Radboud University Nijmegen

Department of theoretical high energy physics

Quantum Gravity corrections to the Unruh effect

Author:

Fleur Versteegen

Supervisor:

Dr Frank Saueressig

18/07/2016

Abstract: A common feature shared by many quantum gravity models is modifications of two-point functions at energy scales around the Planck scale. Generically, these modifications induce non-trivial profiles for the spectral dimension characterizing the underlying quantum spacetime. This thesis investigates the consequences of these modifications within the Unruh radiation detected by an accelerated detector in Minkowski space. While the Unruh temperature, as a purely geometric effect, is protected from quantum gravity corrections, the induced emission rate of the accelerated detector receives distinct corrections in the prefactor multiplying the Bose-Einstein distribution. Essentially, the modified two-point functions change the effective dimension of spacetime seen by the accelerated detector. The resulting Unruh dimension has a close relation to the spectral dimension commonly measured in quantum gravity models.

Contents

1 Introduction

intro

Quantum gravity, as the name suggests, focuses on the quantization of gravity. There are numerous reasons for pursuing this endeavour, while simultaneously there are reasons as to why gravity on microscopic scale does not seem to effect daily life Krishnan:2010un [1]. In particle physics the effects of quantum gravity are (usually) negligible as the energies encountered in the corresponding experiments are well below the Planck energy scale. For the Planck length, time and mass

$$L_P = \left(\frac{G\hbar}{c^3}\right)^{1/2}, \quad T_P = \frac{L_P}{c}, \quad M_P = \frac{\hbar T_P}{L_P^2}, \tag{1.1}$$

the Planck energy is defined as

$$E_P = M_P c^2 \approx 10^{19} GeV. \tag{1.2}$$

Keeping in mind that most particle experiments are still in the range of $10^4 GeV$, it should not come as a surprise that trans-Planckian events are not (directly) measurable. One possibility to establish quantum gravity effects is by attempting to recognize ultra-violet (UV) contributions that propagate through to lower, detectable energies. To accomplish this, it is necessary to construct a theoretical framework describing physics on trans-Planckian scales. One could of course wonder where the expected breakdown of the present model comes from. That is: what keeps us from simply quantizing general gravity following the procedures dictated by quantum field theory? As in general relativity it is the metric that describes the gravitational field, quantization of this field could be interpreted as the quantization of geometry. This approach is known as covariant quantization and suffers from conceptual problems rendering it inadequate. The route to follow requires a perturbative description of the theory (metric) in terms of E/E_P, where the series would be truncated once the desired order is reached. The resulting theory would be an effective field theory, valid below and up to the perturbation order. While this may work for other theories, a gravity-specific difficulty arises once we pass the Planck scale as there $E/E_P \approx 1$, indicating we are dealing with a non-renormalizable theory. This tells us that the effective field theory is no longer valid and any predictive properties are lost. It is expected then that at these high energies (small distances) scales, there is a range of degrees of freedom that make their appearance while remaining concealed at low energies (long distances).

Another conundrum arises when one tries to define observables in a theory of quantized gravity. As in the classical limit (e.g. general relativity) the theory is required to be diffeomorphism invariant, it seems reasonable to demand the same for its quantized extension. Consequently, it seems reasonable to demand that any theory of quantum gravity is background independent i.e. quantum observables should be background independent. Then there is the question of locality as well. How can one define what is local and what is not if there is no unique coordinate frame to depend on?

In section (sec:curved spacetime 2.2) it will be shown that equal-time canonical quantization can be applied if one chooses a spacetime that admits a Cauchy surface (e.g. the spacetime is globally hyperbolic). If there is no such Cauchy surface, however, applying equal-time canonical quantization would violate diffeomorphism invariance and lead to an ill-defined time evolution of the theory.

Different theories trying to resolve these problems (and many more) are at the moment under construction. For later reference, Sect. sect:QG 4 will consist of a compact collection of multiple such theories.

To study effects originating from quantum gravity, one can analyze dimensional flows. Dimensional flows are a feature commonly encountered in virtually all approaches to quantum gravity and quantum gravity inspired models Carlip:2009kf,Carlip:2012md [2, 3]. The most prominent example of a dimensional flow occurs in Kaluza-Klein theories where the dimensionality of spacetime increases below the compactification scale. An even more intriguing phenomenon of this form is dynamical dimensional reduction where a specific dimensionality of spacetime decreases at short distances. The prototypical example for this mechanism is provided by Causal Dynamical Triangulations [4] where a random walk sees a two-dimensional spacetime at short distances while long walks exhibit a four-dimensional behavior [5]. Similar features are encountered in Asymptotic Safety [6, 7, 8, 9], Loop Quantum Gravity [10, 11, 12, 13, 14], Horava-Lifshitz gravity [15, 16], Causal Set Theory [17, 18, 19], κ-Minkowski space [20, 21, 22], non-commutative geometry [23, 24], non-local theories [25, 26], minimal length models [27], and based on the Hagedorn temperature seen by a gas of strings [28].

The indicator commonly used to study dimensional flows is the spectral dimension (see Sect. 3). The (typically Euclidean) quantum spacetime is equipped with an artificial diffusion process for a test particle. One then studies the return probability of the particle as a function of the diffusion time σ. The mathematical definition of the spectral dimension d_s is obtained in the limit of infinitesimal diffusion time $\sigma \to 0$. On a manifold the spectral dimension agrees with the topological dimension d. In the context of quantum gravity, where the properties of the underlying spacetime may depend on the length scales probed by the diffusing particle, it is useful to define a generalized spectral dimension $D_s(\sigma)$ where the limit $\sigma \to 0$ is omitted. The most common behavior of $D_s(\sigma)$ encountered in quantum gravity interpolates between $D_s = 4$ on macroscopic scales and $D_s = 2$ at short distances. This observation has also triggered the investigation of multi-scale geometries serving as a phenomenological model of quantum gravity inspired spacetimes [29].

The spectral dimension bears a close relation to the two-point correlation function $\widetilde{G}$ of the diffusing particle (see Sect. 2 for a recap on Green functions). For a massless scalar particle propagating on a four-dimensional Euclidean space one has $\widetilde{G} = p^{-2}$, which leads to a scale-independent spectral dimension $D_s = 4$. Non-trivial D_s-profiles are created if the two-point correlation function acquires an anomalous dimension. Based on this close connection, the interpretation of the spectral dimension as the Hausdorff dimension of the momentum space has been advocated in [30]. Note that a non-trivial spectral dimension does not necessarily involve the breaking of Lorentz invariance, since $\widetilde{G}(p^2)$ may be a function of the momentum four-vector squared and thus a Lorentz invariant quantity. However, this function can in principle have more general forms than those allowed in a local quantum field theory. One relevant example is a two-point function arising in a nonlocal field theory, defined as a theory whose equations of motion have an infinite number of derivatives. This form is ubiquitous in Causal Set studies [31].

The fictitious nature of the diffusion process underlying the spectral dimension then raises the crucial question whether the flow of the spectral dimension can be seen in a physical observable quantity. The main goal of this research is to explicitly demonstrate that this is indeed the case: the non-trivial momentum profiles leave an imprint in the Unruh effect felt by an accelerated detector. More precisely, the effective dimension of spacetime seen by the Unruh detector is determined by the spectral dimension.

The Unruh effect [32, 33, 34] (also see [49, 35] for reviews) is one of the most intriguing phenomena occurring within quantum field theory in Minkowski space. Essentially, it predicts that to an accelerated observer (Rindler observer) the Minkowski vacuum appears as a thermal state whose temperature is proportional to the acceleration parameter. This acceleration radiation can leave imprints in a variety of phenomenological contexts: for instance in the transverse polarization of electrons and positrons in particle storage rings (Sokulov-Ternov effect) [36, 37], at the onset of quark gluon plasma formation due to heavy ions collisions [38], on the dynamics of electrons in Penning traps, of ultra-intense lasers, and atoms in microwave cavities (see [49] and references therein), or in the Berry phase acquired by the accelerated detector [39]. Recently it has also been shown that the low energy signatures of Unruh radiation are very sensitive to high energy nonlocality [40].

On theoretical grounds the Unruh effect can be derived by defining creation and annihilation operators with respect to the positive and negative frequency modes associated with the Minkowski and Rindler space and relating them through a Bogoliubov transform, see e.g. [41] for a pedagogical exposition or Sect. 5. The origin of the thermal spectrum is essentially geometrical, in the sense that it depends solely on the presence of a horizon in the Rindler frame. As a geometric effect, the Unruh temperature is insensitive to the specific form of the Lagrangian or the interactions under consideration and thermality of the spectrum is essentially ensured by Lorentz invariance [42]. It will be shown that this also holds for the broad class of quantum gravity corrections considered in this work.[1] While not affecting the thermal nature of the Unruh radiation, quantum gravity induced modifications of the two-point function affect the profile functions multiplying the thermal distribution in a more or less radical way.

In order to make the connection between dimensional flows and modifications in the Unruh effect as close as possible, the detector approach [45] will be followed. The central idea is to consider a detector made from a two-level system with an upper, excited state 2 and a lower state 1 being separated by the energy $\Delta E \equiv E_2 - E_1 > 0$ coupled to a scalar field. The transition probabilities induced by the scalar can be expressed in terms of the positive-frequency Wightman function of the Minkowski vacuum state. The emission rates of the detector can be computed by evaluating a Fourier transform of the two-point function along the worldline of an accelerated observer. For a standard massless scalar field, it is then rather straightforward to show that the Green's function evaluated on the worldline satisfies a Kubo-Martin-Schwinger (KMS) condition (see Sect. 2.1.3) where the periodicity in Euclidean time depends on the properties of the worldline only. The resulting Unruh temperature is proportional to the acceleration a. This setup also makes clear that corrections to the two-point functions, e.g. induced by quantum fluctuations at small scales, may leave their fingerprints in the transition rate of the Unruh detector. Both, a dynamical dimensional flow and corrections to the transition rate, can be traced back to the same source: a non-trivial momentum dependence of the two-point function.

In this work the focus will lie on the asymptotic structure of the detector-induced emission rates in a fixed Minkowski background.[2] We will show that different types of dimensional flows leave distinct signatures in the detector rates. In particular, in the case of dimensional reduction at high energies, one finds a suppression of the rates, whereas for a dimensional *enhancement* at high energies, as in Kaluza-Klein models, the rate increases. Since the transition probability of the Unruh detector is clearly a signature which is observable at least in principle, we expect that it can be used to make phenomenological predictions from quantum gravity, allowing a direct comparison between various approaches.

The first half of this thesis (Sect. 2 to Sect. 4) can be seen as a pedagogical introduction of concepts and tools needed to acquire the results derived in the sections that follow. Sect. 2 shortly recaps the quantization of massless scalar fields in Minkowski and curved spacetime, after which Sect. 3 derives the diffusion equation and discusses the origin of

[1] For similar studies in the context of anisotropic dispersion relations and a minimal length scale see [43, 44, 45]

[2] Throughout the work, effects related to the "switching function" χ, which controls the time dependence of the detector coupling strength, will not be taken into account. See [46, 47] for details.

the spectral dimension from diffusion processes. For later purposes the KMS condition is derived in Sect. 2.1.3. As a final part of the introduction, Sect. 4 discusses the basic concepts of quantum gravity and approaches therein followed by a direct derivation of the Unruh effect in Sect. 5. The original research carried out is organized as follows. Sect. 6 briefly reviews the detector approach to the Unruh effect. Dimensional flows entail specific modifications of the two-point correlation functions entering into the detector approach and we derive the master formula capturing the resulting corrections to the Unruh effect in Sect. 7. In Sect. 8 we define the Unruh dimension as the effective dimension seen by the detector and relate it to the spectral dimension. In Sect. 9 we apply this formula to specific examples taken from phenomenologically motivated multi-scale models (Sect. 9.1), Kaluza-Klein theory (Sect. 9.2), spectral actions (Sect. 9.3), and Causal Set Theory (Sect. 9.4). We close with a brief discussion of our findings in Sect. 10.

2 Quantum Field Theory

In this section, the general methodology for second quantization is briefly recapped. The first half covers the quantization of a scalar field ϕ on a Minkowski background [48], whereas the second half generalizes the developed methodologies to curved backgrounds given certain specific conditions on the curved manifold.

2.1 Scalar field quantization in Minkowski spacetime

There are two essential requirements the quantized fields will have to meet; Lorentz invariance (i.e. spacetime obeys Poincaré symmetry) and causality. One can then take a Hilbert space constructed of relativistic particle states and define fields to gain a notion of observables acting on the Hilbert space. For example, a free scalar field is classically an infinite collection of Harmonic oscillator modes, with Hamiltonian

$$H = \frac{1}{2m}p^2 + \frac{1}{2}m\omega^2 q^2, \tag{2.1}$$

where p is the momentum and q a coordinate in real space. To quantize, one can promote the Hamiltonian, momentum and space coordinate to operators, $(q,p) \to (\hat{q},\hat{p})$ and demanding $\hat{p}$ and $\hat{q}$ satisfy $[\hat{q},\hat{p}] = i\hat{1}$. The momentum and space coordinate can then be defined in terms of $\hat{a}^\dagger$ and $\hat{a}$, the creation and annihilation operators respectively. Doing so leads to

$$\hat{H} = \frac{1}{2m}\hat{p}^2 + \frac{1}{2}m\omega^2 \hat{q}^2. \tag{2.2}$$

Introducing creation/annihilation operators yields

$$\hat{q} \equiv \frac{\hat{a} + \hat{a}^\dagger}{\sqrt{2\omega}}, \qquad \hat{p} \equiv -i\omega\frac{\hat{a} + \hat{a}^\dagger}{\sqrt{2\omega}}, \tag{2.3}$$

such that the (discrete) bosonic commutation relations are satisfied: $[\hat{a},\hat{a}^\dagger] = \hat{1}$. The subtlety here is that there are an infinite number of linear oscillators that need to be quantized (i.e. there are infinitely many degrees of freedom). However, as the theory under consideration is a free theory, the degrees of freedom evolve independently. To see this, consider a field component satisfying the Klein-Gordon equation; $(\Box + m^2)f(\vec{x},t) = 0$

where $f(\vec{x},t) \in \mathbb{R}$. Performing a Fourier decomposition gives

$$f(\vec{x},t) = \int \frac{d\vec{p}}{(2\pi)^3} e^{i\vec{p}\cdot\vec{x}} g(\vec{p},t), \tag{2.4}$$

where now for each Fourier mode $\vec{p} = (p_x, p_x, p_z)$ the Klein-Gordon equation

$$\left(\partial_t^2 + (\vec{p}^2 + m^2)\right) g(\vec{p},t) = 0, \tag{2.5}$$

is satisfied by $g(\vec{p},t)$ with frequency $\omega \equiv \sqrt{\vec{p}^2 + m^2}$. As the modes are now decoupled, the general solution to the Klein-Gordon equation is that of a linear superposition of harmonic oscillators. This justifies the quantization procedure as described above.

Making the transition from discrete to continuous, the position operator $\hat{q}$ becomes a field

$$\hat{\phi}(\vec{x}) = \int \frac{d\vec{p}}{(2\pi)^3} \frac{1}{2\omega} \left(\hat{a}_{\vec{p}} e^{i\vec{p}\cdot\vec{x}} + \hat{a}^\dagger_{\vec{p}} e^{-i\vec{p}\cdot\vec{x}}\right), \tag{2.6}$$

where now

$$[\hat{a}_{\vec{p}}, \hat{a}^\dagger_{\vec{p}'}] = (2\pi)^3 \delta(\vec{p} - \vec{p}')\hat{1}. \tag{2.7}$$

So far the fields exhibit no time dependency yet. To discuss the consequences of causality, however, a time dependent formalism has to be developed. Suppose then that the field under consideration has a time dependence, i.e. $\hat{\phi} \equiv \hat{\phi}(x) = \hat{\phi}(\vec{x},t)$. As the time evolution of operators is described by means of the Hamiltonian operator, letting $\hat{H}$ work on the creation/annihilation operators would give the time dependent field. In this procedure one makes use of the fact that $[\hat{H}, \hat{a}_{\vec{p}}] = -\omega \hat{a}_{\vec{p}}$ and $[\hat{H}, \hat{a}^\dagger_{\vec{p}}] = \omega \hat{a}^\dagger_{\vec{p}}$. By repeatedly applying $\hat{H}$ on $\hat{a}_{\vec{p}}$ and $\hat{a}^\dagger_{\vec{p}}$ (or equivalently, on $\hat{\phi}$), the exponential map of $\hat{H}$ can be constructed such that the evaluation of $\hat{\phi}(x) = e^{i\hat{H}t}\hat{\phi}(\vec{x})e^{-i\hat{H}t}$ can be performed. One can also take a different route and use the Lorentz invariant momentum space measure

$$\begin{aligned} \int \frac{d^4p}{(2\pi)^3} \delta(p^2 - m^2)\Theta(p^0) &= \int \frac{d^4p}{(2\pi)^3} \left(\frac{\delta(p_0 - \omega)}{2\omega} + \frac{\delta(p_0 + \omega)}{2\omega}\right) \Theta(p^0) \\ &= \int \frac{d\vec{p}}{(2\pi)^3} \frac{1}{2\omega}. \end{aligned} \tag{2.8}$$

eq:LorInv

Note that the Heaviside step function restricts p^0 to be positive and thus the second delta function drops out when m is real. Applying this to $\hat{\phi}$ results in

$$\hat{\phi}(x) = \int \frac{d\vec{p}}{(2\pi)^3} \frac{1}{2\omega} \left(\hat{a}_{\vec{p}} e^{-ip\cdot x} + \hat{a}^\dagger_{\vec{p}} e^{ip\cdot x}\right)_{p_0=\omega}. \tag{2.9}$$

To check if this formalism respects causality, one can evaluate $[\hat{\phi}(x), \hat{\phi}(y)]$ and check whether it gives zero when $(x-y)^2 < 0$ (i.e. for spacelike separations of the spacetime points x and y). In the explicit check, one can use that

$$\left[\hat{\phi}(x), \hat{\phi}(y)\right] = \int \frac{d\vec{p}}{(2\pi)^3} \frac{1}{2\omega} \left(e^{-ip\cdot(x-y)} - e^{ip\cdot(x-y)}\right)_{p_0=\omega}, \tag{2.10}$$

is Lorentz invariant due to (eq:LorInv 2.8). Another useful property is that taking $x \to -x$, $y \to -y$ yields the same expression if $x_0 - y_0 = 0$. This can be checked by taking $\vec{p} \to -\vec{p}$. As for $(x-y)^2 < 0$ there is always a Lorentz transformation such that $x_0' - y_0' = 0$, the commutator above indeed evaluates to zero. Furthermore (eq:LorInv 2.8) can be used to derive the 1-particle completeness relation by considering that

$$|\vec{k}\rangle = \int \frac{d\vec{p}}{(2\pi)^3}\frac{1}{2\omega}\,|\vec{p}\rangle\,\langle\vec{p}|\vec{k}\rangle\,, \tag{2.11}$$

which implies a completeness relation of the form

$$\hat{1} = \int \frac{d\vec{p}}{(2\pi)^3}\frac{1}{2\omega}\,|\vec{p}\rangle\,\langle\vec{p}|\,. \tag{2.12}$$

Note that in the examples above, there is a notion of locality in the sense that the Lagrangian contains no interaction terms that couple a field at spacetime point x to a field at spacetime point y.

An alternative route to quantization would be to start out with a classical field theory that already satisfies the requirements imposed by relativity and apply canonical quantization to the fields. In the case of the free Klein-Gordon theory, this entails starting out with the classical Lagrangian for a real scalar field and extracting the Klein-Gordon equation by means of the Euler-Lagrange equation. The fields ϕ_j and their conjugate momenta $\pi_k = \partial_t\phi_k$ become operators that satisfy the equal time canonical commutation relations, i.e.

$$\begin{aligned}
&[\hat{\phi}_j(x), \hat{\pi}_k(y)] = i\delta_{jk}\delta^3(\vec{x}-\vec{y}),\\
&[\hat{\phi}_j(x), \hat{\phi}_k(y)] = 0,\\
&[\hat{\pi}_j(x), \hat{\pi}_k(y)] = 0,
\end{aligned} \tag{2.13}$$

eq:comm flat

where the labels j and k rever to the j^{th} and k^{th} field.

2.1.1 Two-point functions

To evaluate the vacuum expectation values of free fields, $\langle 0|\,[\hat{\phi}(x),\hat{\phi}(y)]\,|0\rangle$, it is necessary to invert the equation of motion of the theory. In the case of the free scalar field, this entails constructing the Green function of the operator $(\Box + m^2)$. Let $G(x-y)$ be this Green function in real space and $\tilde{G}(p)$ denote its momentum space representation, that is

$$\begin{gathered}
iG(x-y) = \int \frac{d^4p}{(2\pi)^4}\tilde{G}(p)e^{-ip\cdot(x-y)}\\
\text{where}\\
(-p^2+m^2)\tilde{G}(p) = -i \quad\Rightarrow\quad \tilde{G}(p) = \frac{i}{p^2-m^2},
\end{gathered} \tag{2.14}$$

here $G(x-y)$ is the Green function in real space, see Fig. fig:G 1. The integral over $\tilde{G}$ contains divergencies at $p_0 = \omega$ and $p_0 = -\omega$ which cause the Fourier integral to blow up. To obtain a finite result, the contour integral procedure is implemented. There are several options one can choose from to circle around these poles, depending on the type of process under consideration (e.g. depending on the boundary conditions). For taking into account influences from the past, the poles are shifted into the negative imaginary part of the plane by an amount $i\epsilon$ which is taken to zero after integration. The resulting contour integral carries the name *retarded* Green function $G_R(x-y) = -\theta(x^0-y^0)G(x-y)$. The exact opposite procedure, i.e. shifting the poles upwards along the positive imaginary axis, takes influences from the future into account and is known as the *advanced* Green function $G_A(x-y) = \theta(y^0-x^0)G(x-y)$, see Fig. fig:RetAdv 2. The Green function $G(x-y)$ can be split into

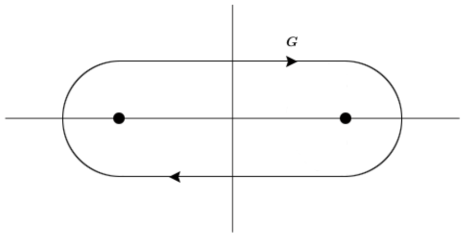

Figure 1: Green function

fig:G

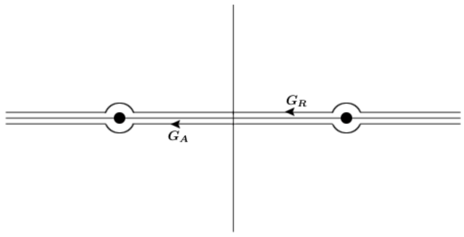

Figure 2: Retarded and advanced Green function

fig:RetAdv

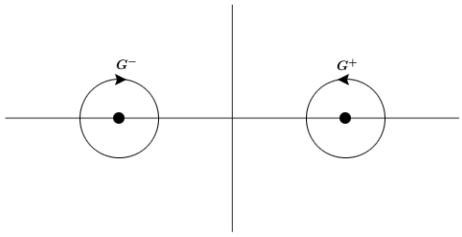

Figure 3: Positive and negative Wightman functions

fig:Wightman

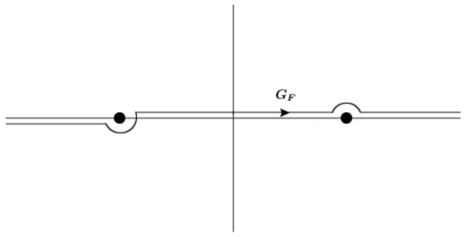

Figure 4: Feynmann propagator

fig:Feynmann

a positive/negative frequency part, i.e. a contour integral that circles around the pole in the positive/negative real part of the plane. These positive and negative frequency parts are denoted as $G^+(x-y) = \langle 0| \hat{\phi}(x)\hat{\phi}(y) |0\rangle$ and $G^-(x-y) = \langle 0| \hat{\phi}(y)\hat{\phi}(x) |0\rangle$ respectively, satisfy $iG(x-y) = G^+(x-y) - G^-(x-y)$ and are referred to as the positive and negative *Wightman* functions, see Fig. 3. Another useful contour is the *Feynman* Green function $G_F(x-y)$ which can be constructed from the Wightman functions as $G_F(x-y) = \theta(x^0 - y^0)G^+(x-y) + \theta(y^0 - x^0)G^-(x-y)$ and yields the time-ordered product of the fields, see Fig. 4.

2.1.2 Källén-Lehmann spectral representation

For later purposes, it is convenient to introduce the *Källén-Lehmann spectral representation.* When dealing with a theory that allows interaction terms, the Källén-Lehmann spectral representation gives the form of the Green function in terms of a sum over Green functions describing a free theory. Consider the vacuum expectation value of a complex scalar field, whit groundstate $|\lambda_{GS}\rangle$, $\langle \lambda_{GS}| \hat{\phi}(x)\hat{\phi}^\dagger(y) |\lambda_{GS}\rangle$, which can be rewritten by using the completeness relation

$$\hat{1} = |\lambda_{GS}\rangle \langle \lambda_{GS}| + \sum_{\lambda} \int \frac{d\vec{p}}{(2\pi)^3} \frac{|\lambda_{\vec{p}}\rangle \langle \lambda_{\vec{p}}|}{2E_\lambda}, \tag{2.15}$$

into

$$
\begin{aligned}
\langle\lambda_{GS}|\,\hat{\phi}(x)\hat{\phi}^\dagger(y)\,|\lambda_{GS}\rangle &= \langle\lambda_{GS}|\,\hat{\phi}(x)\,|\lambda_{GS}\rangle\,\langle\lambda_{GS}|\,\hat{\phi}^\dagger(y)\,|\lambda_{GS}\rangle \\
&\quad + \sum_\lambda \int \frac{d\vec{p}}{(2\pi)^3}\frac{\langle\lambda_{GS}|\,\hat{\phi}(x)\,|\lambda_{\vec{p}}\rangle\,\langle\lambda_{\vec{p}}|\,\hat{\phi}^\dagger(y)\,|\lambda_{GS}\rangle}{2E_\lambda}.
\end{aligned}
\tag{2.16}
$$

eq:KL

Here $|\lambda_{GS}\rangle$ denotes the ground state of the interacting theory (the free theory equivalent would be $|0\rangle$), $|\lambda_{\vec{p}}\rangle$ denotes an excited state and $E_\lambda = \sqrt{\vec{p}^2 + m_\lambda^2}$ with m_λ the mass belonging to a zero-momentum state (i.e. $p_0^\mu = (m_\lambda, \vec{0})$). Note that m_λ cannot be thought of as the mass belonging to a particular particle as the theory under consideration is an interacting theory. If the sum over λ yields a complete set of states and if these states are eigenstates of the momentum four-vector, then on the account of invariance under translations and Lorentz transformations, it is possible to write

$$
\begin{aligned}
\langle\lambda_{GS}|\,\hat{\phi}(x)\,|\lambda_{\vec{p}}\rangle\,\langle\lambda_{\vec{p}}|\,\hat{\phi}^\dagger(y)\,|\lambda_{GS}\rangle &= \langle\lambda_{GS}|\,e^{i\hat{P}\cdot x}\hat{\phi}(x)e^{-i\hat{P}\cdot x}\,|\lambda_{\vec{p}}\rangle\,\langle\lambda_{\vec{p}}|\,e^{-i\hat{P}\cdot y}\hat{\phi}^\dagger(y)e^{i\hat{P}\cdot y}\,|\lambda_{GS}\rangle \\
&= e^{-ip\cdot(x-y)}\,\langle\lambda_{GS}|\,\hat{\phi}(0)\,|\lambda_{\vec{p}}\rangle\,\langle\lambda_{\vec{p}}|\,\hat{\phi}^\dagger(0)\,|\lambda_{GS}\rangle\Big|_{p^0=E_{\vec{p}}}.
\end{aligned}
\tag{2.17}
$$

Here $\hat{P}$ is the generator of spacetime translations such that $\hat{P}^\mu = (\hat{H} - E_0\hat{1}, \hat{\vec{P}})$ with eigenvalues $p^\mu = (E - E_0, \vec{p})$. As mentioned before, the purpose of the Källén-Lehmann representation is to write an interacting theory as a sum over free theories. To meet this requirement, it is necessary to rewrite the expression above in terms of $\lambda_{\vec{0}}$ instead of $\lambda_{\vec{p}}$. Let $\hat{U}(\Lambda)$ be the (unitary) boost operator, then one can show that $\hat{U}(\Lambda)\,|\lambda_{\vec{0}}\rangle = |\lambda_{\vec{p}}\rangle$ by using that the generator $\hat{P}^\mu$, and thus its eigenvalues, transforms as a contravariant vector under boosts, i.e. $\hat{U}^{-1}(\Lambda)\hat{P}^\mu\hat{U}(\Lambda) = \Lambda^\mu{}_\nu\hat{P}^\nu$. Likewise, the ground state of the theory $|\lambda_{GS}\rangle$ should be invariant under the Poincaré group, suggesting that $e^{i\hat{P}\cdot x}\,|\lambda_{GS}\rangle = |\lambda_{GS}\rangle$ and $\hat{U}(\Lambda)\,|\lambda_{GS}\rangle = |\Lambda_{GS}\rangle$. Taking this into account, those brakets containing an excited state become

$$
\begin{aligned}
e^{-ip\cdot x}\,\langle\lambda_{GS}|\,\hat{\phi}(0)\,|\lambda_{\vec{p}}\rangle\Big|_{p^0=E_{\vec{p}}} &= e^{-ip\cdot x}\,\langle\lambda_{GS}|\,\hat{U}^{-1}\hat{U}\hat{\phi}(0)\hat{U}^{-1}\hat{U}\,|\lambda_{\vec{p}}\rangle\Big|_{p_0=E_{\vec{p}}} \\
&= e^{-ip\cdot x}\,\langle\lambda_{GS}|\,\hat{\phi}(0)\,|\lambda_{\vec{\Lambda p}}\rangle\Big|_{p^0=E_{\vec{p}}} \\
&= e^{-ip\cdot x}\,\langle\lambda_{GS}|\,\hat{\phi}(0)\,|\lambda_{\vec{0}}\rangle\Big|_{p^0=E_{\vec{p}}},
\end{aligned}
\tag{2.18}
$$

where in the last line the Lorentz transformation was chosen such that $\vec{\Lambda p} = \vec{0}$. For the ground-state term of (2.16), one can write

$$
\langle\lambda_{GS}|\,\hat{\phi}(x)\,|\lambda_{GS}\rangle = \langle\lambda_{GS}|\,\hat{\phi}(0)\,|\lambda_{GS}\rangle = vev. \tag{2.19}
$$

The vacuum expectation value (vev) of $\hat{\phi}$ yields a delta function and in most cases it is subtracted by redefining the field $\hat{\phi}(x) \to \hat{\phi}(x) - vev$. Assuming this has been done and that $x^0 > y^0$, (2.16) becomes

$$
\begin{aligned}
\langle\lambda_{GS}|\,\hat{\phi}(x)\hat{\phi}^\dagger(y)\,|\lambda_{GS}\rangle &= \sum_\lambda \int \frac{d\vec{p}}{(2\pi)^3}\,e^{-ip\cdot(x-y)}\frac{\langle\lambda_{GS}|\,\hat{\phi}(0)\,|\lambda_{\vec{0}}\rangle\,\langle\lambda_{\vec{0}}|\,\hat{\phi}^\dagger(0)\,|\lambda_{GS}\rangle}{2E_\lambda}\Bigg|_{p^0=E_{\vec{p}}} \\
&= \sum_\lambda \left|\langle\lambda_{GS}|\,\hat{\phi}(0)\,|\lambda_{\vec{0}}\rangle\right|^2 \int \frac{dp}{(2\pi)^4}\frac{ie^{-ip\cdot(x-y)}}{p^2 - m_\lambda^2 + i\epsilon} \\
&= \int_0^\infty d\mu^2 \rho(\mu^2) G^+(x-y;\mu^2),
\end{aligned}
\tag{2.20}
$$

eq:spectralden

where G^+ is the positive-frequency Wightman function and

$$\rho(\mu^2) = \sum_\lambda \delta(\mu^2 - m_\lambda^2) \left| \langle \lambda_{GS} | \, \hat{\phi}(0) \, | \lambda_{\vec{0}} \rangle \right|^2, \tag{2.21}$$

is known as the *spectral density* with squared invariant mass μ^2. If instead $y^0 > x^0$ in (2.20), the above equation would have yielded the negative-frequency Wightman function G^-.

2.1.3 KMS condition

The KMS (Kubo, Martin-Schwinger) condition provides a description of (thermal) equilibrium states without having to restrict oneself to systems with a finite number of degrees of freedom. In general it is the Gibbs' distribution that is most commonly used to describe equilibrium states. For the case of a canonical ensemble, the probability of a system X being in the non-degenerate state x (or the random variable X to have value x) is given by

$$P(X = x) = \frac{1}{Z} e^{-\beta E}. \tag{2.22}$$

Here β is the inverse temperature, E is the energy of the state x and $Z = \mathrm{Tr} e^{-\beta E}$ is the (normalizing) partition function. Problems arise when one takes the thermodynamic limit (taking the size to infinity) and thus an alternative procedure is needed.

For an observable $\hat{O}$, the time evolution can be written as

$$\hat{o}_t(\hat{O}) = e^{i\hat{H}t} O e^{-i\hat{H}t}, \tag{2.23}$$

and a Gibbs state ω_β of the observable $\hat{O}$ is defined as:

$$\omega_\beta(\hat{O}) = \frac{1}{Z} \mathrm{Tr}(e^{-\beta \hat{H}} \hat{O}). \tag{2.24}$$

If one then takes two observables $\hat{O}$ and $\hat{P}$ and, by using the cyclic properties of the trace, computes the Gibbs state as

$$\begin{aligned}
\omega_\beta(\hat{o}_t(\hat{O})\hat{P}) &= \frac{1}{Z} \mathrm{Tr}\left(e^{-\beta \hat{H}} e^{i\hat{H}t} \hat{O} e^{-i\hat{H}t} \hat{P} \right) \\
&= \frac{1}{Z} \mathrm{Tr}\left(\hat{P} e^{i\hat{H}(t+i\beta)} \hat{O} e^{-i\hat{H}t} \right) \\
&= \omega_\beta \left(\hat{P} e^{i\hat{H}(t+i\beta)} \hat{O} e^{-i\hat{H}(t+i\beta)} \right) \\
&= \omega_\beta(\hat{P} \hat{o}_{t+i\beta}(\hat{O})),
\end{aligned} \tag{2.25}$$

then the definition of a (τ, β)-KMS state can be taken as

$$\omega(\hat{P} \tau_{i\beta}(\hat{O})) = \omega(\hat{O}\hat{P}). \tag{2.26}$$

The upshot of the short derivation above is that when one is treating a system in a KMS thermal equilibrium, the property (2.26) automatically holds. An application of the KMS condition can be found in Sect. 6.2

2.2 Scalar field quantization in curved spacetime

Even though this thesis only considers flat spacetime, it is instructive to take a closer look at quantization in curved spacetime [1] as Rindler space exhibits properties similar to those in curved spacetime, Sect. 5. The main problem of quantization in curved spacetime is that Poincaré symmetry has been demoted from a global to a local symmetry as compared to flat spacetime. As a consequence, it is no longer sensible to use irreducible representations of the Poincaré group for the construction of one-particle states. One notion that we can still depend on, however, is that of causality. To quantize a scalar field in curved spacetime, one can develop a one-particle Hilbert space such that the field operations on this space are causal. The simplest example one can work through is again that of the curved spacetime Klein-Gordon equation

$$\left(\Box + m^2\right)\phi = 0, \tag{2.27}$$

where $\Box = -g^{\mu\nu}\nabla_\mu\nabla_\nu$, the curved spacetime d'Alembertian. The Klein-Gordon equation is the equation of motion of the minimally coupled action (i.e. there is only a coupling to the invariant spacetime volume)

$$S = \int d^4x \frac{\sqrt{|g|}}{2}\left(g^{\mu\nu}\partial_\mu\phi\partial_\nu\phi - m^2\phi^2\right), \tag{2.28}$$

respecting diffeomorphism invariance. Note that in flat spacetime, diffeomorphism invariance reduces to Poincaré invariance as boosts, rotations and translations allow for one coordinate system to be transformed into another. In flat spacetime the natural next step would be to construct the solutions to the (flat spacetime) Klein-Gordon equation and note that there exists an isomorphism between states in the one-particle Hilbert space and the positive frequency solutions of the Klein-Gordon equation (hermitian conjugation of these solutions give the negative frequency modes). The existence of this isomorphism allows for the Hilbert space to be constructed as the space of positive frequency solutions of the Klein-Gordon equation. A similar method in curved spacetime requires one to demand that the manifold, M, on which quantization takes place, is globally hyperbolic. Equivalently, one demands that M has a global Cauchy surface. A Cauchy surface S is a spatial slice such that for any point $p \in M$ in the future of the surface, the (past-directed) inextendible curve from p to S crosses S only once. Here inextindible denotes a curve without fixed end-points and in the particular case of a Cauchy surface the curves cannot be closed either. If M in its whole can be described by the initial data on a Cauchy surface, then one says M has a global Cauchy surface and is thus globally hyperbolic.

The essential consequence of the above is that it ensures the entire future/past can be determined by the initial data on one spatial slice. One can then introduce canonical equal-time commutators according to

$$\begin{aligned}
[\hat{\phi}(x), n^\mu\partial_\mu\hat{\phi}(y)]_S &= \frac{i}{\sqrt{|h|}}\delta^3(\vec{x}-\vec{y}) \\
[\hat{\phi}(x), \hat{\phi}(y)]_S &= 0 \\
[n^\mu\partial_\mu\hat{\phi}(x), n^\nu\partial_\nu\hat{\phi}(y)]_S &= 0.
\end{aligned} \tag{2.29}$$

Here S is the Cauchy slice, n^μ the normal to the surface and h the determinant of the induced metric on the Cauchy slice. Note that $n^\mu\partial_\mu\hat{\phi}(x)$ is a (covariant) generalization of the conjugate momenta, as in flat space the normal to the Cauchy surface is given by the time coordinate (i.e. $n^\mu\partial_\mu = \partial_t$) and the equations (2.29) coincide with (2.13). It can be shown that if the canonical equal time commutators hold on one spacelike slice, then they do so on any other spacelike slice as well, given that the field, $\hat{\phi}$, satisfies the Klein-Gordon equation.

At this stage in flat spacetime, there was the possibility to expand solutions to the Klein-Gordon equation in their Fourier basis. In curved spacetime one has to proceed with caution, as a Fourier decomposition might be ill defined. A strategy to circumvent this problem, is to assume that in the far past spacetime was approximately flat, such that a basis of solutions once existed. The next step is then to evolve these solutions forward in time, such that they form a complete basis of solutions in the curved spacetime. The reason this works, is exactly because the commutation relations are independent of the spacelike slice S.

Defining the Klein-Gordon inner product of two (plain-wave) solutions to the Klein-Gordon equation as

$$\langle u_p, u_{p'} \rangle = i \int_S d^3x \sqrt{|h|} n^\mu \left(u_p^* \partial_\mu u_{p'} - u_{p'} \partial_\mu u_p^* \right), \tag{2.30}$$

the orthogonality conditions on the basis can be written as

$$\begin{aligned} \langle u_p, u_{p'} \rangle &= (2\pi)^3 2p^0 \delta^3(\vec{p} - \vec{p}'), \\ \langle u_p, u_{p'}^* \rangle &= 0, \\ \langle u_p^*, u_{p'}^* \rangle &= -(2\pi)^3 2p^0 \delta^3(\vec{p} - \vec{p}'). \end{aligned} \tag{2.31}$$

The field $\hat{\phi}$ is again the superposition of these solutions and the a_p, $a_p^\dagger$ are given by

$$a_p = \left\langle u_p, \hat{\phi} \right\rangle, \qquad a_p^\dagger = -\left\langle u_p^\dagger, \hat{\phi} \right\rangle. \tag{2.32}$$

The difference between quantization in curved spacetime with respect to flat spacetime, comes from the choice of basis solutions u_p. In flat spacetime this choice was unique as there is a timelike Killing vector that advocates a natural choice for the time coordinate. In curved spacetime, however, there is no such "obvious" choice which has as a consequence that there is no unique choice for the basis of solutions. As a result, it is not clear what one perceives as positive/negative frequency modes and the notion of a particle becomes an ambiguity in itself. Analogous to flat spacetime, the existence of a timelike Killing vector (e.g. a stationary spacetime)[3] gives a natural choice for the basis in curved spacetime as well. However, this Killing vector might not be well-defined globally. In some cases, one can then perform an analytic continuation to the part of spacetime where the Killing vector is not well-defined. A particularly interesting situation is Rindler spacetime, where it is exactly this continuation from which the Unruh effect can be derived Crispino:2007eb [49].

3 Effective dimension of spacetime as seen by diffusion

sect:spectral

The spectral dimension can be used to probe the possibility of dimensional reduction generated by various processes. In qauntum gravity, for example, it is a convenient tool to determine the spacetime dimension as felt by an effective field theory in the high energy limit. This concept can be introduced by analyzing the behavior of a test particle undergoing a diffusion process, described by the so called *diffusion equation* (also known as the heat equation). To derive the diffusion equation, consider a microscopic system governed by an ensemble of non-interacting particles submerged into a fluid. As the timescales on which

[3]If the timelike Killing vector is orthogonal to the Cauchy surface, then the spacetime is static as well.

the particles move and collide with one-another is significantly smaller than the timescale on which measurements are performed (i.e. approximately a factor $10^{12}s$ smaller), the particles seem to move randomly (that is, subject to Brownian motion). The diffusion equation is essentially a statistical tool that allows for the description of the movement of an ensemble of identical particles that share their boundary and initial conditions. In this context, the solution to the diffusion equation yields a probability distribution rather than the deterministic value for e.g. the position of a particle. To be more precise, if $c(\vec{x}, t)$ is a solution of the diffusion equation, then c gives the probability distribution to find a particle in a small neighborhood of $\vec{x}$ at a time t.

Rather than immediately evaluating the continuous case, it is instructive to start with a discussion on discrete random walks, following [50]. That is, consider an infinite d-dimensional lattice in Euclidean space. Each site can be described by a d-dimensional vector $\vec{x} = x^i \vec{e}_{(i)}$ where the basis vectors $\vec{e}_{(i)}$ are orthonormal to each other $\vec{e}_{(i)} \cdot \vec{e}_{(j)} = \delta_{ij}$, the x^i are integer multiples of the lattice spacing $a = 1$ (thus the lattice is hypercubic) and every site has $q = 2d$ neighbors. For a walker moving instantaneously and at random between neighboring sites, allowing a time interval $\Delta t = 1$ between every move, the probability of reaching a certain neighboring site is $\frac{1}{q} = \frac{1}{2d}$. Furthermore, the system is set up such that the walker has no recollection about whether the next site has been visited previously (i.e. the process is Markovian and does not depend on the history of the walker, with the exception of the initial site which serves as an initial condition).

Using the initial data $(\vec{x}_0, t_0)$, the conditional probability for a walker to have moved to site $\vec{x}_1$ at time t_1 is given by $P(\vec{x}_1, t_1; \vec{x}_0, t_0)_{(1,1)}$, where the subscripts refer to the lattice spacing and timestep. To calculate this probability, first note that

$$P(\vec{x}_1, t_0; \vec{x}_0, t_0)_{(1,1)} = \prod_{i=1}^{d} \delta_{x_0^i x_1^i}, \tag{3.1}$$

the probability for a walker to be positioned at sites $\vec{x}_0$ and $\vec{x}_1$ simultaneously. Obviously the equation above yields 1 for $\vec{x}_1 = \vec{x}_0$ and 0 otherwise. Furthermore, the probability for the walker to be *somewhere* on the lattice at time $t_1 > t_0$ is given by

$$\sum_{\vec{x}_1} P(\vec{x}_1, t_1; \vec{x}_0, t_0)_{(1,1)} = 1, \tag{3.2}$$

and yields a normalization condition. Note that due to translation invariance in both time and space, P only depends on $t_1 - t_0$ and $x_1 - x_0$. To make the transition to continuous space, it is beneficial to relate the probabilities at different times to one another. As the probability for the walker to be at $\vec{x}$ at time $t + 1$ depends on whether at time t the walker was at $\vec{x} \pm \vec{e}_i$, a neighbor of $\vec{x}$, the probabilities can be written as a recurrence relation

$$P(\vec{x}, t + 1; \vec{x}_0, t_0)_{(1,1)} = \frac{1}{2d} \sum_i P(\vec{x} \pm \vec{e}_i, t; \vec{x}_0, t_0)_{(1,1)}. \tag{3.3}$$

To see the change in time of the probabilities, subtract $P(\vec{x}, t; \vec{x}_0, t_0)$

$$
\begin{aligned}
&P(\vec{x}, t+1; \vec{x}_0, t_0)_{(1,1)} - P(\vec{x}, t; \vec{x}_0, t_0)_{(1,1)} \\
&= \frac{1}{2d} \sum_{i=1}^{d} P(\vec{x} \pm \vec{e}_i, t; \vec{x}_0, t_0)_{(1,1)} - P(\vec{x}, t; \vec{x}_0, t_0)_{(1,1)} \\
&= \frac{1}{2d} \sum_{i=1}^{d} \left[P(\vec{x} + \vec{e}_i, t; \vec{x}_0, t_0)_{(1,1)} + P(\vec{x} - \vec{e}_i, t; \vec{x}_0, t_0)_{(1,1)} \right] - P(\vec{x}, t; \vec{x}_0, t_0)_{(1,1)} \qquad (3.4) \\
&= \frac{1}{2d} \sum_{i=1}^{d} \left[P(\vec{x} + \vec{e}_i, t; \vec{x}_0, t_0)_{(1,1)} + P(\vec{x} - \vec{e}_i, t; \vec{x}_0, t_0)_{(1,1)} - 2P(\vec{x}, t; \vec{x}_0, t_0)_{(1,1)} \right] \\
&= \Delta_D P(\vec{x}, t; \vec{x}_0, t_0)_{(1,1)},
\end{aligned}
$$

eq:diffdisc

where Δ_D functions as a discrete Laplace operator. As the equation above relates a change in time to a second order change in position, it is straightforward to generalize this equation to its continuous equivalent

$$\left(\partial_t - \partial_E^2 \right) P(\vec{x}, t; \vec{x}_0, t_0)_{(1,1)} = 0. \tag{3.5}$$

eq:diffcont

That is, the diffusion equation in continuous space. Here ∂_E denotes the partial derivative with respect to to Euclidean space.

To compute the continuous solution, first consider the discrete equation (eq:diffdisc 3.4). Performing a Fourier transformation yields

$$P(\vec{x}, t; \vec{x}_0, t_0)_{(1,1)} = \int_{-\pi}^{\pi} \frac{d^d\vec{k}}{(2\pi)^d} e^{i\vec{k}\cdot\vec{x}} \tilde{P}(\vec{k}, t; \vec{x}_0, t_0)_{(1,1)}, \tag{3.6}$$

which together with

$$P(\vec{x}, t+1; \vec{x}_0, t_0)_{(1,1)} = \frac{1}{2d} \sum_{i=1}^{d} \left[P(\vec{x} + \vec{e}_i, t; \vec{x}_0, t_0)_{(1,1)} + P(\vec{x} - \vec{e}_i, t; \vec{x}_0, t_0)_{(1,1)} \right], \tag{3.7}$$

implies that

$$\tilde{P}(\vec{k}, t+1)_{(1,1)} = \frac{1}{d} \sum_{i=1}^{d} \cos(k_i) \tilde{P}(\vec{k}, t; \vec{x}_0, t_0)_{(1,1)}, \tag{3.8}$$

subject to the boundary condition

$$\tilde{P}(\vec{k}, t_0; \vec{x}_0, t_0)_{(1,1)} = e^{-i\vec{k}\cdot\vec{x}_0} \qquad \text{or} \qquad P(\vec{x}, t_0; \vec{x}_0, t_0)_{(1,1)} = \delta^d(\vec{x} - \vec{x}_0). \tag{3.9}$$

The probability to find a particle at time t on site $\vec{x}$ now reads

$$P(\vec{x}, t; \vec{x}_0, t_0)_{(1,1)} = \int_{-\pi}^{\pi} \frac{d^d\vec{k}}{(2\pi)^d} e^{i\vec{k}\cdot(\vec{x}-\vec{x}_0)} \left(\frac{1}{d} \sum_{i=1}^{d} cos(k_i) \right)^{t-t_0}. \tag{3.10}$$

The continuum limit in this case is given by taking the lattice spacing and the time interval between walks to zero. For this purpose, let the lattice spacing be given by a and the time interval by τ such that

$$P(\vec{x} - \vec{x}_0; t - t_0)_{(a,\tau)} = \int_{-\pi/a}^{\pi/a} \frac{d^d\vec{k}}{(2\pi)^d} a^d e^{i\vec{k}\cdot(\vec{x}-\vec{x}_0)} \left(\frac{1}{d} \sum_{i=1}^{d} cos(ak_i) \right)^{\frac{t-t_0}{\tau}}. \tag{3.11}$$

Dividing by a^d (i.e. the volume of a hypercube with an edge length a) and taking the limit, yields

$$
\begin{aligned}
\lim_{a,\tau\to 0} P(\vec{x}-\vec{x}_0; t-t_0)_{(a,\tau)} &= \lim_{a,\tau\to 0} \int_{-\pi/a}^{\pi/a} \frac{d^d\vec{k}}{(2\pi)^d} e^{i\vec{k}\cdot(\vec{x}-\vec{x}_0)} \left(\frac{1}{d}\sum_{i=1}^{d}\cos\left(ak_i\right)\right)^{\frac{t-t_0}{\tau}} \\
&= \int_{-\infty}^{\infty} \frac{d^d\vec{k}}{(2\pi)^d} e^{i\vec{k}(\vec{x}-\vec{x}_0)} e^{-\vec{k}^2(t-t_0)} \qquad (3.12) \\
&= \frac{e^{-\frac{(\vec{x}-\vec{x}_0)^2}{4(t-t_0)}}}{(4\pi(t-t_0))^{d/2}},
\end{aligned}
$$

eq:Gauss

where the identification $\tau = \frac{a^2}{2d}$ was made in the expansion

$$
\begin{aligned}
\left(\frac{1}{d}\sum_{i=1}^{d}\cos\left(ak_i\right)\right)^{\frac{t-t_0}{\tau}} &= \left(1-\frac{a^2}{2d}\vec{k}^2+\dots\right)^{(t-t_0)/\tau}, \\
&\approx e^{-(t-t_0)\vec{k}^2}
\end{aligned}
\tag{3.13}
$$

and it was used that the resulting exponential can be written as

$$
e^{i\vec{k}(\vec{x}-\vec{x}_0)-\vec{k}^2(t-t_0)} = e^{-\frac{(\vec{x}-\vec{x}_0)^2}{4(t-t_0)}} e^{-(t-t_0)\left(\vec{k}+\frac{i(\vec{x}-\vec{x}_0)}{2(t-t_0)}\right)^2}, \tag{3.14}
$$

after which a change of integration variables $z^2 = (t-t_0)\left(\vec{k}+\frac{i(\vec{x}-\vec{x}_0)}{2(t-t_0)}\right)^2$ yields the desired result (eq:Gauss 3.12). For future reference, note that the spatial separation of two sites is a property intrinsic to the manifold, while the time coordinate, t, is not. In this context t can be interpreted as the laboratory time i.e. the walk time as measured by an outside observer. To avoid confusion, define $\sigma \equiv t - t_0 = t$ the so-called fictitious diffusion time, where t_0 was set to 0. The probability can then be written as

$$
P(\vec{x}, \vec{x}_0; \sigma) = \frac{e^{-\frac{(\vec{x}-\vec{x}_0)^2}{4\sigma}}}{(4\pi\sigma)^{d/2}}, \tag{3.15}
$$

where the subscripts were omitted.

The next step on the road to spectral dimensions is to take a look at the return probability. That is, the probability that after a given time $\sigma > 0$, the walker is yet again positioned at $\vec{x}_0$

$$
P_r(\sigma) \equiv P(\vec{x}_0, \vec{x}_0; \sigma) = (4\pi\sigma)^{-d/2}. \tag{3.16}
$$

Note that the return probability is equivalent to taking the trace of P

$$
\mathrm{Tr}P(\vec{x}, \vec{x}_0; \sigma) = \int d^d\vec{x} \frac{e^{-\frac{(\vec{x}-\vec{x}_0)^2}{4\sigma}}}{(4\pi\sigma)^{d/2}} \delta^d(\vec{x}-\vec{x}_0) = P(\vec{x}_0, \vec{x}_0; \sigma). \tag{3.17}
$$

The mathematical definition of the spectral dimension, d_s, takes the limit $\sigma \to 0$ such that

$$
d_s \equiv -2 \lim_{\sigma\to 0} \frac{d\ln P_r(\sigma)}{d\ln\sigma}. \tag{3.18}
$$

Intuitively one takes the diffusion time, and thus the length of the diffusion path, to zero such that the length of the path becomes smaller than the radius of curvature. In the case of a flat and smooth spacetime, the spectral dimension coincides with the topological dimension of the manifold, d. Fractal spacetimes are an example where these definitions of dimension do not (necessarily) coincide.

As for the purpose of this thesis it is the flow of the spectral dimension that is of interest, an alternative definition where one omits the limit is considered

$$D_s \equiv -2\frac{d\ln P_r(\sigma)}{d\ln\sigma}. \tag{3.19}$$

See Sect. 8 for a derivation of D_s in the context of a modified differential operator and its relation to two-point functions.

4 Quantum Gravity models

sect:QG

The purpose of this section is to give a pedagogical introduction to a collection of theories/frameworks within quantum gravity. In Sect. 9 these theories will reappear in the form of examples within the formulation developed in Sect. 6 and onwards.

4.1 Causal Sets

One of the attempts to face some of the problems mentioned above above is posed in the form of causal set theory [51]. Theories within this framework are based upon the path-integral approach to quantum field theory. Loosely said, the path-integral is a sum over all the histories within a theory and can be used as a quantization procedure. Some of the necessary ingredients are a history-space and a quantum measure for each collection of histories. For example, the amplitude to go from a state defined by a metric and matter field, g_1, ϕ_1 at time t_1 to a state at time t_2 with metric and matter field g_2, ϕ_2 is defined as [52]

$$\langle g_2, \phi_2, t_2 | g_1, \phi_1, t_1\rangle = \int D[g]D[\phi]e^{iS[g,\phi]}, \tag{4.1}$$

where S is the action, $D[g]$, $D[\phi]$ a measure on the history-space of all metrics and matter fields respectively. It is then apparent that the integral includes all field and metric configurations obeying the desired boundary conditions.

The reason this quantization procedure is often favored within quantum gravity can be granted to the fact that other quantization procedures bring technical and conceptual difficulties. Attempting to directly quantize operators renders the physical interpretation of the theory non-trivial as a consequence of the complicated structure of the Einstein equations. Canonical quantization yields the problems mentioned above; splitting spacetime into spatial and a temporal dimensions contradicts the fundamental principles of relativity. Nevertheless, the path-integral approach has its own drawbacks, some of which can be avoided by treating spacetime as a discrete set rather than a continuous manifold. In the discrete setting the path-integral becomes a sum with a natural short-distance cut-off at the Planck-scale. It is this discrete cut-off that allows one to handle the difficulties arising from the continuous procedure.

There are numerous discrete approaches under construction at this moment, one of which is causal set theory. In causal set theory one assumes that a continuous manifold has an underlying discrete structure, used to determine the history-spaces of a theory. As the name suggests, the structure of these discrete sets is imposed by the causal ordering of spacetime points. Given such a causal relation and a Lorentzian manifold, points on this manifold form a partially ordered set (poset), satisfying

$$\begin{aligned}&\text{Transitivity: } (\forall x,y,z \in C)\ (x \prec y \prec z \Rightarrow x \prec z)\\&\text{Irreflexibility: } (\forall x \in C)\ (x \not\prec x)\\&\text{Local Finiteness: } (\forall x,z \in C)\ (\mathbf{card}\ \ \{y \in C \mid x \prec y \prec z\} < \infty).\end{aligned} \tag{4.2}$$

Here $x \prec y$ indicates that x is in the causal past of y. Note that the second condition (irreflexibility) assures that there are no closed causal loops (the manifold is referred to as weakly causal). The discreteness of the set is assured by the condition of local finiteness where **card** C indicates the cardinality[4] of the set C. In the causal set context this demand enforces that there is a finite number of points between any two points. As a direct consequence, a causal set can only count a finite number of elements.

As mentioned before, the classical (low energy/large distance) limit of any quantum gravity theory should yield general relativity. To assure this, the (in general shared) view in causal set theory is that some of the considered histories have to be reasonably well approximated by Lorentzian manifolds. To make this statement more precise, the principles of embedding need to be invoked. For a causal set, C, to be embedded into a spacetime, (M, g), the elements of C have to be identified with points in (M, g) and the order linking these elements is imposed by the causal order of the spacetime. Up till here no discreteness scale has been introduced yet, which makes it impossible to develop an adequate procedure for "measuring" volumes. Consequently there is no natural framework to determine if the density of elements is such that they contain enough causal relations to be correctly embedded into a given manifold. To resolve this problem, one sprinkles elements into a region with a given volume. Sprinkling a manifold entails the use of a Poisson distribution to randomly select a number of points on the manifold. The Poisson probability distribution is given by

$$P(n) = \frac{(\rho V)^n\, e^{-\rho V}}{n!}, \tag{4.3}$$

where n is the number of points, V the volume of a certain region and ρ the sprinkling density of the Planckian order. Once ρ and n are set, the only input for the Poisson process is the volume V. If there is a high probability that the causal set could have been established from sprinkling the manifold, then the manifold approximates the causal set. The definition of a high probability is case sensitive in this context. Note that the definition above naturally implies that the number of elements sprinkled into a given region correspond to the volume of that region. It is then said that the causal set obeys a faithful embedding into the manifold.

It is important to realize that not every causal set can be properly embedded into a manifold. Even more alarming, a causal set that has been faithfully embedded into a certain region of Minkowski space might no longer satisfy the rules of faithful embedding once some of the causal relations between points have been changed. An equivalent statement would be that small fluctuations within the theory change the physical meaning of certain properties. To remove the importance of these fluctuations, one may invoke the methodology of coarse-graining. In essence, coarse-graining a causal set C entails the removal of some points, yielding a new causal set C' with lower density ρ'.

At this point, one might wonder what the benefits of causal set theory are. The manner in which it distinguishes itself from, for example, lattice based theories can be

[4]Cardinality is a measure for the number of elements/points contained in a set

[4]The theory might even be rendered unphysical if it no longer satisfies the classic limit.

captured within the occurrence of local Lorentz invariance. In the discussion above, a lot of attention was granted to defining a causal set in such a way that (the sprinklinf of) a manifold can be thought of as an approximation to said causal set. This suggests that if one considers Minkowski spacetime, the discrete theory assigned to its microscopic structure should be such that it does not impose violation of Lorentz invariance upon the continuous manifold. In other words, the underlying discrete theory is not permitted to invoke a preferred reference Lorentz frame. It is not hard to imagine that a lattice based theory would do exactly this, as its particular structure violates rotational invariance. In the case of causal sets, however, the elements/points have been distributed randomly, leaving the approximating Minkowskian manifold without a preferred frame.

4.2 Spectral Actions

A frequently used approach to various calculations involving manifolds and their geometries comes from the principle of spectral actions [53][54]. In this approach, the geometry of a Manifold M is described through a spectral triple consisting of an involutive algebra $\mathcal{A}$, a Hilbert space $\mathcal{H}$ and an unbounded, selfadjoint, Dirac operator D living on $\mathcal{H}$. The inverse of the Dirac operator D can be used to construct the line element[5] ds and an involutive algebra ($*$-algebra) is an algebra A with a conjugate linear map $* : A \mapsto A$ such that $(ab)^* = b^* a^*$ and $(a^*)^* = a$.

For a Riemannian compact spin manifold, the spectral triple is given by the $\mathcal{A} = C^\infty(M)$ of continuous, infinitely differentiable functions on M, a spin-manifold $\mathcal{H} = L^2(M, X)$ of L^2-spinors and D is the Dirac operator of the Levi-Cevita spin connection. Intuitively, a spin-manifold allows for the definition of spinor bundles which in their turn associate a spin representation to every point on M of which the elements are spinors. For a mathematically precise definition of spin geometries see chapter 4 of [55]. The points on the manifold, M, are characters of $\mathcal{A}$ (hence the trace over the representation φ of the algebra $\mathcal{A}$) which can be recognized as homomorphisms $\rho : \mathcal{A} \to \mathbb{C}$.

To define a notion of distance, the metric needs to be defined. For a Riemannian manifold, the line-element squared is expanded in the local coordinates to find the standard form

$$ds^2 = g_{\mu\nu} dx^\mu dx^\nu, \tag{4.4}$$

such that the distance between two points (x, y) is given by

$$d(x, y) = \text{Inf} \int_\gamma ds, \tag{4.5}$$

that is, the length of the shortest path between x and y. In the language of commutative geometry the distance between two points is given by

$$d(x, y) = \text{Sup}\{|f(x) - f(y)|; f \in \mathcal{A}, \| [D, f] \| \leq 1\}. \tag{4.6}$$

One of the benefits of the spectral triple approach, is that the physical action only depends on the spectrum $\Sigma \subset \mathbb{R}$ of the Dirac operator D. As an example, one can study the standard model [54, 56], also see [57, 58, 55] for reviews.

Let S denote the action of the standard model and gravity (i.e. including the coupling between gravity and matter), then there are certain symmetries that need to be taken into account. The total action has to be invariant under the group of diffeomorphisms of a particular manifold M, denoted by $\text{Diff}(M)$, and under the group $\mathcal{G}$ of gauge

[5]For a Riemannian manifold, $D^2 \propto \nabla^2$, the d-dimensional Laplacian

transformations working on the matter-part of the action. Letting $\mathcal{G}$ work on M, one obtains a mapping from M to a smaller gauge group G which can be readily identified as $G = SU(3) \times SU(2) \times U(1)$, the group describing the Standard Model. To find the full symmetry group of S, it is necessary to define the concept of (inner) automorphisms $\mathrm{Aut}(\mathcal{A})$. An automorphism can be seen as a symmetry of an object that maps the object to itself without altering its structure. In that sense the automorphism of an object is an isomorphism with respect to the object itself. A diffeomorphism can then be seen as an automorphism $a \in \mathrm{Aut}(\mathcal{A})$ of the coordinate algebra. In fact, for the standard model it is the inner automorphism of $\mathcal{A}$ that corresponds to internal symmetries while the outer automorphism (the quotient $\mathrm{Aut}(\mathcal{A})/\mathrm{Inn}(\mathcal{A})$) correspond to diffeomorphisms. With this in mind, the full group of symmetries $\mathcal{V}$ is given by the outer semidirect product between $\mathcal{G}$ and $\mathrm{Diff}(M)$

$$\mathcal{V} = \mathcal{G} \rtimes \mathrm{Diff}(M). \tag{4.7}$$

Where the outer semidirect product can be obtained from the direct product, by considering a group A and two subgroups A_1, A_2 that satisfy

$$\begin{aligned} &A_1 \text{ and } A_2 \text{ are normal in } A, \\ &A_1 \cap A_2 = 1, \\ &A_1 A_2 = A. \end{aligned} \tag{4.8}$$

Then A is isomorphic to the direct product $A_1 \times A_2$. The semi-direct product is constructed by taking A_2 such that it is not normal in A, consequently elements from A_1 and A_2 do not necessarily commute (if they do, then the semi-direct product becomes a direct product). A second demand on semidirect products is the existence of a homomorphism from A_2 to the group of automorphisms of A_1

$$\phi : A_2 \to \mathrm{Aut}(A_1). \tag{4.9}$$

Assuming the demands above are satisfied, one can write

$$A = A_1 \rtimes A_2. \tag{4.10}$$

The question is now whether there is a space that directly obeys the symmetry group $\mathcal{V}$. As it turns out, there is no such commutative space but there are almost-commutative spaces that satisfy this demand.

For a given symmetry group, determining the algebra $\mathcal{A}$ comes down to finding an algebra for which the automorphisms on $\mathcal{H}$ are such that $\mathrm{Aut}(\mathcal{A}) = \mathcal{V}$. In other words, the algebra has to respect the (total) symmetry group of the theory. For the standard model $\mathcal{A}$ is found to be

$$\mathcal{A} = C^\infty(M) \otimes \mathcal{A}_F, \tag{4.11}$$

where $\mathcal{A}_F$ is a finite dimensional algebra. The Hilbert space and Dirac operator belonging to this algebra can be found by exploiting the (tensor product) structure of $\mathcal{A}$

$$\mathcal{H} = L^2(M, X) \otimes \mathcal{H}_F \quad \text{and} \quad \mathcal{D} = \not{\partial}_M \otimes 1 + \gamma_5 \otimes D_F, \tag{4.12}$$

where $\mathcal{H}_F$ and D_F are the Hilbert space and Dirac operator on the finite space. Similarly, $L^2(M, X)$ and $\not{\partial}_M$ refer to the corresponding quantities of the manifold M.

Leaving out neutrino mixing, the algebra $\mathcal{A}_F$ describes the underlying geometrical definition of the standard model. It turns out that the (inner) fluctuations of the metric will give rise to the gauge bosons, and thus one replaces the Dirac operator D by a fluctuating Dirac operator that will be denoted as $\tilde{D}^2 = -(\nabla^2 - E)$, where E is an endomorphism capturing the particle content of the theory. This new expression $\tilde{D}$ is a result from the fact that the connection ∇ is not unique on the vector bundle. The fermionic part of the action can be written as $S_F(\psi, A) = \langle \psi, \tilde{\mathcal{D}}\psi \rangle$ where ψ denotes the fermion field. For the purpose of this thesis only the bosonic (scalar) action is required, and thus the fermionic action will not be discussed further (see Sect. 9.3). The bosonic action is given by

$$S_B(\tilde{D}) = \mathrm{Tr}(\chi(\tilde{D}^2/\Lambda^2)), \tag{4.13}$$

where Λ is the typical scale of the theory and χ a positive, even function from $\mathbb{R}$ to $\mathbb{R}$ such that the operator $\chi(\tilde{D}^2/\Lambda^2)$ decays at $\pm\infty$. The bosonic action has to respect diffeomorphism invariance (the fermionic as well for that matter). Only the eigenvalues of the Dirac operator satisfy this condition à priori, and thus it seems only natural that the bosonic action yields functions of those eigenvalues that are below the characteristic scale Λ.

4.3 Kaluza-Klein theories

In the first half of the 20$^{\text{th}}$ century, Kaluza noticed that a five-dimensional spacetime can be constructed by a four-dimensional metric coupled to a scalar field and the electromagnetic vector potential [59]. Using this setup, Kaluza was able to derive the four-dimensional field equations, describing gravity, electromagnetism and a scalar field. There was, however, a drawback to this theory. Kaluza had to enforce the so-called *cylinder condition*, which essentially states that the four-dimensional metric has to be independent of the extra fifth dimension. As this imposed a rather extreme symmetry, the physics community started looking for an alternative description of this fifth dimension. It was Klein that justified Kaluza's ansatz by suggesting to make the fifth dimension periodic and very small (e.g. he introduced the concept of *compactification*).

In Kaluza-Klein theory, the fifth dimension is taken to be a circle with a very small circumference (radius) such that the metric essentially does not depend on the fifth coordinate x^5. More concretely, the five-dimensional manifold can by written as

$$\mathcal{M}^{(5)} = \mathcal{M}^{(4)} \times U(1). \tag{4.14}$$

As the fifth dimension is compact (i.e. it is the circle group), this approach was named compactification and is nowadays frequently applied in string theory. Using the fact that the metric is now periodic in the fifth dimension, the metric can be decomposed into its Fourier modes as

$$\tilde{g}_{AB}(x, x^5) = \sum_{-\infty}^{\infty} g^{(n)}_{AB}(x) e^{inx^5/R}, \qquad x^5 \in [0, 2\pi R], \tag{4.15}$$

where, the indices A, B run from 0 to 4, n denotes the Fourier mode and R is the compactification radius. Any fields living on this five-dimensional manifold $\mathcal{M}^5$ obey a Fourier decomposition in the circle coordinate similar to the metric field.

$$\phi(x, x_5) = \sum_{n=-\infty}^{+\infty} \phi_n(x)\, e^{i\frac{n}{R}x_5}\,, \qquad x_5 \in [0, 2\pi R]\,. \tag{4.16}$$

The Fourier coefficients $\phi_n(x)$ depend on the coordinates on $\mathbb{R}^4$ and are called Kaluza-Klein modes. For a real scalar field ϕ they obey the reality condition $\phi_{-n} = \phi_n^*$. Substituting this mode expansion into the action of a free scalar field in five dimensions yields

$$\int d^5x\,\tfrac{1}{2}\,\left[(\partial_\mu\phi)^2-(\partial_5\phi)^2\right]=2\pi R\int d^4x\sum_{n=-\infty}^{+\infty}\tfrac{1}{2}\left[|\partial_\mu\phi_n|^2-\frac{n^2}{R^2}|\phi_n|^2\right]. \tag{4.17}$$

In Sect. 9.2 the model above will be examined more closely, yielding the two-point function and properties derived thereof.

5 The Unruh effect

sect:unruh

The notion of an observer, accelerating with respect to the Minkowski vacuum, observing a thermal spectrum of particles is known as the *Unruh effect*. The key to understanding this effect is the difference between the definitions of positive frequency modes and thus the interpretation of particles. Here we will derive the Unruh effect for a massless and massive scalar field in $1+1$-dimensions [41]. The generalization to $3+1$ dimensions can be found in Sect. 5.2.

The derivation starts by considering an inertial observer in Minkowski spacetime and parameterizing the observer's trajectory in terms of its proper time. Likewise, the trajectory of an observer accelerating through Minkowski spacetime (i.e. an inertial observer in *Rindler* spacetime) will be parametrized in terms of the accelerated observer's proper time. Of course, strictly speaking, Rindler spacetime is simply (a patch of) Minkowski spacetime written in a different (accelerated) coordinate frame. Hence, Rindler spacetime is flat. It is then due to Einstein's equivalence principle that the accelerated frame exhibits traits similar to as if it was positioned in a gravitational field (e.g. the existence of an horizon becomes apparent). Once the parameterizations have been established, one can apply second quantization and find the scalar fields expanded in Minkowski and Rindler modes. As the two trajectories are related, the resulting (quantized) fields describe the same scalar field and are thus the same. The difference between the two descriptions lies in the definition of creation/annihilation operators and thus their vacua. By expressing the creation/annihilation operators belonging to one description in terms of the other, the differences concerning particle interpretation become clear. This is what is known as a *Bogolyubov* transformation.

5.1 1+1 dimensions

sect:unruh1

In two dimensions the Minkowski metric is given by

$$ds^2=dt^2-dx^2. \tag{5.1}$$

eq:metric2d

For an observer following a trajectory $x^\alpha(\tau)$, where τ is the proper time used to parametrize this trajectory, the 2-velocity is given by

$$\dot{x}^\alpha(\tau)=\frac{dx^\alpha(\tau)}{d\tau}=\big(\dot{t}(\tau),\dot{x}(\tau)\big) \tag{5.2}$$

and normalised such that

$$\eta_{\alpha\beta}\dot{x}^\alpha\dot{x}^\beta=1. \tag{5.3}$$

eq:velocity

The 2-acceleration is then $a^\alpha=\ddot{x}^\alpha(\tau)$ and satisfies

$$\eta_{\alpha\beta}a^\alpha\dot{x}^\beta=0. \tag{5.4}$$

eq:velacc

In the inertial frame of the observer undergoing constant acceleration, we have $\dot{x}(\tau) = 0$ and thus $\dot{x}^\alpha(\tau) = (1, 0)$. It can then be deduced from (5.4) that $a^\alpha(\tau) = (0, a)$ with a a constant. In any inertial frame we find then

$$\eta_{\alpha\beta} a^\alpha(\tau) a^\beta(\tau) = -a^2. \tag{5.5}$$

To determine the trajectory of an accelerated observer we first switch to lightcone coordinates, defined in the inertial frame as

$$u \equiv t - x, \quad v \equiv t + x \tag{5.6}$$

eq:lightcone

which transforms (5.1) into

$$ds^2 = du dv = g_{\alpha\beta} d\tilde{x}^\alpha d\tilde{x}^\beta \tag{5.7}$$

where $\tilde{x}^0 \equiv u$, $\tilde{x}^1 \equiv v$ and the Minkowski metric in lightcone coordinates is

$$g_{\alpha\beta} = \begin{pmatrix} 0 & 1/2 \\ 1/2 & 0 \end{pmatrix}. \tag{5.8}$$

eq:metriclight

The trajectory can then be expressed in lightcone coordinates as

$$x^\alpha(\tau) = (u(\tau), v(\tau)), \tag{5.9}$$

which, together with $g_{\alpha\beta}$, (5.3) and (5.4), yields

$$\begin{aligned} \dot{u}(\tau)\dot{v}(\tau) &= 1, \\ \ddot{u}(\tau)\ddot{v}(\tau) &= -a^2. \end{aligned} \tag{5.10}$$

eq:relationuv

The first of these two equations gives $\dot{u} = \frac{1}{\dot{v}}$ and thus $\ddot{u} = -\frac{\ddot{v}}{\dot{v}^2}$, such that the second equation can be used to obtain

$$\left(\frac{\ddot{v}}{\dot{v}}\right)^2 = a^2. \tag{5.11}$$

Integration of the equation above gives the following solution for $v(\tau)$

$$v(\tau) = \frac{A}{a} e^{a\tau} + B \quad \rightarrow \quad v(\tau) = \frac{1}{a} e^{a\tau}, \tag{5.12}$$

where the integration constants A, B have been put to one and zero by performing a Lorentz transformation and shifting the origin respectively. To find $u(\tau)$ we use the relation $\dot{u} = \frac{1}{\dot{v}}$

$$u(\tau) = -\frac{1}{Aa} e^{-a\tau} + C \quad \rightarrow \quad u(\tau) = -\frac{1}{a} e^{-a\tau}. \tag{5.13}$$

eq:defu

The trajectory of the inertial observer has now been fully parametrized in terms of τ.

Next we will look for the comoving frame of an accelerated observer in terms of the coordinates (ξ^0, ξ^1). The coordinate system should be defined such that at $\xi^1 = 0$ the observer is at rest and along the observer's worldline the time coordinate ξ^0 should coincide with the proper time τ. To make field quantization easier later on, we also want the metric in the comoving frame to be conformally flat, that is

$$ds^2 = \chi^2(\xi^0, \xi^1) \left[(d\xi^0)^2 - (d\xi^1)^2 \right], \tag{5.14}$$

eq:metricconfc

where $\chi(\xi^0, \xi^1)$ will be found by imposing proper conditions later on. Similar to the derivation for the inertial observer, the lightcone coordinates are defined as

$$\tilde{u} \equiv \xi^0 - \xi^1, \qquad \tilde{v} \equiv \xi^0 + \xi^1 \tag{5.15}$$

such that (5.14) becomes

$$ds^2 = \chi^2(\tilde{u}, \tilde{v}) d\tilde{u} d\tilde{v}. \tag{5.16}$$

In the comoving frame one has $\xi^0 = \tau$ and $\xi^1 = 0$, yielding for the worldline

$$\tilde{v}(\tau) = \tau, \qquad \tilde{u}(\tau) = \tau \tag{5.17}$$

and the conformal factor along this worldline

$$d\tau^2 = ds^2 = \chi^2(\tilde{u} = \tau, \tilde{v} = \tau) d\tau^2 \tag{5.18}$$

gives

$$\chi^2(\tilde{u} = \tau, \tilde{v} = \tau) = 1. \tag{5.19}$$

eq:Omega

Using that physics should be coordinate independent (e.g. diffeomorphism invariance holds), the metric can be written as

$$ds^2 = du dv = \chi^2(\tilde{u}, \tilde{v}) d\tilde{u} d\tilde{v}. \tag{5.20}$$

eq:unruhmetric

Note that there are no $d\tilde{u}^2$ and $d\tilde{v}^2$ terms appearing in the equation above, thus u and v only depend on one of the coordinates $\tilde{u}$ or $\tilde{v}$. Choosing $u = u(\tilde{u})$ and $v = v(\tilde{v})$ gives the exact form of these functions by considering

$$\frac{du(\tau)}{d\tau} = \frac{du(\tilde{u})}{d\tilde{u}} \frac{d\tilde{u}(\tau)}{d\tau}. \tag{5.21}$$

Using partial differentiation and

$$\frac{du(\tau)}{d\tau} = -au(\tau) \quad \text{and} \quad \frac{d\tilde{u}(\tau)}{d\tau} = 1, \tag{5.22}$$

yields

$$\frac{du(\tilde{u})}{d\tilde{u}} = -au, \tag{5.23}$$

and thus

$$u = Ce^{-a\tilde{u}}. \tag{5.24}$$

Similarly

$$v = De^{a\tilde{v}}. \tag{5.25}$$

Then the integration constants C and D from (5.19) become

$$\begin{aligned} 1 &= \chi^2(\tilde{u} = \tau, \tilde{v} = \tau) \\ &= \left.\frac{du}{d\tilde{u}} \frac{dv}{d\tilde{v}}\right|_{\tilde{u}=\tau, \tilde{v}=\tau} = -a^2 CD e^{-a\tau} e^{a\tau} \\ &= -a^2 CD. \end{aligned} \tag{5.26}$$

Hence

$$u = -\frac{1}{a} e^{-a\tilde{u}}, \qquad v = \frac{1}{a} e^{a\tilde{v}}. \tag{5.27}$$

eq:RindlerCoor

The line element in the accelerated frame can now be written as

$$ds^2 = e^{a(\tilde{v} - \tilde{u})} d\tilde{u} d\tilde{v} = e^{2a\xi^1} \left[(d\xi^0)^2 - (d\xi^1)^2 \right]. \tag{5.28}$$

eq:rindler2dme

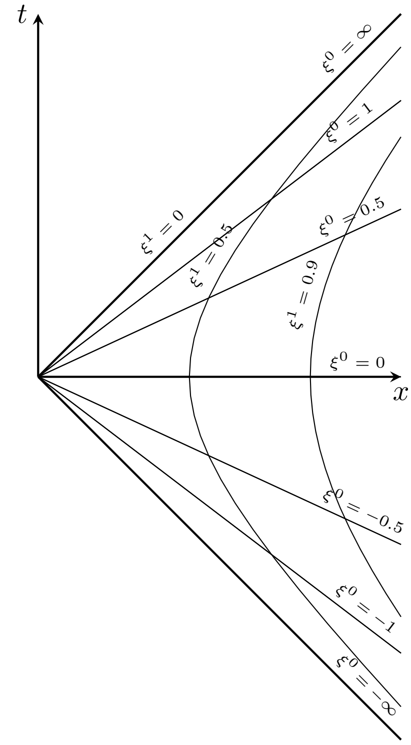

fig:Rindler

Figure 5: Minkowski spacetime in Rindler coordinates.

This is the metric on *Rindler* spacetime. Note that by expressing the inertial Minkowski coordinates (t, x) in terms of the Rindler coordinates (ξ^0, ξ^1) one obtains

$$\begin{aligned} t &= \frac{1}{2}(u+v) = \frac{1}{a}e^{a\xi^1}\sinh(a\xi^0), \\ x &= \frac{1}{2}(-u+v) = \frac{1}{a}e^{a\xi^1}\cosh(a\xi^0), \end{aligned} \tag{5.29}$$

eq:MinkInRind

where the Rindler coordinates have ranges $-\infty < \xi^0, \xi^1 < \infty$.

From figure 5 one can see that a Rindler observer, moving on a trajectory with $\xi^1 =$ const, never crosses the Killing horizons located at $\xi^0 = \pm\infty$. As a result, the observer is confined to the right Rindler wedge. Referring back to Sect. 2.2, the constant ξ^0 surfaces are Cauchy surfaces, i.e. Rindler spacetime is globally hyperbolic. It is this property that will allow the introduction of equal-time commutators needed to quantize the scalar fields in the following sections.

5.1.1 Massles scalar field

The current task at hand is to quantize a scalar field in Rindler/Minkowski spacetime. To do this we will need to define which modes register as positive/negative frequency modes in both the inertial as well as the accelerated frame. An inertial observer would define positive/negative modes with respect to the Minkowski time coordinate t, while an accelerated observer would use the time coordinate $\tau = \xi^0$. As the line elements are related by a conformal transformation, we will see that a mode registering as a positive frequency mode for an inertial observer registers in the accelerated frame as a superposition of positive and negative frequency modes.

In the case of a massless scalar field in $1+1$-dimensions the action is given by

$$S = \frac{1}{2} \int d^2x \sqrt{-g} g^{\alpha\beta} \phi_{,\alpha} \phi_{,\beta}, \tag{5.30}$$

eq:action2d

where $d^2x = dtdx$. As the inertial and accelerated frame are conformally related the Lagrangian as well as the action are left invariant under this particular change of coordinate system. That is

$$\begin{aligned} & dtdx\sqrt{-g}g^{\alpha\beta} = d\xi^0 d\xi^1 \sqrt{-g'} g'^{\alpha\beta} \\ & = d\xi^0 d\xi^1 \left(\chi^2 \sqrt{-g}\right) \left(\chi^{-2} g^{\alpha\beta}\right) = d\xi^0 d\xi^1 \sqrt{-g} g^{\alpha\beta}. \end{aligned} \tag{5.31}$$

Rewriting (5.30) in terms of (u, v) and $(\tilde{u}, \tilde{v})$ yields

$$S = 2 \int du dv \partial_u \phi \partial_v \phi = 2 \int d\tilde{u} d\tilde{v} \partial_{\tilde{u}} \phi \partial_{\tilde{v}} \phi, \tag{5.32}$$

where the factor of $4 = 2^2$ with respect to (5.30) arises from the inverse of (5.8). As we are dealing with a massless scalar field without any form of interaction, the equations of motion become $\partial_\alpha \frac{\partial L}{\partial(\partial_\alpha \phi)} = 0$ and thus

$$\partial_u \partial_v \phi = 0 \quad \text{and} \quad \partial_{\tilde{u}} \partial_{\tilde{v}} \phi = 0. \tag{5.33}$$

eq:unruh2deqm

The solutions to these equation are straightforward to compute and we write them as

$$\phi(u, v) \propto e^{-i\omega u} + e^{-i\omega v} \qquad \text{and} \qquad \phi(\tilde{u}, \tilde{v}) \propto e^{-i\Omega \tilde{u}} + e^{-i\Omega \tilde{v}}. \tag{5.34}$$

Here, the modes $\phi \propto e^{-i\omega u}$ and $\phi \propto e^{-i\Omega \tilde{u}}$ describe right moving, positive frequency modes with respect to t and τ. Likewise, the left moving parts of the solutions is given by $\phi \propto e^{-i\omega v}$ and $\phi \propto e^{-i\Omega \tilde{v}}$. Where, $\Omega \in [0, \infty]$, in what follows can be interpreted as the frequency corresponding to a specific mode in Rindler spacetime.

Now that the solutions to the equations of motion have been found, the field ϕ can be written as an operator $\hat{\phi}$. Suppressing the left moving part of the solutions, the fields have the following mode expansion

$$\begin{aligned} \hat{\phi} &= \int_0^\infty \frac{d\omega}{(2\pi)^{1/2}} \frac{1}{\sqrt{2\omega}} \left(e^{-i\omega u} \hat{a}_\omega + e^{i\omega u} \hat{a}_\omega^\dagger\right) \\ &= \int_0^\infty \frac{d\Omega}{(2\pi)^{1/2}} \frac{1}{\sqrt{2\Omega}} \left(e^{-i\Omega \tilde{u}} \hat{b}_\Omega + e^{i\Omega \tilde{u}} \hat{b}_\Omega^\dagger\right). \end{aligned} \tag{5.35}$$

eq:unruhphi

The creation and annihilation operators satisfy the bosonic commutation relations where

$$\left[\hat{a}_\omega, \hat{a}_{\omega'}^\dagger\right] = \delta(\omega - \omega'), \qquad \left[\hat{b}_\Omega, \hat{b}_{\Omega'}^\dagger\right] = \delta(\Omega - \Omega'), \tag{5.36}$$

eq:commboson

are the only non-zero commutators. To find the number of particles an observer accelerating with respect to Minkowski spacetime (Rindler observer) would observe in the Minkowski vacuum, we need to let the number operator defined in Rindler spacetime work on the Minkowski vacuum. That is

$$\left\langle \hat{N}_\Omega \right\rangle \equiv \langle 0_M | \hat{b}_\Omega^\dagger \hat{b}_\Omega | 0_M \rangle, \tag{5.37}$$

eq:numberop

where $|0_M\rangle$ denotes the Minkowski vacuum and $|0_R\rangle$ the Rindler vacuum. The vacua are defined such that

$$\hat{a}_\omega |0_M\rangle = 0, \qquad \hat{b}_\Omega |0_R\rangle = 0. \tag{5.38}$$

To evaluate the number operator, the creation/annihilation operators $\hat{b}_\Omega^\dagger$ and $\hat{b}_\Omega$ need to be expressed in terms of $\hat{a}_\omega^\dagger$ and $\hat{a}_\omega$. By doing so it will become apparent that the Minkowski and Rindler observer do not share the same vacuum.

The relation between the creation/annihilation can be found through the use of Bogolyubov transformations of the form[6]

$$\hat{b}_\Omega = \int_0^\infty d\omega \left[\alpha_{\Omega\omega}\hat{a}_\omega - \beta_{\Omega\omega}\hat{a}_\omega^\dagger\right]. \tag{5.39}$$

eq:Bogolyubov

eq:commboson

From the commutation relations (5.36) the normalization of the Bogolyubov coefficients becomes

$$\left[\hat{b}_\Omega, \hat{b}_{\Omega'}^\dagger\right] = \int_0^\infty d\omega (\alpha_{\Omega\omega}\alpha_{\Omega'\omega}^* - \beta_{\Omega\omega}\beta_{\Omega'\omega}^*) = \delta(\Omega - \Omega'). \tag{5.40}$$

eq:Bogolyubov eq:unruhphi

By substitution of (5.39) into (5.35) the coefficient of $\hat{a}_\omega$ is computed as

$$\frac{1}{\sqrt{\omega}} e^{-i\omega u} = \int_0^\infty \frac{d\Omega'}{\sqrt{\Omega'}} \left(\alpha_{\Omega'\omega} e^{-i\Omega'\tilde{u}} - \beta_{\Omega'\omega}^* e^{i\Omega'\tilde{u}}\right). \tag{5.41}$$

Multiplying through with $e^{\pm i\Omega\tilde{u}}$, where $\Omega > 0$, and integrating over $\tilde{u}$ results in

$$\begin{aligned}
\int_{-\infty}^\infty d\tilde{u} \frac{1}{\sqrt{\omega}} e^{-i\omega u \pm i\Omega\tilde{u}} &= \int_{-\infty}^\infty d\tilde{u} \int_0^\infty \frac{d\Omega'}{\sqrt{\Omega'}} \left(\alpha_{\Omega'\omega} e^{-i\Omega'\tilde{u} \pm i\Omega\tilde{u}} - \beta_{\Omega'\omega}^* e^{i\Omega'\tilde{u} \pm i\Omega\tilde{u}}\right) \\
&= \int_{-\infty}^\infty d\tilde{u} \int_0^\infty \frac{d\Omega'}{\sqrt{\Omega'}} \left(\alpha_{\Omega'\omega} e^{i(\pm\Omega - \Omega')\tilde{u}} - \beta_{\Omega'\omega}^* e^{i(\pm\Omega + \Omega')\tilde{u}}\right) \\
&= \int_0^\infty \frac{d\Omega'}{\sqrt{\Omega'}} \left(\alpha_{\Omega'\omega} 2\pi\delta(\pm\Omega - \Omega') - \beta_{\Omega'\omega}^* 2\pi\delta(\pm\Omega + \Omega')\right)
\end{aligned} \tag{5.42}$$

Note that the integral over Ω' runs from 0 to ∞ and thus, for one particular choice of Ω, can only be non-zero for either $\alpha_{\Omega'\omega}$ or $\beta_{\Omega'\omega}^*$ but not both. Choosing the $+\Omega$ solution one finds

$$\int_{-\infty}^\infty d\tilde{u} \frac{1}{\sqrt{\omega}} e^{-i\omega u + i\Omega\tilde{u}} = \frac{2\pi}{\sqrt{\Omega}} \alpha_{\Omega\omega}, \tag{5.43}$$

which can be solved for $\alpha_{\Omega\omega}$

$$\alpha_{\Omega\omega} = \frac{1}{2\pi}\sqrt{\frac{\Omega}{\omega}} \int_{-\infty}^\infty d\tilde{u} e^{-i\omega u + i\Omega\tilde{u}}. \tag{5.44}$$

[6] As the Rindler coordinates only cover the $x > |t|$ quarter of Minkowski spacetime, this mapping is surjective (onto) but not injective (one-to-one). That is, the inverse mapping is not defined.

Using that $\frac{\partial \tilde{u}}{\partial u} = \frac{1}{au}$ and the logarithm is only defined between 0 and $+\infty$, this integral can be carried out analytically

$$\begin{aligned} \alpha_{\Omega\omega} &= \frac{1}{2\pi}\sqrt{\frac{\Omega}{\omega}} \int_0^\infty du \frac{1}{au} e^{-i\omega u} e^{\frac{i\Omega}{a}\ln(au)} \\ &= \frac{1}{2\pi}\sqrt{\frac{\Omega}{\omega}} \int_{-\infty}^0 du (-au)^{\frac{-i\Omega}{a}-1} e^{i\omega u} \\ &= \frac{1}{2\pi a}\sqrt{\frac{\Omega}{\omega}} e^{\frac{\pi\Omega}{2a}} \left(\frac{\omega}{a}\right)^{\frac{i\Omega}{a}} \Gamma\left(-\frac{i\Omega}{a}\right). \end{aligned} \tag{5.45}$$

eq:alpha

The computation of $\beta^*_{\Omega'\omega}$ follows a similar reasoning and yields

$$\beta^*_{\Omega\omega} = -\frac{1}{2\pi a}\sqrt{\frac{\Omega}{\omega}} e^{-\frac{\pi\Omega}{2a}} \left(\frac{\omega}{a}\right)^{\frac{i\Omega}{a}} \Gamma\left(-\frac{i\Omega}{a}\right). \tag{5.46}$$

Note that $\alpha_{\Omega\omega}$ and $\beta_{\Omega\omega}$ satisfy the relation

$$|\alpha_{\Omega\omega}|^2 = e^{\frac{2\pi\Omega}{a}} |\beta_{\Omega\omega}|^2 . \tag{5.47}$$

eq:alphabeta

The last step is to compute the number of particles detected by an accelerated observer, using the formula (eq:numberop 5.37)

$$\begin{aligned} \left\langle \hat{N}_\Omega \right\rangle &= \int d\omega \beta_{\omega\Omega} \beta^*_{\omega\Omega'} \\ &= \frac{\sqrt{\Omega\Omega'}}{4\pi^2 a^2} e^{-\frac{\pi}{2a}(\Omega+\Omega')} \Gamma\left(-\frac{i\Omega}{a}\right) \Gamma\left(\frac{i\Omega'}{a}\right) \int \frac{d\omega}{\omega} \left(\frac{\omega}{a}\right)^{\frac{i}{a}(\Omega-\Omega')} \\ &= \frac{\sqrt{\Omega\Omega'}}{4\pi^2 a^2} e^{-\frac{\pi}{2a}(\Omega+\Omega')} \Gamma\left(-\frac{i\Omega}{a}\right) \Gamma\left(\frac{i\Omega'}{a}\right) \int \frac{d\omega}{\omega} e^{\frac{i}{a}(\Omega-\Omega')\ln\left(\frac{\omega}{a}\right)}. \end{aligned} \tag{5.48}$$

The integral above can be easily solved by making a change of integration variables $y = \ln\left(\frac{\omega}{a}\right)$

$$\begin{aligned} \left\langle \hat{N}_\Omega \right\rangle &= \frac{\sqrt{\Omega\Omega'}}{4\pi^2 a} e^{-\frac{\pi}{2a}(\Omega+\Omega')} \Gamma\left(-\frac{i\Omega}{a}\right) \Gamma\left(\frac{i\Omega'}{a}\right) \int dy e^{\frac{i}{a}(\Omega-\Omega')y} \\ &= \frac{\sqrt{\Omega\Omega'}}{2\pi a} e^{-\frac{\pi}{2a}(\Omega+\Omega')} \Gamma\left(-\frac{i\Omega}{a}\right) \Gamma\left(\frac{i\Omega'}{a}\right) \delta(\Omega-\Omega'), \end{aligned} \tag{5.49}$$

selecting the $\Omega' = \Omega$ then gives

$$\begin{aligned} \left\langle \hat{N}_\Omega \right\rangle &= \frac{\Omega}{2\pi a} e^{-\frac{\pi\Omega}{a}} \left|\Gamma\left(-\frac{i\Omega}{a}\right)\right|^2 \delta(0) \\ &= \frac{\Omega}{2\pi a} e^{-\frac{\pi\Omega}{a}} \frac{a\pi}{\Omega \sinh\left(\frac{\pi\Omega}{a}\right)} \delta(0) \\ &= \frac{e^{-\frac{\pi}{a}\Omega}}{2\sinh\left(\frac{\pi\Omega}{a}\right)} \delta(0) \\ &= \left(e^{\frac{2\pi\Omega}{a}} - 1\right)^{-1} \delta(0). \end{aligned} \tag{5.50}$$

Here it was used that $\Gamma(ix) = \frac{1}{ix}\Gamma(1+ix)$ and $|\Gamma(1+ix)|^2 = x\frac{\pi}{\sinh(\pi x)}$. The divergent $\delta(0)$ term is a consequence of the infinite volume of space and can be divided out, yielding the mean number-density

$$\langle \hat{n} \rangle = \frac{\left\langle \hat{N}_\Omega \right\rangle}{V} = \left(e^{\frac{2\pi\Omega}{a}} - 1\right)^{-1} \tag{5.51}$$

From the calculation above, it is apparent that the observed radiation spectrum follows the Bose-Einstein distribution with temperature $T = \frac{a}{2\pi}$.

5.1.2 Massive scalar field

The procedure above can be applied to a massive scalar field as well. In this case the action for an inertial observer becomes

$$S_t = \frac{1}{2}\int dtdx \left[(\phi_{,t})^2 - (\phi_{,x})^2 - m^2\phi^2\right] \tag{5.52}$$

and for an accelerated observer

$$S_\tau = \frac{1}{2}\int d\xi^0 d\xi^1 \left[\left(\phi_{,\xi^0}\right)^2 - \left(\phi_{,\xi^1}\right)^2 - e^{2a\xi^1} m^2\phi^2\right]. \tag{5.53}$$

Note that due to the mass term the actions are no longer conformally related. The equation of motion for the inertial observer becomes

$$\left(\partial_t^2 - \partial_x^2 + m^2\right)\phi(x,t) = 0 \tag{5.54}$$

which has as solution

$$\phi(x,t) \propto e^{-ip^\mu x_\mu} \tag{5.55}$$

where $x^\mu = (t, x)$, $p^\mu = (p_0, p_1)$, $p_0 = \sqrt{p_1^2 + m^2}$ and we only wrote the right-moving part of the solution. Quantizing this solution yields

$$\hat{\phi}(t,x) = \int \frac{dp_1}{(2\pi)^{1/2}} \frac{1}{\sqrt{2p_0}} \left(\hat{a}_{p_0} e^{-ip^\mu x_\mu} + \hat{a}_{p_0}^\dagger e^{ip^\mu x_\mu}\right). \tag{5.56}$$

For the accelerated observer we need to solve

$$\left(\partial_{\xi^0}^2 - \partial_{\xi^1}^2 + e^{2a\xi^1} m^2\right)\phi(\xi^0, \xi^1) = 0, \tag{5.57}$$

eq:unruh2dmass

where the factor $e^{2a\xi^1}$ comes from the metric (5.28). Following [49] we can apply separation of variables and write $\phi(\xi^0,\xi^1) = f_{q_0}(\xi^1)e^{-iq_0\xi^0}$, with q_0 a positive constant, such that the equation above becomes

$$\left(-q_0^2 - \partial_{\xi^1}^2 + e^{2a\xi^1} m^2\right) f_{q_0}(\xi^1) = 0. \tag{5.58}$$

eq:mass2dKG

For $\xi^1 \to -\infty$ the solutions $f_{q_0}(\xi^1)$ will start to rapidly oscillate as $e^{\pm iq_0\xi^1}$ and for $\xi^1 \to +\infty$ they will approach zero. In the first case we can approximate $f_{q_0}(\xi^1)$ for $\xi^1 \to -\infty$ as

$$f_{q_0}(\xi^1) \approx \frac{1}{\sqrt{2\pi}} \left(e^{i(q_0\xi^1 + \epsilon(q_0))} + e^{-i(q_0\xi^1+\epsilon(q_0))}\right), \tag{5.59}$$

with $\epsilon(q_0)$ a real constant. This leads to the normalization condition

$$\int\limits_{-\infty}^{\infty} d\xi^1 f_{q_0}^*(\xi^1) f_{q_0'}(\xi^1) = \delta(q_0 - q_0'). \tag{5.60}$$

Together with (eq:unruh2dmasseom 5.57) the equation above yields the solutions

$$f_{q_0}(\xi^1) = \sqrt{\frac{2q_0 \sinh\left(\frac{\pi q_0}{a}\right)}{\pi^2 a}} K_{\frac{iq_0}{a}}\left(\frac{m}{a} e^{a\xi^1}\right), \tag{5.61}$$

eq:unruh2dmass

where $K_{\frac{iq_0}{a}}\left(\frac{m}{a} e^{a\xi^1}\right)$ is the modified Bessel function. Thus

$$\phi(\xi^0, \xi^1) = \sqrt{\frac{2q_0 \sinh\left(\frac{\pi q_0}{a}\right)}{\pi^2 a}} K_{\frac{iq_0}{a}}\left(\frac{m}{a} e^{a\xi^1}\right) e^{-iq_0\xi^0}. \tag{5.62}$$

Quantisation of $\phi(\xi^0, \xi^1)$ gives

$$\hat{\phi}(\xi^0, \xi^1) = \int_0^\infty \frac{dq_0}{(2\pi)^{1/2}} \frac{1}{\sqrt{2q_0}} \left(\hat{b}_{q_0} f_{q_0} e^{-iq_0\xi^0} + \hat{b}^\dagger_{q_0} f^*_{q_0} e^{iq_0\xi^0}\right). \tag{5.63}$$

The next step is to write both $\hat{\phi}(\xi^0, \xi^1)$ and $\hat{\phi}(t, x)$ in terms of the lightcone coordinates. Noting that the Bogoliubov coefficients are independent of the coordinates, one can choose a convenient point in spacetime to perform the evaluation of the fields. To simplify the integrals observe that on the future Killing horizon, where $t = x$ and $|t| > 0$ one has $t = \frac{u+v}{2} = \frac{v}{2}$ and thus

$$\hat{\phi}(t, x) \overset{t=x}{=\!=} \int \frac{dp_1}{(2\pi)^{1/2}} \frac{1}{\sqrt{2p_0}} \left(\hat{a}_{p_0} e^{-i(-p_0+p_1)\frac{v}{2}} + \hat{a}^\dagger_{p_0} e^{i(-p_0+p_1)\frac{v}{2}}\right). \tag{5.64}$$

Also, for $\xi^1 \to -\infty$ the modified Bessel function can be approximated such that

$$\begin{aligned} f_{q_0}(\xi^1) &= \sqrt{\frac{2q_0 \sinh\left(\frac{\pi q_0}{a}\right)}{\pi^2 a}} K_{\frac{iq_0}{a}}\left(\frac{m}{a} e^{a\xi^1}\right) \\ &= \sqrt{\frac{2q_0 \sinh\left(\frac{\pi q_0}{a}\right)}{\pi^2 a}} \frac{i\pi}{2\sinh\left(\frac{\pi q_0}{a}\right)} \left[\frac{\left(\frac{m}{2a} e^{a\xi^1}\right)^{\frac{iq_0}{a}}}{\Gamma\left(1 + \frac{iq_0}{a}\right)} - \frac{\left(\frac{m}{2a} e^{a\xi^1}\right)^{\frac{-iq_0}{a}}}{\Gamma\left(1 - \frac{iq_0}{a}\right)}\right] \\ &= \frac{i\sqrt{q_0}}{\sqrt{2a\sinh\left(\frac{\pi q_0}{a}\right)}} \left[\frac{\left(\frac{m}{2a}\right)^{\frac{iq_0}{a}} e^{iq_0\xi^1}}{\Gamma\left(1 + \frac{iq_0}{a}\right)} - \frac{\left(\frac{m}{2a}\right)^{\frac{-iq_0}{a}} e^{-iq_0\xi^1}}{\Gamma\left(1 - \frac{iq_0}{a}\right)}\right]. \end{aligned} \tag{5.65}$$

Leaving out the expression $\hat{b}^\dagger_{q_0}$ to lighten the derivation, the expression for the field in terms of Rindler coordinates becomes

$$\begin{aligned} \hat{\phi}(\xi^0, \xi^1) &= \int \frac{dq_0}{(2\pi)^{1/2}} \frac{1}{\sqrt{2q_0}} \frac{i\sqrt{q_0}}{\sqrt{2a\sinh\left(\frac{\pi q_0}{a}\right)}} \left[\frac{\left(\frac{m}{2a}\right)^{\frac{iq_0}{a}} e^{iq_0\xi^1}}{\Gamma\left(1 + \frac{iq_0}{a}\right)} - \frac{\left(\frac{m}{2a}\right)^{\frac{-iq_0}{a}} e^{-iq_0\xi^1}}{\Gamma\left(1 - \frac{iq_0}{a}\right)}\right] \hat{b}_{q_0} e^{-iq_0\xi^0} \\ &= \int \frac{dq_0}{(4\pi)^{1/2}} \frac{i}{\sqrt{2a\sinh\left(\frac{\pi q_0}{a}\right)}} \left[\frac{\left(\frac{m}{2a}\right)^{\frac{iq_0}{a}} e^{-iq_0\tilde{u}}}{\Gamma\left(1 + \frac{iq_0}{a}\right)} - \frac{\left(\frac{m}{2a}\right)^{\frac{-iq_0}{a}} e^{-iq_0\tilde{v}}}{\Gamma\left(1 - \frac{iq_0}{a}\right)}\right] \hat{b}_{q_0}. \end{aligned} \tag{5.66}$$

However, for $\xi^1 \to -\infty$ we have $-\tilde{u} = -(\xi^0 - \xi^1) \to -\infty$, and thus $e^{-iq_0\tilde{u}} \to 0$, leaving

$$\hat{\phi}(\xi^0, \xi^1) = -\int \frac{dq_0}{(4\pi)^{1/2}} \frac{i}{\sqrt{2a\sinh\left(\frac{\pi q_0}{a}\right)}} \frac{\left(\frac{m}{2a}\right)^{\frac{-iq_0}{a}}}{\Gamma\left(1 - \frac{iq_0}{a}\right)} e^{-iq_0\tilde{v}} \hat{b}_{q_0}. \tag{5.67}$$

If we now follow the same procedure as in the previous section (i.e. plug in the Bogolyubov transformation (5.39), multiply through with $\exp\left(iq_0\tilde{v}\right)$ and integrate over $\tilde{v}$) we find

$$\int \frac{d\tilde{v}}{\sqrt{8\pi^2 p_0}} e^{i(p_0+p_1)\frac{v}{2}+iq_0\tilde{v}} = -\int \frac{dq_0' i\sqrt{\pi}}{\sqrt{2a\sinh\left(\frac{\pi q_0'}{a}\right)}} \frac{\left(\frac{m}{2a}\right)^{\frac{-iq_0'}{a}}}{\Gamma\left(1-\frac{iq_0'}{a}\right)} \left[\alpha_{q_0'p_0}\delta(q_0'-q_0) - \beta^*_{q_0'p_0}\delta(q_0'+q_0)\right]. \tag{5.68}$$

Focusing on α first we find

$$\begin{aligned}
\alpha_{q_0p_0} &= \frac{i\sqrt{a\sinh\left(\frac{\pi q_0}{a}\right)}\Gamma\left(1-\frac{iq_0}{a}\right)}{\left(\frac{m}{2a}\right)^{\frac{-iq_0}{a}}} \int \frac{d\tilde{v}}{\sqrt{4\pi^3 p_0}} e^{i(p_0+p_1)\frac{v}{2}+iq_0\tilde{v}} \\
&= \frac{i\sqrt{a\sinh\left(\frac{\pi q_0}{a}\right)}\Gamma\left(1-\frac{iq_0}{a}\right)}{\left(\frac{m}{2a}\right)^{\frac{-iq_0}{a}}} \int \frac{dv}{\sqrt{4\pi^3 p_0}} (av)^{-1+\frac{iq_0}{a}} e^{i\frac{p_0-p_1}{2}\frac{v}{2}} \\
&= \frac{i\sqrt{a\sinh\left(\frac{\pi q_0}{a}\right)}\Gamma\left(1-\frac{iq_0}{a}\right)}{\left(\frac{m}{2a}\right)^{\frac{-iq_0}{a}}\sqrt{4\pi^3 p_0}} \frac{\Gamma\left(\frac{iq_0}{a}\right)}{a} \left(i\frac{p_0-p_1}{2a}\right)^{\frac{-iq_0}{a}} \\
&= \frac{e^{\frac{\pi q_0}{2a}}}{\sqrt{4\pi a p_0 \sinh\left(\frac{\pi q_0}{a}\right)}} \left(\frac{p_0+p_1}{p_0-p_1}\right)^{-\frac{iq_0}{2a}},
\end{aligned} \tag{5.69}$$

where it was used again that

$$\Gamma\left(\frac{iq_0}{a}\right)\Gamma\left(1-\frac{iq_0}{a}\right) = \frac{a}{iq_0}\Gamma\left(1-\frac{iq_0}{a}\right)\Gamma\left(1+\frac{iq_0}{a}\right) = \frac{\pi}{i\sinh\left(\frac{\pi q_0}{a}\right)}, \tag{5.70}$$

and $i^c = e^{\frac{i\pi c}{2}}$, $m = \sqrt{(p_0+p_1)(p_0-p_1)}$.

Likewise the solution for $\beta_{q_0p_0}$ is found to be

$$\beta_{q_0p_0} = -\frac{e^{-\frac{\pi q_0}{2a}}}{\sqrt{4\pi a p_0 \sinh\left(\frac{\pi q_0}{a}\right)}} \left(\frac{p_0+p_1}{p_0-p_1}\right)^{-\frac{iq_0}{2a}}, \tag{5.71}$$

such that the number operator (5.37) becomes

$$\begin{aligned}
\left\langle \hat{N}_{q_0} \right\rangle &= \int dp_1 \beta_{p_0q_0}\beta^*_{p_0q_0'} \\
&= \frac{e^{-\frac{\pi}{2a}(q_0+q_0')}}{4\pi a\left(\sinh\left(\frac{\pi q_0}{a}\right)\sinh\left(\frac{\pi q_0'}{a}\right)\right)^{1/2}} \int \frac{dp_1}{p_0} e^{-\frac{i}{2a}(q_0-q_0')\ln\left(\frac{p_0+p_1}{p_0-p_1}\right)}.
\end{aligned} \tag{5.72}$$

Similar to the massless case, this integral can be solved by making a change of variables $y = \frac{1}{2}\ln\left(\frac{p_0+p_1}{p_0-p_1}\right)$ such that $dp_1 = p_0 dy$ and hence

$$\begin{aligned}
\left\langle \hat{N}_{q_0} \right\rangle &= \frac{e^{-\frac{\pi}{2a}(q_0+q_0')}}{4\pi a\left(\sinh\left(\frac{\pi q_0}{a}\right)\sinh\left(\frac{\pi q_0'}{a}\right)\right)^{1/2}} \int dy e^{-\frac{i}{a}(q_0-q_0')y} \\
&= \frac{e^{-\frac{\pi}{2a}(q_0+q_0')}}{2\left(\sinh\left(\frac{\pi q_0}{a}\right)\sinh\left(\frac{\pi q_0'}{a}\right)\right)^{1/2}} \delta(q_0-q_0'),
\end{aligned} \tag{5.73}$$

taking $q_0' = q_0$ the number density becomes

$$\langle \hat{n} \rangle = \frac{\left\langle \hat{N}_{q_0} \right\rangle}{V} = \left(e^{\frac{2\pi q_0}{a}} - 1 \right)^{-1}, \tag{5.74}$$

the Bose-Einstein distribution with temperature $\frac{a}{2\pi}$. It can then be concluded that the number-operator has the exact same form regardless of the mass of the scalar field.

5.2 3+1 dimensions

To make the step to (3+1) dimensions we first have to redefine the inertial and accelerated frame. The Minkowski metric in 3+1 dimensions becomes

$$ds^2 = dt^2 - dx^2 - dy^2 - dz^2, \tag{5.75}$$

and the normalization conditions in 3+1 dimensions differ from (5.3) and (5.4) only in the sense that α and β now run from 0 to 3. Putting the accelerated trajectory in the t, x-plane such that $u^\alpha(\tau) = (1, 0, 0, 0)$ and $a^\alpha(\tau) = (0, a, 0, 0)$ (thus the acceleration is captured by the $x(\tau)$ coordinate) the metric in lightcone coordinates (5.6) becomes

$$ds^2 = dudv + dy^2 + dz^2 = g_{\alpha\beta} dx^\alpha dx^\beta, \tag{5.76}$$

where now

$$g_{\alpha\beta} = \begin{pmatrix} 0 & 1/2 & 0 & 0 \\ 1/2 & 0 & 0 & 0 \\ 0 & 0 & 1 & 0 \\ 0 & 0 & 0 & 1 \end{pmatrix}. \tag{5.77}$$

The trajectory in lightcone coordinates can then be written as $x^\alpha(\tau) = (u(\tau), v(\tau), 0, 0)$ and equations (5.10) through (5.13) still hold. In $1+1$-dimensions we moved on from here to defining a comoving frame for the accelerated observer in terms of the coordinates (ξ^0, ξ^1). In the $3+1$-dimensional case we have coordinates $(\xi^0, \xi^1, \xi^2, \xi^3)$. However, as the acceleration only affects the (t, x)-plane, one can make the identification $\xi^2 = y$, $\xi^3 = z$. The observer still needs to be at rest for $\xi^1 = y = z = 0$ and the proper time along the worldline should be equal to ξ^0. Furthermore, for the first two coordinates we can demand the metric of the comoving frame to be proportional to the metric in the inertial frame. Hence

$$ds^2 = \chi^2(\xi^0, \xi^1) \left[(d\xi^0)^2 - (d\xi^1)^2 \right] - dy^2 - dz^2. \tag{5.78}$$

Then we can follow the same procedure as before and define the lightcone coordinates $\tilde{u} \equiv \xi^0 - \xi^1$ and $\tilde{v} \equiv \xi^0 + \xi^1$.

$$ds^2 = \chi^2(\tilde{u}, \tilde{v}) d\tilde{u} d\tilde{v} - dy^2 - dz^2. \tag{5.79}$$

5.2.1 Massless scalar field

The relation between the first two components of the metrics (5.76) and (5.79) is the same as in $(1+1)$-dimensions (5.20) but the metric is no longer conformally flat. As a result the action is no longer conformally invariant. We find then

$$S_t = \frac{1}{2} \int \left[(\partial_t \phi)^2 - (\partial_x \phi)^2 - (\partial_y \phi)^2 - (\partial_z \phi)^2 \right] dtdxdydz, \tag{5.80}$$

the action of the fields quantized with respect to the Minkowski time t, and

$$S_\tau = \frac{1}{2}\int \left[(\partial_{\xi^0}\phi)^2 - (\partial_{\xi^1}\phi)^2 - e^{2a\xi^1}((\partial_y\phi)^2 + (\partial_z\phi)^2)\right] d\xi^0 d\xi^1 dy dz, \tag{5.81}$$

the action of the fields quantized with respect to the proper time $\tau = \xi^0$. The equations of motion become

$$(\partial_t^2 - \partial_x^2 - \partial_{\vec{x}_\perp}^2)\phi = 0 \quad \text{and} \quad (\partial_{\xi^0}^2 - \partial_{\xi^1}^2 - e^{2a\xi^1}\partial_{\vec{x}_\perp}^2)\phi = 0, \tag{5.82}$$

where $\vec{x}_\perp = (y, z)$. For the modes in the inertial frame, the solution is given by

$$\phi(t, \vec{x}) \propto e^{-i(\omega u - \vec{k}\cdot\vec{x}_\perp)}. \tag{5.83}$$

Note that the equation of motion for 4-dimensional Rindler spacetime has the same form as the massive 2-dimensional equation from the previous section. Writing the Rindler field as

$$\hat{\phi}(\xi^0, \xi^1, \vec{x}_\perp) = f_{q_0\vec{q}_\perp}(\xi^1)e^{-i(q_0\xi_0 - \vec{q}_\perp\cdot\vec{x}_\perp)}, \tag{5.84}$$

where $\vec{q}_\perp \equiv (q_2, q_3)$ the equation of motion becomes

$$(-q_0^2 - \partial_{\xi^1}^2 + e^{2a\xi^1}\vec{q}_\perp)f_{q_0\vec{q}_\perp}(\xi^1) = 0. \tag{5.85}$$

The derivation of the solution is equivalent to the derivation following (eq:mass2dKG 5.58) with the replacement $m^2 = \vec{q}_\perp$ where the dispersion relation is such that $\vec{q}_0 = \sqrt{q_1^2 + \vec{q}_\perp^2}$. Taking advantage of this the fields can be readily obtained as

$$\begin{aligned}
\hat{\phi}(\xi^0, \xi^1, \vec{x}_\perp) &= \int\limits_{-\infty}^{\infty} \frac{dq_1 d\vec{q}_\perp}{(2\pi)^{3/2}}\frac{1}{\sqrt{2q_0}}\left(\hat{b}_{q_0\vec{q}_\perp} f_{q_0\vec{q}_\perp} e^{-i(q_0\xi^0 - \vec{q}_\perp\cdot\vec{x}_\perp)} + \hat{b}^\dagger_{q_0\vec{q}_\perp} f^*_{q_0\vec{q}_\perp} e^{i(q_0\xi^0 - \vec{q}_\perp\cdot\vec{x}_\perp)}\right), \\
\hat{\phi}(t, \vec{x}) &= \int\limits_{-\infty}^{\infty} \frac{dp_1 d\vec{p}_\perp}{(2\pi)^{3/2}}\frac{1}{\sqrt{2p_0}}\left(\hat{a}_{p_0\vec{p}_\perp} e^{-i(p_0 t - \vec{p}_\perp\cdot\vec{x}_\perp)} + \hat{a}^\dagger_{p_0\vec{p}_\perp} e^{i(p_0 t - \vec{p}_\perp\cdot\vec{x}_\perp)}\right).
\end{aligned} \tag{5.86}$$

The creation and annihilation operators, (eq:commboson 5.36), satisfy the 4-dimensional bosonic commutation relations

$$\left[\hat{a}_{p_0\vec{p}_\perp}, \hat{a}^\dagger_{p_0'\vec{p}_\perp'}\right] = \delta(p_0 - p_0')\delta^2(\vec{p}_\perp - \vec{p}_\perp'), \qquad \left[\hat{b}_{q_0\vec{q}_\perp}, \hat{b}^\dagger_{q_0\vec{q}_\perp}\right] = \delta(q_0 - q_0')\delta^2(\vec{q}_\perp - \vec{q}_\perp'). \tag{5.87}$$

Note that the exponentials depending on $\vec{x}_\perp$ are equal for both $\hat{\phi}(\xi^0, \xi^1, \vec{x}_\perp)$ and $\hat{\phi}(t, x, \vec{x}_\perp)$. As a result these terms will drop out after multiplication by $e^{-i\vec{q}_\perp'\cdot\vec{x}_\perp}$ or $e^{-i\vec{p}_\perp'\cdot\vec{x}_\perp}$ followed by integration over $\vec{x}_\perp$ and $\vec{q}_\perp$ or $\vec{p}_\perp$.

The Bogoliubov coefficients can be read of from the massless 2-dimensional case and yield

$$\begin{aligned}
\alpha_{q_0p_0} &= \frac{e^{\frac{\pi q_0}{2a}}}{\sqrt{4\pi a p_0 \sinh\left(\frac{\pi q_0}{a}\right)}}\left(\frac{p_0 + p_1}{p_0 - p_1}\right)^{-\frac{iq_0}{2a}}, \\
\beta_{q_0p_0} &= -\frac{e^{-\frac{\pi q_0}{2a}}}{\sqrt{4\pi a p_0 \sinh\left(\frac{\pi q_0}{a}\right)}}\left(\frac{p_0 + p_1}{p_0 - p_1}\right)^{-\frac{iq_0}{2a}}.
\end{aligned} \tag{5.88}$$

The number operator in 4 dimensions becomes

$$\left\langle \hat{N}_{q_0\vec{q}_\perp}\right\rangle = \int dp_0 \int d\vec{p}_\perp \left|\beta_{q_0p_0}\right|^2. \tag{5.89}$$

Instead of plugging in the explicit coefficients, one can make use of the completeness relation in 4 dimensions

$$\int dp_0 d\vec{p}_\perp (\alpha_{q_0 p_0}\alpha^*_{q_0' p_0} - \beta_{q_0 p_0}\beta^*_{q_0' p_0}) = \delta(q_0 - q_0')\delta^2(\vec{q}_\perp - \vec{q}_\perp'), \tag{5.90}$$

and the relation

$$|\alpha_{q_0 p_0}|^2 = e^{\frac{2\pi q_0}{a}} |\beta_{q_0 p_0}|^2, \tag{5.91}$$

to obtain

$$\left\langle \hat{N}_{q_0 \vec{q}_\perp} \right\rangle = \left(e^{\frac{2\pi\Omega}{a}} - 1\right)^{-1} \delta(0)\delta^3(\vec{0}). \tag{5.92}$$

Dividing out the volume as before yields the number density

$$\langle \hat{n} \rangle = \frac{\left\langle \hat{N}_{q_0 \vec{q}_\perp} \right\rangle}{V} = \left(e^{\frac{2\pi\Omega}{a}} - 1\right)^{-1}. \tag{5.93}$$

5.2.2 Massive scalar field

Similar to the previous section, most of our equations remain valid. The Euler-Lagrange equation now yields the massive Klein-Gordon equation in $3+1$-dimensions

$$\left(\partial_t^2 - \partial_x^2 - \partial_{\vec{x}_\perp}^2 + m^2\right)\phi(t, x, \vec{x}_\perp) = 0, \tag{5.94}$$

for the inertial observer. The solution to this equation is given by

$$\phi \propto e^{-ip^\mu x_\mu}, \tag{5.95}$$

where now $p^\mu = (p_0, p_1, \vec{p}_\perp)$, $x^\mu = (t, x, \vec{x}_\perp)$ and $p_0 = \sqrt{p_1^2 + \vec{p}_\perp + m^2}$ and $\vec{x}_\perp$, $\vec{p}_\perp$ are defined as before. For the accelerated observer we use Rindler coordinates such that $\phi(\xi^0, \xi^1, \vec{x}_\perp)$ has to satisfy

$$\left(\partial_{\xi^0}^2 - \partial_{\xi^1}^2 - e^{2a\xi^1}\left(\partial_{\vec{x}_\perp}^2 - m^2\right)\right)\phi(\xi^0, \xi^1, \vec{x}_\perp) = 0. \tag{5.96}$$

This equation can be solved equivalently to the massless case yielding

$$\left(-q_0^2 - \partial_{\xi^1}^2 + e^{2a\xi^1} m_{\vec{q}_\perp}^2\right)\phi(\xi^0, \xi^1, \vec{x}_\perp) = 0, \tag{5.97}$$

where $m_q^2 = q_2^2 + q_3^2 + m^2$ can be seen as a shifted mass. The solution is given by (eq:unruh2dmasssol 5.61) if we make the substitution $m \to m_q$

$$f_{q_0 \vec{q}_\perp}(\xi^1) = \sqrt{\frac{2q_0 \sinh\left(\frac{\pi q_0}{a}\right)}{\pi^2 a}} K_{\frac{iq_0}{a}}\left(\frac{m_q}{a} e^{a\xi^1}\right), \tag{5.98}$$

which gives for ϕ

$$\phi(\xi^0, \xi^1, \vec{x}_\perp) = \sqrt{\frac{2q_0 \sinh\left(\frac{\pi q_0}{a}\right)}{\pi^2 a}} K_{\frac{iq_0}{a}}\left(\frac{m_q}{a} e^{a\xi^1}\right) e^{-i(q_0\xi^0 - \vec{q}_\perp \cdot \vec{x}_\perp)}. \tag{5.99}$$

Making the substitution $m \to m_q$ in (eq:unruh2dmassalpha 5.69) leads to

$$\begin{aligned}
\alpha_{q_0 p_0} &= \frac{e^{\frac{\pi q_0}{2a}}}{\sqrt{4\pi a p_0 \sinh\left(\frac{\pi q_0}{a}\right)}} \left(\frac{p_0 + p_1}{p_0 - p_1}\right)^{-\frac{iq_0}{2a}}, \\
\beta_{q_0 p_0} &= -\frac{e^{-\frac{\pi q_0}{2a}}}{\sqrt{4\pi a p_0 \sinh\left(\frac{\pi q_0}{a}\right)}} \left(\frac{p_0 + p_1}{p_0 - p_1}\right)^{-\frac{iq_0}{2a}},
\end{aligned} \tag{5.100}$$

where it was used again that $m_q = \sqrt{\vec{q}_\perp^2 + m^2} = \sqrt{q_0^2 - q_1^2} = \sqrt{(q_0 - q_1)(q_0 + q_1)}$. The number density can then be obtained as

$$\langle \hat{n} \rangle = \frac{\left\langle \hat{N}_{q_0 \vec{q}_\perp} \right\rangle}{V} = \left(e^{\frac{2\pi\Omega}{a}} - 1 \right)^{-1} . \tag{5.101}$$

From the calculations performed above, it is clear that the number density is independent of the mass of the field and the dimensions of spacetime (for $d \geq 2$). The Unruh effect turns out to be a purely geometric effect. It arises for a generic Lorentz-invariant matter theory simply because of the properties of the Rindler frame (see Sect. 5.1 for more details).

Consider a generic Lorentz invariant Green's function $G_M(x, x') = G_M(x - x')$ for an interacting theory in Minkowski space. When evaluated on the worldline (5.29) of a uniformly accelerated observer, it will be a function of the Rindler coordinates $(\vec{x}_\perp, \tau)$ and $(\vec{x}'_\perp, \tau')$. Since the theory is Lorentz invariant, G_M can only depend on $(x - x')^2$. Using the relation

$$\begin{aligned} (t - t')^2 - (x - x')^2 &= a^{-2} \left[(\sinh a\tau - \sinh a\tau')^2 - (\cosh a\tau - \cosh a\tau')^2 \right] \\ &= 2a^{-2} \left(\cosh(a\Delta\tau) - 1 \right) , \end{aligned} \tag{5.102}$$

with $\Delta\tau = \tau - \tau'$, the Rindler Green's function has a τ dependence of the form $G_R(\cosh a\Delta\tau)$. Focusing for simplicity on $\tau' = 0$, a Wick rotation $t = it_E$ will induce, through $t = a^{-1} \sinh a\tau$, a corresponding Wick rotation in Rindler time, $\tau = i\tau_E$. But this then means that a general Rindler two-point function will be periodic in Rindler time, since $G_R(\cosh a\tau) \to G_R^{(E)}(\cos a\tau_E) = G_R^{(E)}(\cos(a\tau_E + 2\pi))$. We thus see that the periodicity $\beta = 2\pi/a$ implies a temperature $T = a/2\pi$.

As a consequence of this property, possible corrections to the Unruh effect arising from quantum gravity models, will not propagate through to the number density. In the following section, a framework based on the emission rate will be developed, exactly with the intention to capture signatures originating from quantum gravity.

6 Rates from correlators

The rest of this work will follow the detector approach to the Unruh effect [35, 60, 61, 45]. The advantage of this approach is that it considers observable quantities, namely emission and absorption rates of the accelerated detector. The response of the accelerated detector then indicates that it is immersed in a thermal bath of particles. This framework is ideally suited for studying corrections to the Unruh effect by using effective two-point correlation functions incorporating quantum gravity effects. We first review the formalism following [45] before applying it to dimensional flows in Sects. 7, 8, and 9.

6.1 Particle detectors and two-point functions

The simplest model of a particle detector is a quantum mechanical system with two internal energy states $|E_2\rangle$ and $|E_1\rangle$, with energies $E_2 > E_1$. The detector moves along a worldline $x(\tau)$ parameterized by the detector's proper time τ and interacts with a scalar field $\Phi(x)$ by absorbing or emitting its quanta. The coupling of Φ to the detector is modeled by a monopole moment operator $m(\tau)$ acting on the internal detector eigenstates through the Lagrangian

$$L_I = g\, m(\tau) \Phi(x(\tau)) . \tag{6.1}$$

We will consider in the following the two cases of a detector moving inertially in Minkowski space, and one moving along a uniformly accelerated trajectory, which defines the Rindler space (see Sect. 5.1). Let us denote the Minkowski vacuum by $|0_M\rangle$, the Rindler vacuum by $|0_R\rangle$, and the one-particle state of the field Φ with spatial momentum $\vec{k}$ by $|\vec{k}\rangle$. There are three possible processes giving a non-zero rate. Following the nomenclature used in [45] we can also give them a thermodynamic interpretation, since it will turn out that Rindler correlators are thermal. First, the inertial detector can be in the excited state with energy E_2. This is a spontaneous emission process and corresponds to the transition $|E_2\rangle|0_M\rangle \rightarrow |E_1\rangle|\vec{k}\rangle$ for an observer comoving with the detector. Second, the accelerating detector can be in the excited state with energy E_2. This is an induced emission process and instead corresponds to the transition $|E_2\rangle|0_R\rangle \rightarrow |E_1\rangle|\vec{k}\rangle$ for an inertial observer in Minkowski space (or equivalently $|E_2\rangle|0_M\rangle \rightarrow |E_1\rangle|\vec{k}\rangle$ for an *accelerating* one). Finally, an accelerating detector in the ground state $E = E_1$ corresponds to absorption, or the transition $|E_1\rangle|0_M\rangle \rightarrow |E_2\rangle|\vec{k}\rangle$. Notice that the term absorption here is meant purely as an analogy with two state systems, since the one-particle state $|\vec{k}\rangle$ still appears as a final state.

The transition probability can be expressed in terms of the two-point function of the field. To first order in time-dependent perturbation theory, the amplitude for the detector-field interaction takes the form

$$\mathcal{A}(\vec{k}) = ig\langle E_f|m(0)|E_i\rangle \int d\tau e^{i(E_f-E_i)\tau}\langle\vec{k}|\Phi(x(\tau))|0_M\rangle \ . \tag{6.2}$$

The transition probability is the square of the amplitude, integrated over all possible final states

$$P_{i\to f} = \int d^3k|\mathcal{A}(\vec{k})|^2 \,. \tag{6.3}$$

For $E_f = E_1$ and $E_i = E_2$ this gives the total, spontaneous plus induced, emission probability.

The field Φ can be expanded in its normal mode basis, according to the choice of vacuum. If we define the annihilation operators in Minkowski space as $a_{\vec{k}}|0_M\rangle = 0$, and those in Rindler space (we work implicitly in the right wedge) as $b_{\vec{k}}|0_R\rangle = 0$, then the field has the expansions:

$$\Phi(x) = \int d^3k \left(u_{\vec{k}}a_{\vec{k}} + u^*_{\vec{k}}a^\dagger_{\vec{k}}\right) = \int d^3k \left(v_{\omega\vec{k}_\perp}b_{\omega\vec{k}_\perp} + v^*_{\omega\vec{k}_\perp}b^\dagger_{\omega\vec{k}_\perp}\right) \ . \tag{6.4}$$

We used the notation $\vec{k}_\perp = (k_y, k_z)$, these coordinates are left untouched by the Rindler coordinate transformation. Here the mode functions in the Minkowski basis are

$$u_{\vec{k}} = \frac{1}{\sqrt{2(2\pi)^3 w}}e^{-i(wt-\vec{k}\vec{x})} \,, \tag{6.5}$$

where $w \equiv \sqrt{\vec{k}^2 + m^2}$, whereas in the Rindler basis with coordinates $(\tau, \xi, \vec{x}_\perp)$ they are given in terms of a modified Bessel function $K_\nu(x)$ as [49]

$$v_{\omega\vec{k}_\perp} = \left[\frac{\sinh(\pi\omega/a)}{4\pi^2 a}\right]^{1/2} K_{i\omega/a}\left(\frac{\sqrt{\vec{k}_\perp^2 + m^2}}{a}e^{a\xi}\right) e^{-i(\omega\tau - \vec{k}_\perp\cdot\vec{x}_\perp)} \,. \tag{6.6}$$

The sum over all possible one-particle states needed to obtain the transition probabilities leads to a sum over modes $\sum_{\vec{k}} u_{\vec{k}}(x_1)u^*_{\vec{k}}(x_2)$. Upon using the completeness of states this gives rise to the two-point function for the Minkowski vacuum. Defining $C \equiv g^2 |\langle E_f|m(0)|E_i\rangle|^2$, one finds

$$\begin{aligned} P_{i\to f} &= C \int d^3k \int_{-\infty}^{\infty} d\tau_1 \int_{-\infty}^{\infty} d\tau_2\, e^{i(E_f-E_i)(\tau_1-\tau_2)} \langle \vec{k}|\Phi(x(\tau_1))|0_M\rangle\langle 0_M|\Phi(x(\tau_2))|\vec{k}\rangle \\ &= C \int_{-\infty}^{\infty} d\tau_1 \int_{-\infty}^{\infty} d\tau_2\, e^{i(E_f-E_i)(\tau_1-\tau_2)} \langle 0_M|\Phi(x(\tau_2))\Phi(x(\tau_1))|0_M\rangle. \end{aligned} \tag{6.7}$$

Performing the integration over all the final states first, the expression for the transition probabilities then becomes [45]

$$P_{i\to f} = C\, F(\Delta E)\ , \tag{6.8}$$

where $F(\Delta E)$ is the so-called response function

$$F(\Delta E) = \int_{-\infty}^{\infty} d\tau_1 \int_{-\infty}^{\infty} d\tau_2\, e^{-i(E_f-E_i)\Delta\tau} G_M(\Delta\tau - i\epsilon)\ . \tag{6.9}$$

Here $\Delta\tau \equiv \tau_1 - \tau_2$ (from now on the limit $\epsilon \to 0^+$ is understood). For the massive case, the response function is essentially given by the Fourier transform of the Wightman two-point function $G_M(\Delta\tau - i\epsilon)$ evaluated on the detector's trajectory.

In the following we will be interested in the emission case, with $E_i = E_2$ and $E_f = E_1$ and $\Delta E \equiv E_2 - E_1$ is taken positive by definition. For the case of the detector undergoing constant acceleration the total transition probability (6.8) contains contributions from spontaneous and induced emission. Subtracting the spontaneous emission probability one arrives at the following formula for the induced emission response function

$$F_I(\Delta E) = \int_{-\infty}^{\infty} d\tau_1 d\tau_2\, e^{i\Delta E\Delta\tau} \left[G_M(\Delta\tau - i\epsilon) - G_R(\Delta\tau - i\epsilon)\right]\ . \tag{6.10}$$

Here G_M is the vacuum (Wightman) two-point function for an observer on the accelerated trajectory in the Minkowski vacuum,

$$G_M\left(x, x'\right) = \langle 0_M|\, \Phi\left(x\right) \Phi\left(x'\right) |0_M\rangle\ , \tag{6.11}$$

and G_R is the vacuum two-point function of an accelerated observer in the Rindler vacuum,

$$G_R\left(x, x'\right) = \langle 0_R|\, \Phi\left(x\right) \Phi\left(x'\right) |0_R\rangle\ . \tag{6.12}$$

Practically, it is convenient to work with the induced transition rate per unit time given by

$$\dot{P}_{i\to f} = g^2\, |\langle E_f|m(0)|E_i\rangle|^2\, \dot{F}_I(\Delta E)\ , \tag{6.13}$$

with

$$\dot{F}_I(\Delta E) = \int_{-\infty}^{+\infty} d\Delta\tau\, e^{i\Delta E\Delta\tau}\ \left[G_M(\Delta\tau - i\epsilon) - G_R(\Delta\tau - i\epsilon)\right]\ . \tag{6.14}$$

This equation is the relation between physical rates and two-point functions that we will use in the following. In order to ease our notation we will set $\Delta\tau = \tau$ and $\Delta E = E$ from now on.

The Wightman function for a massive scalar field with mass m in Minkowski space entering into (6.14) is given by

$$G_+(\vec{x}, t) = -i \int \frac{d^3\vec{p}}{(2\pi)^3} \oint_{\gamma_+} \frac{dp^0}{2\pi}\, \widetilde{G}(p^2)\, e^{i\vec{p}\cdot\vec{x} - ip^0 t}\ , \tag{6.15}$$

where

$$\widetilde{G}(p^2) = \frac{1}{p^2 - m^2} = \frac{1}{(p^0 + \sqrt{\vec{p}^2 + m^2})(p^0 - \sqrt{\vec{p}^2 + m^2})} \,. \qquad (6.16)$$

The contour γ_+ encircles the first order pole located at $p^0 = \sqrt{\vec{p}^2 + m^2}$. Carrying out the Fourier integral the positive-frequency Wightman function in Minkowski space is given by (see, e.g., [35])

$$G_M(x, x') = -\frac{im}{4\pi^2} \frac{K_1\left(im\sqrt{(t - t' - i\epsilon)^2 - (\vec{x} - \vec{x}')^2}\right)}{\sqrt{(t - t' - i\epsilon)^2 - (\vec{x} - \vec{x}')^2}} \,. \qquad (6.17)$$

Here K_1 is the modified Bessel function of the second kind. In the massless limit (6.17) reduces to the Wightman function of a massless scalar field in position space [35, 45]

$$G_M(x, x') = -\frac{1}{4\pi^2} \frac{1}{(t - t' - i\epsilon)^2 - (\vec{x} - \vec{x}')^2} \,. \qquad (6.18)$$

The Wightman function in Rindler space is just the same evaluated on the worldline of the uniformly accelerated detector[7]

$$t = a^{-1}\sinh(a\tau)\,, \quad x = a^{-1}\cosh(a\tau)\,, \quad y = 0\,, \quad z = 0\,. \qquad (6.19)$$

For a thermal system, the induced emission probability coincides with the absorption probability. We can then turn to the proof that the Minkowski vacuum corresponds to a thermal state when probed by an accelerated detector.

6.2 Emergence of thermality

As mentioned in Sect. 5, the Unruh effect arises from the geometry of Rindler spacetime. However, there is a subtlety in the Wick rotation $t = it_E$ when the Wightman function $G_R(\cosh a\tau) \to G_R^{(E)}(\cos a\tau_E) = G_R^{(E)}(\cos(a\tau_E + 2\pi))$. Due to the different domains of analyticity of G_+ and G_- in the complex τ-plane, one actually identifies $G_E(\tau_E) = G_+(i\tau_E)$ for $-2\pi < \tau_E < 0$ and $G_E(\tau_E) = G_-(i\tau_E)$ for $0 < \tau_E < 2\pi$. This is responsible for the change of sign of τ in the KMS condition.

Undoing the Wick rotation we obtain the KMS condition in the form (with obvious change of notation)

$$G_R(\tau) = G_R(-\tau - i\beta)\,. \qquad (6.20)$$

This can be put in another equivalent form, which is more natural when dealing with detector rates [63]. Since the rate is a Fourier transform of the Wightman function, assuming that $G_R(\tau)$ is analytic in the strip $-\beta < \mathrm{Im}\tau < 0$, we have

$$\begin{aligned} \dot{F}(E) &= \int_{-\infty}^{+\infty} d\tau e^{-iE\tau} G_R(\tau - i\epsilon) \\ &= \int_{-\infty}^{+\infty} d\tau e^{-iE(\tau - i\beta + 2i\epsilon)} G_R(\tau - i\beta + i\epsilon) \\ &= e^{-(\beta - 2\epsilon)E} \int_{-\infty}^{+\infty} d\tau e^{iE\tau} G_R(\tau - i\epsilon)\,. \end{aligned} \qquad (6.21)$$

[7] Note that from here one $\xi^1 = 0$ and $\xi^0 = \tau$ with respect to Sect. 5.

Here in the second line we made use of the analyticity assumption to push down the contour in the complex τ-plane by $i(\beta-2\epsilon)$, and in the third line we changed variable of integration to $-\tau$. Taking ϵ to zero, the KMS condition becomes

$$\dot{F}(E)=e^{-\beta E}\dot{F}(-E)\,. \tag{6.22}$$

This relation can also be derived directly in the free massive case from the parity properties of the integrands appearing in the rates.[8] A general proof of the KMS condition for an interacting field theory in any dimension was given in [62].

The Unruh temperature is thus only determined by the Euclidean periodicity, and is protected against corrections as long as the Lorentz invariance of G_M is preserved. In particular, if one computes the average number density $\langle n\rangle$ in Rindler space from thermal considerations alone, one can obtain the usual Planckian distribution with temperature $T=a/2\pi$. As a simple illustration of this fact, in Sect. 6.3 we will derive the Planckian thermal spectrum for a massive scalar field, showing as a byproduct that the temperature is independent of the mass.

6.3 Detector response for massive scalars

The direct computation of the induced emission rate proves to be rather nontrivial. Here we will instead opt for a shortcut, based on the KMS condition.

With reference to the nomenclature previously introduced, let us call $\dot{F}_A$ the absorption rate and $\dot{F}_E$ the emission rate. This last one is the sum of spontaneous and induced emission, $\dot{F}_E=\dot{F}_S+\dot{F}_I$. From the derivation of the formulas for the detector rates in Sect. 6.1, one immediately finds that $\dot{F}_A(-E)=\dot{F}_E(E)$. This is ensured by the fact that the one-particle state $|\vec{k}\rangle$ always appears as a final state, and thus the Wightman function has the same frequency for both processes. The difference then just amounts to the sign of the Fourier exponential term. Using the KMS condition (6.22), this gives

$$\dot{F}_A(E)=e^{-\beta E}\dot{F}_A(-E)=e^{-\beta E}\dot{F}_E(E)=e^{-\beta E}[\dot{F}_I(E)+\dot{F}_S(E)]\,. \tag{6.23}$$

If the induced emission and absorption rates coincide

$$\dot{F}_A(E)=\dot{F}_I(E) \tag{6.24}$$

it follows that

$$\dot{F}_I(E)=\frac{\dot{F}_S(E)}{e^{\beta E}-1}\,. \tag{6.25}$$

Thus one only needs to compute the spontaneous rate to obtain that for induced emission.

Condition (6.24) can be explicitly proven for a free massive scalar field. It is indeed found in this case [63] that

$$\begin{aligned}\dot{F}(E) &= \int_{-\infty}^{+\infty} d\tau e^{-iE\tau}G_R(\tau-i\epsilon)\\ &= 2\pi\int d^2k_\perp\left|v_{\omega\vec{k}_\perp}\right|^2[\theta(E)N(E/a)+\theta(-E)(1+N(|E|/a))]\,,\end{aligned} \tag{6.26}$$

where

$$N(x)=\frac{1}{e^{2\pi x}-1}\,. \tag{6.27}$$

[8] We thank J. Louko for pointing this out to us.

The different terms in (6.26) have a direct interpretation in the language of Sect. 6.1. The first term corresponds to the absorption case, while the second is the sum of the spontaneous and induced emission. Indeed, as a check one can compute directly the spontaneous emission rate by considering an accelerated detector in the Rindler vacuum (which is therefore at rest), with $\xi = 0$ and $\vec{x}_\perp = 0$. An explicit calculation of this term following [45] (see (3.11) in that reference) gives

$$\dot{F}_S(E) = 2\pi \int d^2k_\perp d\omega \left| K_{i\omega/a}\left(\frac{\sqrt{\vec{k}_\perp^2 + m^2}}{a}\right)\right|^2 \frac{\sinh(\pi\omega/a)}{4\pi^4 a}\delta(\omega - E) \tag{6.28}$$

which, using (6.6), precisely reproduces the spontaneous term in (6.26). It is then manifest from (6.26) that (6.24) and (6.25) hold.

Based on (6.25) it then suffices to compute the spontaneous emission rate. Rather than attempting to solve (6.28) analytically, an approximation using the response function will prove to effectively capture the high energy behavior of the spontaneous emission rate. We then consider a detector at rest in the Minkowski vacuum, in general dimension d [35]. The simplest way is to start from (6.9) and substitute the explicit form of the two-point function:

$$F(\Delta E) \approx \int_{-\infty}^{\infty} d\tau_1 \int_{-\infty}^{\infty} d\tau_2\, e^{i\Delta E \Delta\tau} \int \frac{d^dk}{(2\pi)^d}\frac{1}{2\omega} e^{-i\omega(t(\tau_1)-t'(\tau_2)) + i\vec{k}\cdot(\vec{x}(\tau_1)-\vec{x}'(\tau_2))}\,. \tag{6.29}$$

Inverting the τ and k integrations we find

$$\begin{aligned}\dot{F}_S(E) &\approx \int \frac{d^{d-1}k}{(2\pi)^{d-1}}\frac{1}{2\sqrt{k^2+m^2}}\int_{-\infty}^{+\infty} d\tau e^{-i(\sqrt{k^2+m^2}-E)\tau} \\ &= \frac{\pi^{\frac{d-1}{2}}}{\Gamma(\frac{d-1}{2})(2\pi)^{d-2}}\left(E^2 - m^2\right)^{\frac{d-3}{2}}\theta(E-m)\,. \end{aligned} \tag{6.30}$$

Exploiting now relation (6.25), the induced rate function per unit time of the accelerated detector in $d = 4$ becomes

$$\dot{F} \approx \frac{1}{2\pi}\sqrt{E^2 - m^2}\,\theta(E-m)\,\frac{1}{e^{\frac{2\pi E}{a}} - 1}\,. \tag{6.31}$$

Plotting the numerical integration of (6.28) and the approximation (6.31) as a function of the energy, E, one can clearly see that for large energies the approximation agrees with the numerical result. For the case of a massless scalar field, the spontaneous emission rate can be calculated analytically and the approximation becomes exact [63].

The rate function constitutes the main result of this subsection. Taking the limit $m \to 0$, it agrees with the derivation for the massless case given in [35, 45]. The structure of (6.31) then motivates the definition of a profile function $\mathcal{F}(E)$ via

$$\dot{F} \approx \frac{1}{2\pi}\,\mathcal{F}(E)\,\frac{1}{e^{\frac{2\pi E}{a}} - 1}\,. \tag{6.32}$$

For a massless and massive scalar field obeying the Klein-Gordon equation one then has

$$\mathcal{F}^{\text{massless}}(E) = E\,, \qquad \mathcal{F}^{\text{massive}}(E) = \sqrt{E^2 - m^2}\,\theta(E-m)\,. \tag{6.33}$$

For general dimension the profile function is

$$\mathcal{F}(E) = \frac{\pi^{\frac{d-1}{2}}}{\Gamma(\frac{d-1}{2})(2\pi)^{d-3}}\left(E^2 - m^2\right)^{\frac{d-3}{2}}\theta(E-m)\,. \tag{6.34}$$

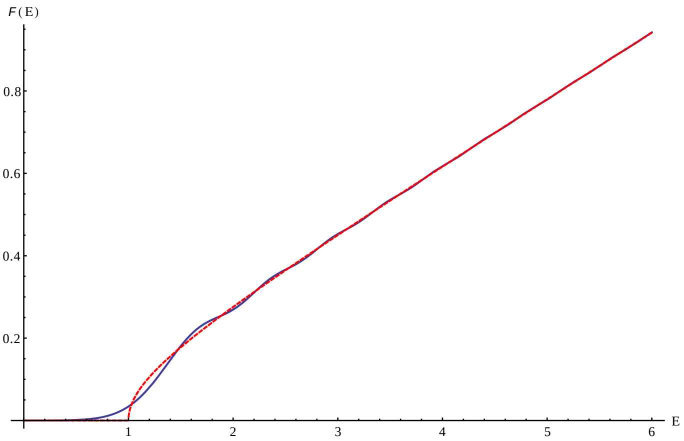

Figure 6: The profile function $\mathcal{F}(E)$ for $a = 0.3$ and $m = 1$. The blue, solid line depicts the numerical integration (6.28) while the red, dashed line shows the approximation (6.31). For large values of E, (6.28) is well approximated by (6.31).

As we will show in the subsequent section, it is this profile function that actually carries information about quantum gravity corrections to the Unruh rate.[9]

As stressed before, the Planckian thermal factor is independent of the details of the field considered. The fact that the mass dependence enters through the prefactor tells us that the signatures of the fields involved will only be present in physical rates, and not in number densities $\langle n \rangle$.

7 Master formulas for modified detector rates

In the presence of a dimensional flow, $\tilde{G}(p^2)$ entering into (6.15), acquires a non-trivial momentum dependence.[10] It is useful to distinguish the two cases where $[\tilde{G}(p^2)]^{-1}$ is a polynomial in p^2 or given by a more general function with a finite number (typically one) of zeros in the complex p^0-plane. These two cases will be discussed in Sects. 7.1 and 7.2, respectively.

7.1 Detector rates from the Ostrogradski decomposition

We start by considering the case in which $\left[\widetilde{G}(p^2)\right]^{-1} \equiv \mathcal{P}_n(p^2)$ is an inhomogeneous polynomial of order n. This covers the class of theories with a general quadratic effective Lagrangian $\mathcal{L} = \frac{1}{2}\phi\,\mathcal{P}_n(-\partial^2)\,\phi$ where $\mathcal{P}_n$ is a local function of the flat space d'Alembertian operator that admits a Taylor expansion around zero momentum. This comprises all local theories in which higher order corrections come in definite powers of momenta. The limiting case $n \to \infty$ can also be considered. In this case the profile function $\mathcal{F}(E)$, (6.32), can be constructed from the Ostrogradski decomposition for a higher-derivative field theory.

The polynomial $\mathcal{P}_n(z)$ has n roots, $\mu_i, i = 1, \ldots, n$ in the complex z-plane. It can then be factorized according to

$$\mathcal{P}_n(z) = c \prod_{i=1}^{n} (z - \mu_i) \tag{7.1}$$

[9]In the subsequent sections, the approximation sign for the profile function will be omitted.

[10]As noted before, this does not necessarily entail the breaking of Lorentz symmetry since $\tilde{G}(p^2)$ may still be a Lorentz invariant function depending on the square of the momentum four-vector only.

where c is a normalization constant. In order to connect to the case of a massive scalar field, the momentum space propagator is decomposed according to

$$[\mathcal{P}_n(z)]^{-1} = \frac{1}{c} \sum_{i=1}^{n} \frac{A_i}{(z-\mu_i)} \tag{7.2}$$

where the coefficients A_i are functions of the roots μ_i. Assuming that $z \neq \mu_i$, (7.1) and (7.2) can be multiplied to obtain the condition

$$\sum_{i=1}^{n} A_i \prod_{j\neq i} (z-\mu_j) = 1\,. \tag{7.3}$$

This condition must hold for any value $z \neq \mu_i$. Since the left-hand-side is a polynomial in z of order $n-1$, (7.3) gives rise to n equations determining the coefficients A_i. Defining the vector $\mathcal{Z} \equiv \left[1, z, \ldots, z^{n-1}\right]$ and introducing the coefficient matrix $\mathcal{C}$ via $\mathcal{C}_{ij}\,\mathcal{Z}_j \equiv \prod_{j\neq i}(z-\mu_j)$, (7.3) entails

$$\sum_{i=1}^{n} A_i\,\mathcal{C}_{ij} = \delta_{1j}\,, \tag{7.4}$$

where δ_{ij} is the Kronecker symbol. This equation can be solved for A_i if $\mathcal{C}$ is invertible, i.e. $\det \mathcal{C} \neq 0$. The general condition for the two-point function to be factorizable then is $\mu_i \neq \mu_j, i \neq j$, i.e., all roots of the polynomial have order one.

Assuming that these conditions are met, the solution for the A_i is given by the first row of the inverse matrix $\mathcal{C}$, $A_i = \left(\mathcal{C}^{-1}\right)_{1i}$. The explicit solution for the A_i is then given by

$$A_i = \left(\prod_{j\neq i}(\mu_i-\mu_j)\right)^{-1}\,. \tag{7.5}$$

For future reference, it is convenient to give the coefficients A_i entering the decomposition (7.2) for the cases $n=2$ and $n=3$ explicitly. For $n=2$,

$$A_1 = \frac{1}{\mu_1-\mu_2}\,, \quad A_2 = \frac{1}{\mu_2-\mu_1}\,, \tag{7.6}$$

while for $n=3$ one has

$$A_1 = \frac{1}{(\mu_1-\mu_2)(\mu_1-\mu_3)}\,,\; A_2 = \frac{1}{(\mu_2-\mu_1)(\mu_2-\mu_3)}\,,\; A_3 = \frac{1}{(\mu_3-\mu_1)(\mu_3-\mu_2)}\,. \tag{7.7}$$

At this stage the following remark is in order. On mathematical grounds the decomposition (7.2) works as long as all roots of the polynomial have order one. On physical grounds there are extra conditions on the roots: comparing (7.2) and (6.16) establishes that $\mu_i = m^2$ should be identified with the square of the particle mass. This implies that roots located at the negative real axis correspond to modes with a negative mass squared. In this case the isolated poles at $p_0 = \pm\sqrt{\vec{p}^2+\mu_i}$ are turned into branch cuts and we will not consider this tachyonic case in the following. Moreover, complex roots always come in pairs $\mu, \bar{\mu}$. This implies that the positive frequency Wightman function contains unstable modes which grow exponentially in the far past and far future (also see [31] for a detailed discussion of this feature). On this basis, we restrict ourselves to polynomials $P_n(p^2)$ whose roots are located at the positive real axis, see Fig. 7.

Since the rate function (6.14) is linear in the Wightman function, it is rather straightforward to obtain the detector response function for the case (7.2). Following the steps of

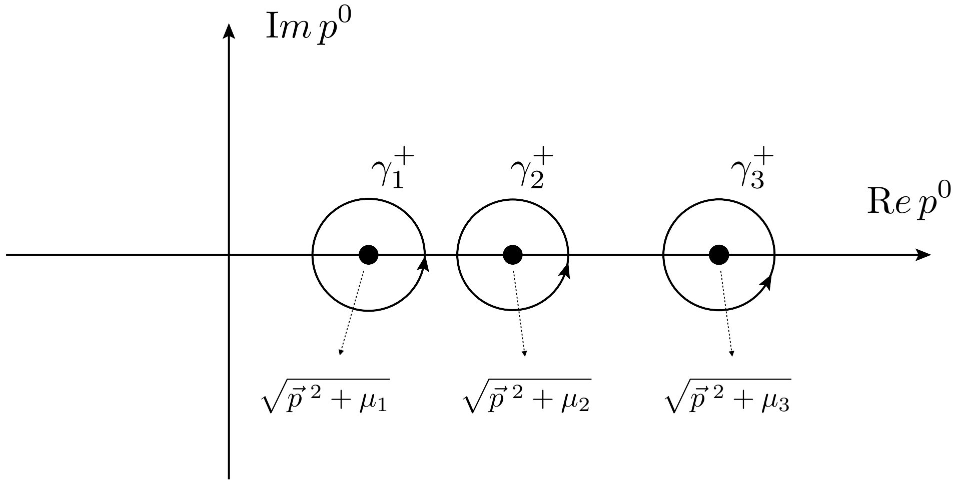

Figure 7: Integration contours for the positive frequency Wightman function based on the Ostrogradski decomposition (7.2) of the function $\widetilde{G}(p^2)$.

Sect. 6.3, we can compute the profile function $\mathcal{F}(E)$ determining the rate (6.32). Substituting the explicit form of the A_i from (7.5) the result reads

$$\mathcal{F}(E) = \frac{1}{c} \sum_{i=1}^{n} \left(\prod_{j \neq i} (\mu_i - \mu_j) \right)^{-1} \sqrt{E^2 - \mu_i}\, \theta(E - \sqrt{\mu_i})\,. \tag{7.8}$$

The rate function is completely determined by the roots of the polynomial $\mathcal{P}_n(p^2)$. It receives new contributions once new channels become available, i.e., if the energy gap E crosses a threshold μ_i where new degrees of freedom enter. Ordering the roots μ_i by their magnitude, i.e., $\mu_j > \mu_i$ for $j > i$, one sees that the sector with μ_j, $j > i$ does not affect the "low-energy" part of the rate function with $E < \mu_i$: the energy gap E of the detector is not large enough to absorb a particle of mass $\sqrt{\mu_j}$, $j > i$. This, in particular, implies that if the polynomial (7.1) arises from an effective field theory description of a system, there are no corrections to the massless Unruh effect below the first threshold $\mu_2 > 0$, provided that the polynomial $\mathcal{P}_n$ is properly normalized. The master formula (7.8) then constitutes the main result of this section.

7.2 Detector rates from the Källen-Lehmann representation

Notably, not all two-point functions proposed in the context of quantum gravity fall in the class where the Ostrogradski-type decomposition is admissible. A prototypical example is provided by Causal Set Theory. Here $\widetilde{G}(p^2)$ interpolates between the standard propagator for a massive scalar field for momenta p^2 below the discretization scale and a nonlocal expression without giving rise to additional poles in the complex p^0-plane [18, 19]. In these cases it is still possible to obtain an explicit formula for the profile function $\mathcal{F}(E)$ based on the Källen-Lehmann representation of the two-point function.

The Källen-Lehmann representation of the positive frequency Wightman function in position space is given by

$$G_+(t, \vec{x}) = \int_0^\infty dm^2\, \rho(m^2)\, G_+^{(0)}(t, \vec{x}; m)\,. \tag{7.9}$$

Here $\rho(m^2)$ denotes a spectral density and $G_+^{(0)}(t, \vec{x}; m)$ is the positive-frequency Wightman function given in (6.17). Substituting the Källen-Lehmann representation into (6.14) and exchanging the order of integration, the computation of the rate function reduces to the one for the massive scalar field carried out in Sect. 6.3. The resulting profile function $\mathcal{F}(E)$, (6.32), is given by

$$\mathcal{F}(E) = \int_0^{E^2} dm^2 \, \rho(m^2) \, \sqrt{E^2 - m^2} \, . \tag{7.10}$$ spectralF

Hence the profile function obtained from the Källen-Lehmann representation is given by the superposition of contributions with mass m weighted by the spectral density $\rho(m^2)$. Only excitations with mass below the energy gap of the detector contribute to the rate function, which is consistent with the expectation that contributions with $m^2 > E^2$ will not excite the detector. The result from the Ostrogradski decomposition, (7.8), can then be understood as a special case where $\rho(m^2)$ is given by a sum of δ-distributions located at $m^2 = \mu_i$.

Dimensional reduction in general seems to be at odd with unitarity. On a manifold with spectral dimension d_s, the asymptotic form of the two-point function in momentum space is

$$G(p^2) \sim (p^2)^{d/d_s} \, . \tag{7.11}$$

Expressing a general two-point function through the Källen-Lehmann representation as in the previous section, we see that, as soon as $d_s < d$, its fall-off properties can only be consistent with the p^{-2} behavior of the spectral representation if we relax the positivity properties of the spectral function $\rho(m^2)$. This automatically entails the presence of negative-normed states and thus a departure from unitarity.

This signals the fact that these types of higher derivative toy models shouldn't be taken too fundamentally. It is likely that dimensional reduction, together with (local) Lorentz invariance, signals the presence of a fundamentally nonlocal theory at small scales. The issue of unitarity for nonlocal theories then is more subtle, see [64] for a more detailed discussion. The higher-derivative toy models can be considered as approximations to a full nonlocal theory, in which unitarity is preserved.

8 Scaling dimensions

sect.3b

The two-point function $\widetilde{G}(p^2)$ serves as the essential input for computing both the spectral dimension D_s seen by a scalar field propagating on the spacetime as well as the rate function of the Unruh detector. Thus, it is conceivable that there is a relation between the rate function of the Unruh detector and the spectral dimension. This section introduces the definitions needed to make this relation precise.

In the computation of the spectral dimension, $p^2 \equiv (p^0)^2 - \vec{p}^{\,2}$ is analytically continued to Euclidean signature $p_E^2 \equiv (p_E^0)^2 + \vec{p}^{\,2} > 0$. Subsequently, one introduces a fiducial diffusion process based on a (modified) diffusion equation

$$\partial_\sigma \, K(x, x'; \sigma) = -F(-\partial_E^2) \, K(x, x'; \sigma) \, , \tag{8.1}$$ diffeq

subject to the boundary condition $K(x, x', 0) = \delta^d(x - x')$. Here σ is the (external) diffusion time, $K(x, x'; \sigma)$ is the diffusion kernel and $F(-\partial_E^2)$ is determined by the equations of motion of the propagating field. In terms of Fourier-modes $F(p_E^2) = (\widetilde{G}(-p_E^2))^{-1}$. The solution of Eq. (8.1) is readily obtained in Fourier-space and reads

$$K(x, x'; \sigma) = \int \frac{d^d p}{(2\pi)^d} \, e^{ip(x-x')} \, e^{-\sigma F(p_E^2)} \, . \tag{8.2}$$

The return probability after diffusion time σ is given by

$$P(\sigma) = \int \frac{d^d p}{(2\pi)^d} \, e^{-\sigma F(p_E^2)} \,, \tag{8.3}$$

and the scale-dependent spectral dimension $D_s(\sigma)$ is defined as

$$D_s(\sigma) = -2 \frac{d \ln P(\sigma)}{d \ln \sigma} \,. \tag{8.4}$$

This definition generalizes the standard definition of the spectral dimension d_s which is recovered by evoking the limit of infinitesimal random walks $\sigma \to 0$. This framework yields the spectral dimension associated with the two-point function $\widetilde{G}(p^2)$ commonly used to assess the dimensionality of spacetime in quantum gravity.

Analyzing the scaling behavior in (8.3) one finds that for the case where $F(p_E^2) \propto p_E^{2+\eta}$ the spectral dimension is given by [7]

$$D_s = \frac{2d}{2+\eta} \,. \tag{8.5}$$

The case of a massless scalar field with $\widetilde{G}(p^2) = p^{-2}$ corresponds to $\eta = 0$ and the spectral dimension agrees with the topological dimension d of the spacetime. In case of a multiscale geometry the scaling law $F(p_E^2) \propto p_E^{2+\eta}$ is obeyed for a certain interval of momenta only. In this case the spectral dimension will depend on the diffusion time σ. If the scaling regime extends over a sufficiently large order of magnitudes, $D_s(\sigma)$ will be approximately constant in this regime, realizing a plateau structure. Typically, such plateaus where $D_s(\sigma)$ is approximately constant are connected by short transition regions where D_s changes rather rapidly, see Fig. 8 for an explicit example illustrating this type of crossover.

In a similar spirit, one can define the effective dimension of spacetime seen by the Unruh detector. Eq. (6.34) indicates that the profile function for a massless scalar field obeying the Klein-Gordon equation in a d-dimensional spacetime scales as

$$\mathcal{F}(E) \propto E^{d-3} \,. \tag{8.6}$$

This motivates defining the effective dimension seen by the Unruh rate, the Unruh dimension D_U, according to

$$D_U(E) \equiv \frac{d \ln \mathcal{F}(E)}{d \ln E} + 3 \,. \tag{8.7}$$

For a massless scalar field with $\widetilde{G}(p^2) = p^{-2}$ or a massive scalar field and energy $E^2 \gg m^2$, D_U is independent of E and coincides with the classical dimension d of the underlying spacetime. Paralleling the discussion of the spectral dimension, this feature changes, however, if $\widetilde{G}(p^2)$ has a non-trivial momentum profile. The examples presented in Sect. 9 indicate that D_U may agree with the spectral dimension in certain cases, but in general the two are different quantities. The Unruh dimension may yield a characterization of quantum spacetimes which is accessible by experiment, at least in principle. Note that the dimensions are only well-defined in plateau regions of sufficient extent and have to be taken with caution during crossovers [7].

A direct comparison between D_U and D_s requires an identification of E and the diffusion time σ. The matching of dimensions in the classical case suggests using

$$\sigma = E^{-2n} \,, \tag{8.8}$$

where $2n$ is the mass-dimension of $\widetilde{G}(p^2)$. We will use this relation in the sequel.

The emission/absorption rates can be related to the density of states of the system interacting with the detector. The density of states as a function of momentum can be defined as $\rho(k) = d\Omega(k)/dk$, where $\Omega(k)$ is the volume of momentum space. Since the spectral dimension d_s is the Hausdorff dimension of momentum space, we can assume that Ω will scale as $\Omega(k) \sim ck^{d_s}$. Then we see that $\rho(k) \propto k^{d_s-1}$, and a smaller value of d_s entails a suppression of the density of states. This in turn will imply a suppression of the various transition rates. Due to the relation between this density of states and the transition rates, we expect a relation between the spectral and Unruh dimensions, D_s and D_U. This relation will indeed be made more precise in the next sections.

9 Unruh rates and dimensional flows

sect.4

We illustrate the general formalism devised in Sect. 7 by first studying corrections to the Unruh rate arising within quantum gravity inspired multiscale models in Sect. 9.1. The connection to Kaluza-Klein theories, spectral actions, and Causal Set Theory will be made in Sects. 9.2, 9.3, and 9.4, respectively.

9.1 Dynamical dimensional reduction

sect.41

In this subsection we investigate modifications of the Unruh rate arising from a particular class of quantum-gravity inspired two-point functions $\widetilde{G}(p^2)$ typically encountered when discussing the flows of the spectral dimension.

Two-scale models

The simplest way to obtain a system exhibiting dynamical dimensional reduction is based on a polynomial, (7.1) with $n = 2$, containing a single mass scale m:

$$\mathcal{P}_2(p^2) = -\frac{1}{m^2}\, p^2\, \left(p^2 - m^2\right)\,. \tag{9.1}$$

ansatz1

Here the normalization c has been chosen such that the model gives rise to a canonically normalized two-point function at low energy. The scaling of this ansatz is given by

$$\mathcal{P}_2(p^2) \propto \begin{cases} p^2\,, & p^2 \ll m^2 \\ p^4\,, & p^2 \gg m^2\,, \end{cases} \tag{9.2}$$

with the crossover occurring at m^2. Evaluating (8.5), the spectral dimension based on this model interpolates between a classical regime with $D_s = 4$ for long diffusion times and $D_s = 2$ for short diffusion times.

The Ostrogradski decomposition (7.2) of (9.1) yields

$$\widetilde{G}(p^2) = \frac{1}{p^2} - \frac{1}{p^2 - m^2}\,. \tag{9.3}$$

2point

The master formula (7.8) gives the following expression for the profile function

$$\mathcal{F}(E) = E - \sqrt{E^2 - m^2}\,\theta(E - m)\,. \tag{9.4}$$

2scalemodel

Expanding $\mathcal{F}$ for small and large E leads to the scaling behavior

$$\begin{aligned} E < m: &\qquad \mathcal{F}(E) = E &\quad \Longleftrightarrow \quad& D_U = 4\,, \\ E \gg m: &\qquad \mathcal{F}(E) = \tfrac{1}{2E} + \mathcal{O}(E^{-2}) &\quad \Longleftrightarrow \quad& D_U = 2\,. \end{aligned} \tag{9.5}$$

2scaleasym

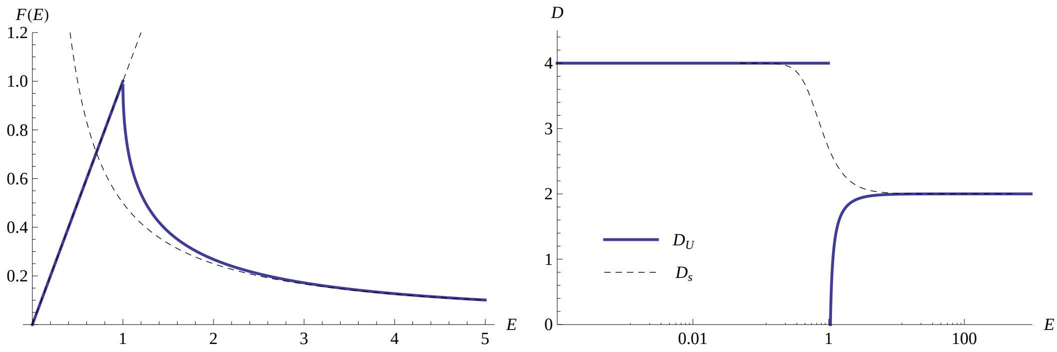

Fig.dimflow1 Figure 8: Profile function $\mathcal{F}(E)$, (9.4), for $m = 1$ (left panel). The asymptotics given in (9.5) are illustrated by the dashed lines. The right panel shows the dimensions D_s (dashed line) and D_U (solid line) resulting from the two-point function (9.3).

This expansion implies that a kinetic term including higher-derivative contributions leads to detector rates which are suppressed at high energies. In particular, whereas for a massless (free or interacting) scalar field with a standard kinetic term the prefactor of the rate grows linearly with energy, the profile function vanishes proportional to E^{-1} at high energies. This also entails that the Unruh dimension D_U interpolates between the classical dimension $D_U = 4$ for small energy and $D_U = 2$ for $E \gg m$.

For $m = 1$ this profile function is shown in the left panel of Fig. 8. Despite the inclusion of modes with a wrong sign kinetic term (poltergeists) in (9.3) the Unruh rate is positive definite, indicating that the model is stable in this respect. The right panel of Fig. 8 shows the spectral dimension (dashed line) and effective dimension seen by the Unruh effect (solid line) where the construction of the spectral dimension is based on the identification (8.8). Both dimensions interpolate between $D = 4$ for $E < m$ and $D = 2$ for $E \gg m$. D_U displays a discontinuity at $E^2 = m^2$ which can be tracked back to the derivative of the square-root becoming singular at this point.

Multi-scale models

At this stage it is instructive to consider a multiscale model which may exhibit more than two scaling regions. The simplest model of this form is build from a third order polynomial $\mathcal{P}_3(p^2)$ with vanishing mass $m_1 = 0$

$$\mathcal{P}_3(p^2) = \frac{1}{m_2^2\, m_3^2}\, p^2\, (p^2 - m_2^2)\, (p^2 - m_3^2)\,, \qquad m_3 > m_2\,. \tag{9.6}$$ ansatz2

Provided that $m_3 \gg m_2$ this ansatz exhibits three scaling regimes

$$\mathcal{P}_3(p^2) \propto \begin{cases} p^2\,, & p^2 \ll m_2^2\,, & D_s = 4 \\ p^4\,, & m_2^2 \ll p^2 \ll m_3^2\,, & D_s = 2 \\ p^6\,, & m_2^3 \gg p^2\,, & D_s = \frac{4}{3}\,, \end{cases} \tag{9.7}$$ 3scalemod

where the spectral dimension has been determined by evaluating (8.5).

Performing the Ostrogradski decomposition for $\mathcal{P}_3(p^2)$ gives

$$\widetilde{G}(p^2) = \frac{1}{p^2} - \frac{m_3^2}{m_3^2 - m_2^2}\,\frac{1}{p^2 - m_2^2} + \frac{m_2^2}{m_3^2 - m_2^2}\,\frac{1}{p^2 - m_3^2}\,. \tag{9.8}$$

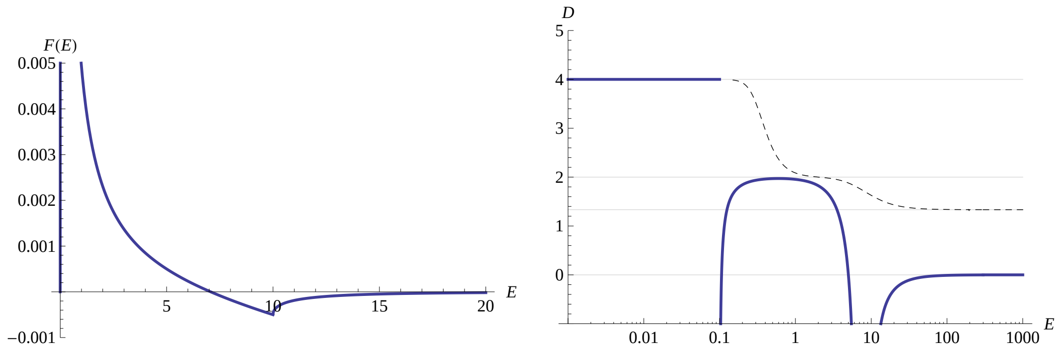

Fig.dimflow2 Figure 9: Illustration of the Unruh effect in a $n = 3$ multiscale model with $m_1 = 0$, $m_2 = 0.1$ and $m_3 = 10$. The resulting profile function $\mathcal{F}(E)$ is shown in the left panel while D_U and D_s are displayed in the right panel. The horizontal gray lines indicate the plateau values of the dimensions at $4, 2, 4/3$ and 0. Notably, D_U and D_s exhibit different asymptotics for $E \gg m_3$.

The resulting profile function then reads

$$\mathcal{F}(E) = E - \frac{m_3^2}{m_3^2 - m_2^2} \sqrt{E^2 - m_2^2}\, \theta(E - m_2) + \frac{m_2^2}{m_3^2 - m_2^2} \sqrt{E^2 - m_3^2}\, \theta(E - m_3) \,. \qquad (9.9)$$

Expanding $\mathcal{F}$ for small and large E leads to the scaling behavior

$$\begin{array}{llcl} E < m_2 : & \mathcal{F}(E) = E & \Longleftrightarrow & D_U = 4 \,, \\ E \gg m_3 : & \mathcal{F}(E) = -\frac{m_2^2 m_3^2}{8E^3} + \mathcal{O}(E^{-4}) & \Longleftrightarrow & D_U = 0 \,. \end{array} \qquad (9.10)$$

3scaleasym

At this stage two remarks are in order. In contrast to the two-scale model, the $n = 3$ case exhibits regions where the profile function $\mathcal{F}(E)$ actually becomes negative. This is illustrated in the example shown in Fig. Fig.dimflow2 9. The form where $\lim_{E\to\infty} F(E) \to 0$ from below then indicates that this feature holds for all values m_2 and m_3. Thus the Unruh rate exhibits an instability for a generic $n = 3$ model.

Furthermore, the spectral and Unruh dimensions shown in the right panel of Fig. Fig.dimflow2 9 show that, contrary to the two-scale model, the asymptotics for D_U and D_s do not agree for $E \gg m_3^2$. In the general case, this may be understood as follows. Considering the general expression (moddetrate 7.8) for $m_1 = 0$, D_U is given by the classical dimension as long as $E < m_2$. Each additional term in the sum creates a new scaling region where D_U decreases by two compared to its previous value. In contrast the pattern for the spectral dimension follows from (spectraldimension 8.5). Combining these relations allows to express the effective dimension seen by the Unruh effect in terms of the spectral dimension

$$D_U = 6 - \frac{8}{D_s} \,. \qquad (9.11)$$

dimrel

Thus, while there is a clear relation between D_U and D_s, the effective dimensions seen by a random walk and the Unruh effect generically do not coincide within the class of multiscale models studied here.

Logarithmic correlation functions

An interesting model which does not fall into the class of multiscale models where the Ostrogradski decomposition can be applied arises from

$$\widetilde{G}(p^2) = p^{-4} \,. \qquad (9.12)$$

p4model

This is the typical fall-off behavior of correlation functions in quantum gravity models which lead to $D_s = 2$ in the ultraviolet. In this case the positive-frequency Wightman function is

$$G_+(\vec{x}, t) = -i \int \frac{d^3k}{(2\pi)^3} \oint_{\gamma_+} \frac{dk^0}{2\pi} \frac{e^{i\vec{k}\cdot\vec{x} - ik^0 t}}{(k^0 + |\vec{k}|)^2 (k^0 - |\vec{k}|)^2} \,. \tag{9.13}$$

Picking up the double pole at $k^0 = |\vec{k}|$, and setting $\vec{x} = 0$ before carrying out the angular momentum integral, one obtains

$$G_+(\vec{x}, t) = -4\pi \int_0^\infty \frac{dk}{(2\pi)^3} k^2 \left[\frac{2}{(2k)^3} + \frac{it}{(2k)^2} \right] e^{-ik(t - i\epsilon)} = I_1 + I_2 \,. \tag{9.14}$$

I12

The second integral is simply

$$I_2 = -\frac{1}{8\pi^2} \,. \tag{9.15}$$

The first integral can be written as a regularized Laplace transform and gives

$$I_1 = \lim_{\epsilon \to 0^+} \lim_{\tilde{\epsilon} \to 0^+} \Gamma(\tilde{\epsilon}) \, (\epsilon + it)^{-\tilde{\epsilon}} = \frac{1}{8\pi^2} \left(\log t + \text{const} \right) \,. \tag{9.16}$$

Thus the resulting positive frequency Wightman function has a logarithmic dependence on the proper distance. Restoring Lorentz invariance, we get

$$G_+(\vec{x}, t) = \frac{1}{8\pi^2} \left[\log \left(\sqrt{(t - t' - i\epsilon)^2 - (\vec{x} - \vec{x}')^2} \right) + \text{const} \right] \,. \tag{9.17}$$

Substituting the Wightman function into the formula for the Unruh rate, (parkereq2 6.14), yields

$$\dot{F}(E) = \frac{1}{8\pi^2} \int_{-\infty}^{\infty} d\tau e^{iE\tau} \left[\log \left(\frac{2 \sinh(\frac{a\tau}{2})}{a\tau} \right) + \text{const} \right] \,. \tag{9.18}$$

The constant terms give rise to terms proportional to $\delta(E)$, indicating an infrared instability of the setup. Since the propagator (p4model 9.12) is thought of describing the asymptotic behavior of the system at high energies we will ignore these terms in the following. Since the argument of the logarithm is an even function in τ the integral can be expressed as a (regularized) Fourier cosine transform

$$\dot{F}(E) = \lim_{\epsilon \to 0^+} \frac{1}{2a\pi^2} \int_0^\infty dx e^{-\epsilon x} \log \left(\frac{\sinh(x)}{x} \right) \cos(\omega x) \,. \tag{9.19}$$

written in terms of the new variables $x = a\tau/2$ and $\omega = 2E/a$. This integral can now be written as $I = I_1 - I_2$, where

$$\begin{aligned} I_1 &= \lim_{\epsilon \to 0^+} \frac{1}{2a\pi^2} \frac{d}{d\alpha} \int_0^\infty dx e^{-\epsilon x} \left(\sinh(x) \right)^\alpha \cos(\omega x) \Big|_{\alpha \to 0} = -\frac{\pi \coth(\frac{\pi\omega}{2})}{2\omega} \,, \\ I_2 &= \lim_{\epsilon \to 0^+} \frac{1}{2a\pi^2} \frac{d}{d\alpha} \int_0^\infty dx e^{-\epsilon x} x^\alpha \cos(\omega x) \Big|_{\alpha \to 0} = -\frac{\pi}{2\omega} \,. \end{aligned} \tag{9.20}$$

Combining the two contributions, the resulting detector rate is given by

$$\dot{F}(E) = \frac{1}{4\pi E} \frac{1}{1 - e^{\frac{2\pi E}{a}}} \,, \tag{9.21}$$

implying that the profile function resulting from a p^{-4} propagator is given by

$$\mathcal{F}(E) = \frac{1}{2E} \qquad \Longleftrightarrow \qquad D_U = 2 \,. \tag{9.22}$$

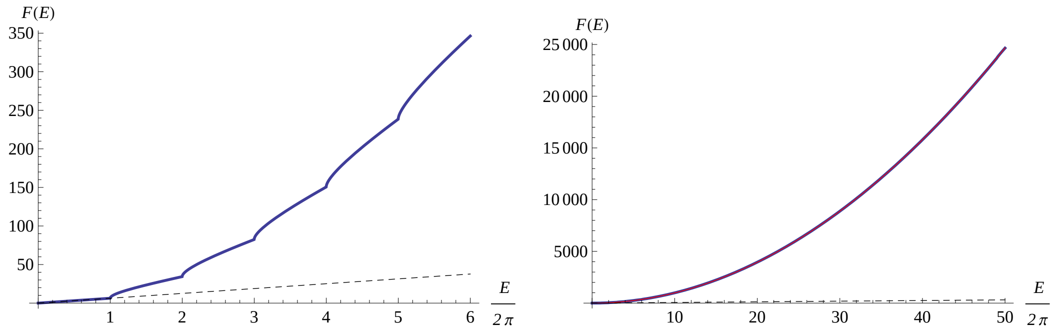

FigKKprofile Figure 10: Profile function $\mathcal{F}(E)$ for a 5-dimensional Kaluza-Klein theory (9.24) with $R = 1/(2\pi)$ (blue, solid line). For guidance the lines $\mathcal{F}(E) = E$ (black, dashed line) and $\mathcal{F}(E) = E^2/4$ (red line, right diagram) have been included. For $E < R^{-1}$ the profile function is linear in E, while for $E \gg R^{-1}$ it increases proportional to E^2.

This is precisely the asymptotic behavior (9.5) found in the two-scale model in the limit $E \gg m$. Thus the direct computation of the detector rate in the p^4-case confirms the drop of the Unruh rate at high energies and constitutes an independent verification of the rate function found in the two-scale case.

sect.43

9.2 Kaluza-Klein theories

A scenario where the dimensional reduction occurs when going towards the *infrared* is provided by Kaluza-Klein theories.[11] In this case the (classical) spacetime is assumed to possess four non-compact and a number of compact spatial dimensions whose typical extension is given by the compactification scale R. At length scales $l \gg R$ the effect of the extra-dimensions is invisible and physics is effectively four-dimensional. We demonstrate that also in this situation the dimensional reduction entails a suppression in the Unruh effect. In the case of Kaluza-Klein theories where the number of effective dimensions increases when going to high energies this implies that the detector rates for energies above the inverse compactification scale are actually *enhanced* as compared to the four-dimensional rate.

For the scalar field (4.16) given in Sect. 4.3, each Kaluza-Klein mode ϕ_n has a two-point function of a scalar field with mass $m_n = n/R$. Taking into account the entire tower of modes, the resulting function $\widetilde{G}(p^2)$ is given by

$$\widetilde{G}(p^2) = \frac{1}{2\pi R} \sum_{n=-\infty}^{\infty} \left(p^2 - \frac{n^2}{R^2} \right)^{-1} . \tag{9.23}$$

Applying the master formula (7.8) to this case then yields the profile function

$$\mathcal{F}(E) = \frac{1}{2\pi R} \left(E + 2 \sum_{n=1}^{\infty} \sqrt{E^2 - (n/R)^2}\, \theta(E - n/R) \right) . \tag{9.24}$$ kkprofile

The shape of this profile function is illustrated in Fig. 10. In contrast to the case of a dynamical dimensional reduction at high energies, all Kaluza-Klein modes contribute to the profile function with the same sign. This leads to an effective enhancement of the

[11] A related discussion of the Unruh detector in Kaluza-Klein theories appeared in Ref. [65] during the final stage of preparing the manuscript.

profile function for $E > R^{-1}$. Explicitly,

$$\begin{aligned} E < 1/R: &\qquad \mathcal{F}(E) \propto E &\quad \Longleftrightarrow \quad& D_U = 4\,, \\ E \gg 1/R: &\qquad \mathcal{F}(E) \propto E^2 &\quad \Longleftrightarrow \quad& D_U = 5\,. \end{aligned} \tag{9.25}$$

The profile function (9.24) interpolates between these two behaviors. Thus also the presence of extra dimensions leaves its imprint on the Unruh rate, adapting the scaling law of the profile function once the energy E exceeds the inverse compactification scale.

9.3 Spectral actions

sect.44

A framework which naturally gives rise to two-point functions $\widetilde{G}(p^2)$ with the properties discussed above are spectral actions. As explained in Sect. 3, the basic idea is that the action describing the dynamics of the theory is generated by the trace of a suitable differential operator, typically the Dirac operator $\mathcal{D}$

$$S_{\chi,\Lambda} = \mathrm{Tr}\big[\chi(\mathcal{D}^2/\Lambda^2)\big]\,. \tag{9.26}$$

SpAct1

Here we focus on the case where $\mathcal{D}^2$ is given in terms of the Laplace operator on flat Euclidean space supplemented by an endomorphism including a real scalar field ϕ:[12]

$$\mathcal{D}^2 = -\left(\nabla^2 \mathbb{1} + E\right)\,, \quad E = -i\gamma^\mu \gamma_5 \partial_\mu \phi - \phi^2\,. \tag{9.27}$$

lapop

The definition of the model is then completed by specifying the function χ.

Nonlocal analytic models

We first discuss the case where $\chi(z) = e^{-z}$. In this case the spectral action (9.26) coincides with the heat-trace of the Laplace-type operator (9.27) which is a well-studied mathematical object, see e.g., [66, 67, 68, 69, 70, 71]. In particular the two-point function of the model is given by

$$S^{(2,\phi)}_{\chi,\Lambda} = \frac{\Lambda^2}{(4\pi)^2} \int d^4x \left[\, \phi\, F_0(-\partial_E^2/\Lambda^2)\, \phi \,\right]. \tag{9.28}$$

spectral2

The structure function F_0 is obtained from the heat-kernel result for the endomorphism E and reads [23]

$$F_0\,(z) = 2\,z\,h\,(z) - 4\,, \tag{9.29}$$

with

$$h(z) = \int_0^1 d\alpha\, e^{-\alpha(1-\alpha)z}. \tag{9.30}$$

The function $h(z)$ is an entire analytic function which is nowhere vanishing in the complex plane. The momentum-dependent two-point function for this model is then obtained by analytically continuing (9.28) to Lorentzian signature

$$\widetilde{G}(p^2) = -\frac{8\pi^2}{\Lambda^2}\,\frac{1}{F_0(-p^2/\Lambda^2)}\,, \tag{9.31}$$

ss1

where p^2 is the Lorentzian momentum four-vector.

[12] The spectral dimension arising in this situation has recently been studied in [24], also see [23] for a related discussion.

A careful study of the two-point function (9.31) reveals several remarkable features. First, the model naturally gives rise to a Higgs mechanism for ϕ. The propagator exhibits a pole at $p^2 \simeq -3.41\Lambda^2$ indicating that the expansion of ϕ around vanishing field value corresponds to expanding at an unstable point in the potential. Restoring the ϕ^4 term[13] leads to a scalar potential

$$V(\phi) = -\mu_H^2 \phi^2 + \lambda\phi^4 + \dots\,, \tag{9.32}$$

with $\mu_H^2 = 2\Lambda^2$. Neglecting the higher-order terms, the potential gives a non-vanishing vacuum expectation value $\langle\phi\rangle = \pm\frac{\mu_H}{\sqrt{2\lambda}}$. Expanding the field around this minimum leads to a potential for the fluctuation field $\tilde{\phi}$

$$V(\tilde{\phi}) = 2\,\mu_H^2\,\tilde{\phi}^2 + \dots\,, \tag{9.33}$$

Thus, when expanded around the minimum of the scalar potential, the structure function entering into (9.31) should be given by

$$F_H(z) = 2\,z\,h(z) + 8\,. \tag{9.34}$$

$F_H(z)$ has a single real root located at $p^2 \simeq 2.56\Lambda^2$. This root corresponds to a positive mass pole in (9.31). In addition there are complex roots located, e.g., at

$$p^2 = -\,(1.32 \pm 21.98i)\,\Lambda^2\,. \tag{9.35}$$

These roots can be traced back to the mass-term contribution in F_0 or F_H and are absent if one considers the $zh(z)$ part only. The presence of complex roots signals that the Wightman function contains modes which increase exponentially for large times. These modes introduce an instability in the Unruh effect, which we will not investigate further. It would be very interesting to see if there are functions χ which give rise to a nonlocal theory avoiding this instability.

Ostrogradski-type models

By making a suitable choice for the function χ one can also generate spectral actions which are local in the sense that the (inverse) two-point function is given by a finite polynomial in p^2.[14] The simplest choice, leading to a two-scale model, uses

$$\chi(z) = (a+z)\,\theta(1-z)\,, \quad a > 0\,. \tag{9.36}$$

Replacing the polynomial multiplying the stepfunction by a polynomial of order n leads to a multiscale model whose inverse propagator is given by a polynomial of order n in p^2.

The spectral action for these cases can be found explicitly by combining the early-time expansion of the heat-kernel in $s \equiv \Lambda^{-2}$

$$\begin{aligned} F_H &= \frac{1}{(4\pi)^2}\frac{1}{s}\sum_{m=0}^{\infty} a_m\,(p_E^2\,s)^m\,, \\ &= \frac{1}{(4\pi)^2}\frac{1}{s}\left(8 + 2\,s\,p_E^2 - \frac{1}{3}\left(s\,p_E^2\right)^2 + \dots\right) \end{aligned} \tag{9.37}$$

with standard Mellin transform techniques [73]

$$S^{(2,\phi)}_{\chi,\Lambda} = \frac{1}{(4\pi)^2}\int \frac{d^4p}{(2\pi)^4}\,\phi\left[\sum_{m=0} Q_{m+1}[\chi]\,a_m\,(p_E^2)^m\right]\phi\,. \tag{9.38}$$

[13] For a discussion of the Higgs mechanism in almost-commutative geometry see Sect. 11.3.2 of [55].
[14] This is closely related to the zeta-function spectral action proposed in [72].

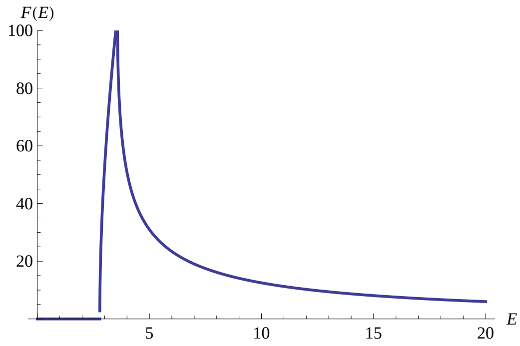

Figure 11: Profile function (9.43) for $a = 3.2$.

The moments Q_n depend on the function χ and, for $n \in \mathbb{Z}$ are given by

$$\begin{aligned} Q_n[\chi] &= \tfrac{1}{\Gamma(n)} \int_0^\infty dz\, z^{n-1}\, \chi(z)\,, \qquad && n > 0\,, \\ Q_{-n}[\chi] &= (-1)^n\, \chi^{(n)}(0)\,, && n \geq 0\,. \end{aligned} \tag{9.39}$$

For the ansatz (9.36) the moments are

$$Q_1[\chi] = a + \frac{1}{2}, \quad Q_0[\chi] = a, \quad Q_{-1}[\chi] = -1, \quad Q_{-2} = Q_{-3} = \ldots = 0. \tag{9.40}$$

Converting to Lorentzian signature, the inverse two-point function based on the expansion of F_H, (9.34) is

$$\mathcal{P}_2(p^2) = -\frac{1}{8\pi^2}\left(8a + 4 - 2ap^2 + \frac{1}{3}p^4\right)\,. \tag{9.41}$$

The two roots of the system are located at

$$\mu_{1,2} = 3a \mp \sqrt{9a^2 - 24a - 12}\,. \tag{9.42}$$

Provided that $2(2+\sqrt{7})/3 < a < (3+\sqrt{15})/2$, both roots are on the positive real axis. Thus the model falls into the class discussed in Sect. 9.1. The profile function is readily obtained by applying the Ostrogradski decomposition to (9.41)

$$\mathcal{F}(E) = \frac{24\pi^2}{\mu_2 - \mu_1}\left(\sqrt{E^2 - \mu_1}\,\theta(E - \sqrt{\mu_1}) - \sqrt{E^2 - \mu_2}\,\theta(E - \sqrt{\mu_2})\right)\,. \tag{9.43}$$

The behavior of this profile function is illustrated in Fig. 11.

For $E^2 < \mu_1$ the profile function vanishes, indicating that the energy gap is too small for the detector to interact with the two massive fields. For $7.77 < E^2 < 12.77$ the profile corresponds to the standard Unruh rate for a field with mass $m^2 = 7.77$. Once E^2 crosses the threshold at 12.77 the profile function decreases and falls of asymptotically as E^{-1} for high energies. Thus spectral actions may give rise to similar profile functions as the multiscale models discussed at the beginning of this section.

9.4 Causal Set inspired theories

A second framework which naturally gives rise to corrections to the Unruh effect are the nonlocal two-point functions emerging in the context of Causal Set Theory. In this case the two-point functions extrapolate between a classical massless or massive propagator at energy scales well below the discretization scale and a discrete D'Alembertian naturally associated with the Causal Set at high energies [31, 74]. In this section we will derive the resulting Unruh signature arising from this setting as well as from Causal Set inspired toy models.

Rate suppression in the full theory

The explicit form of the two point function reads[15]

$$G_+(x^2) = -\frac{i}{2\pi^3}\int_0^\infty d\xi\xi^2 \frac{K_1(i\sqrt{x^2}\xi)}{\sqrt{x^2}\,\xi\, g(\xi^2)}\,, \tag{9.44}$$

2pointcausal

where ξ is a momentum and

$$g(\xi^2) = a + 4\pi\xi^{-1}\sum_{n=0}^{3}\frac{b_n}{n!}C^n \int_0^\infty s^{4(n+1/2)}e^{-Cs}K_1(\xi s)ds\,. \tag{9.45}$$

The parameters are determined based on the analytic properties of the two-point function and given by $a = -\frac{4}{\sqrt{6}}$, $b_0 = \frac{4}{\sqrt{6}}$, $b_1 = -\frac{36}{\sqrt{6}}$, $b_2 = \frac{64}{\sqrt{6}}$, $b_3 = -\frac{32}{\sqrt{6}}$, $C = \frac{\pi}{24}$. The asymptotics of $g(\xi^2)$ has been determined in [31]

$$\begin{aligned}\lim_{\xi^2\to 0}\frac{1}{g(\xi^2)} &= -\frac{1}{\xi^2} + \cdots\,,\\ \lim_{\xi^2\to\infty}\frac{1}{g(\xi^2)} &= -\frac{2\sqrt{6}\pi}{\xi^4} + \cdots\,.\end{aligned} \tag{9.46}$$

asymptotics

We thus see that at high energies the two-point function has a characteristic p^{-4} behavior. The profile function will then asymptotically match the result we already derived in Sect. 5.1, for the logarithmic case, displaying a $1/E$ fall off.

Using the two-point function as above, the equation for the detector rate gives

$$\dot{F} = \frac{-i}{2\pi^3}\int_0^\infty \frac{d\xi\xi^2}{g(\xi^2)}\int_{-\infty}^\infty d\tau e^{-iE\tau}\left(\frac{K_1(\frac{2i\xi}{a}\sinh(\frac{a}{2}(\tau-i\epsilon)))}{\frac{2\xi}{a}\sinh(\frac{a}{2}(\tau-i\epsilon))} - \frac{K_1((\tau-i\epsilon)\xi)}{(\tau-i\epsilon)\xi}\right)\,, \tag{9.47}$$

from which we arrive at the profile function

$$\mathcal{F}(E) = -\frac{2}{\pi}\int_0^E d\xi\xi\frac{\sqrt{E^2-\xi^2}}{g(\xi^2)}\,. \tag{9.48}$$

In principle this relation gives the exact form of the profile function in Causal Set Theory. Its evaluation requires the full form of $g(\xi^2)$ and cannot be based on the asymptotic expansions (9.46) alone. Performing the resulting integral numerically is beyond the scope of the present work. Instead we will focus on a simplified model which allows for an analytic treatment.

A consistent toy model

The central properties of the two-point correlation function for Causal Sets (9.44) are captured by the combination of a massless pole at zero mass combined with a continuum of states with density $\rho(m^2)$ [75]. The resulting positive frequency Wightman function is then given by the sum of the massless one, denoted by $G_+^{(0)}$ and an integral over the continuum of states

$$G_+(t,\vec{x}) = G_+^{(0)}(t,\vec{x};m=0) + \int_0^\infty dm^2\rho(m^2)\,G_+^{(0)}(t,\vec{x};m)\,, \tag{9.49}$$

wfcaus2

[15]We set everywhere the sprinkling density ρ to one.

where $G_+^{(0)}(t, \vec{x}; m)$ denotes the Wightman function for a scalar of mass m. Inspired by [75] it is conceivable that all relevant physics of the Causal Set construction is retained by approximating the density of states by

$$\rho(m^2) = e^{-\alpha m^2} \sum_{n=0}^{N} b_n \, m^{2n} \, . \tag{9.50}$$

Here α is a parameter of order one, b_0 is related to the nonlocality scale, and the remaining b_n's are free parameters.

As a consistency requirement, the simplified model should recover the massless theory in the infrared limit. This is ensured by requiring that the continuum contribution to (9.49) vanishes in the limit where the geodesic distance $Z \equiv (t-t')^2 - (\vec{x} - \vec{x}')^2$ goes to infinity. Substituting (9.50) into (9.49) this condition entails

$$\lim_{Z \to \infty} \sum_{n=0}^{N} b_n \int_0^\infty dm \, e^{-\alpha m^2} \, m^{2n+2} \, \frac{K_1(im\sqrt{Z})}{\sqrt{Z}} = 0 \, . \tag{9.51}$$

Applying the expansion of $K_1(x)$ for large argument the resulting integral reduces to a representation of a Γ-function and falls off as $Z^{-3/4}$ independent of n. From this, it follows that imposing a classical asymptotic behavior in the infrared does not constrain the parameters b_n.[16]

Evaluating (7.10) for (9.49) yields the profile function for this model

$$\mathcal{F}(E) = E + \sum_{n=0}^{N} b_n \int_0^{E^2} dm^2 \, e^{-\alpha m^2} \, m^{2n} \, \sqrt{E^2 - m^2} \, . \tag{9.52}$$

At this stage, it is instructive to study the case $N = 1$ in detail. Setting $\alpha = 1$, the two integrals can be carried out explicitly, giving rise to imaginary error functions

$$\begin{aligned} I_0 &\equiv \int_0^{E^2} dx \, e^{-x} \, \sqrt{E^2 - x} = E - \tfrac{\sqrt{\pi}}{2} \, e^{-E^2} \, \text{Erfi}(E) \, , \\ I_1 &\equiv \int_0^{E^2} dx \, e^{-x} \, x \, \sqrt{E^2 - x} = \tfrac{3}{2} E - \tfrac{\sqrt{\pi}}{4} e^{-E^2} \, (3 + 2E^2) \, \text{Erfi}(E) \, . \end{aligned} \tag{9.53}$$

Expanding the integrals at $E = 0$ one has

$$I_0 \simeq \tfrac{2}{3} E^3 + \ldots \, , \qquad I_1 \simeq \tfrac{4}{15} E^5 + \ldots \, . \tag{9.54}$$

Thus the low-energy behavior is governed by the massless contribution, independently of the values b_0 and b_1. Looking at the asymptotics of the integrals (9.53) for $E^2 \gg 1$, one has

$$I_0 \simeq E - \frac{1}{2E} + \ldots \, , \qquad I_1 \simeq E - \frac{3}{4E} + \ldots \, . \tag{9.55}$$

Hence, for generic values b_0, b_1 the asymptotic scaling for $E \ll 1$ and $E \gg 1$ is identical. In these cases there is no change in the Unruh dimension. For the special value $b_1 = -(b_0 + 1)$, however, the leading term in the high-energy expansion cancels and the asymptotics of the profile function reads

$$\mathcal{F}(E) = \frac{b_0 + 3}{4E} + \ldots \, . \tag{9.56}$$

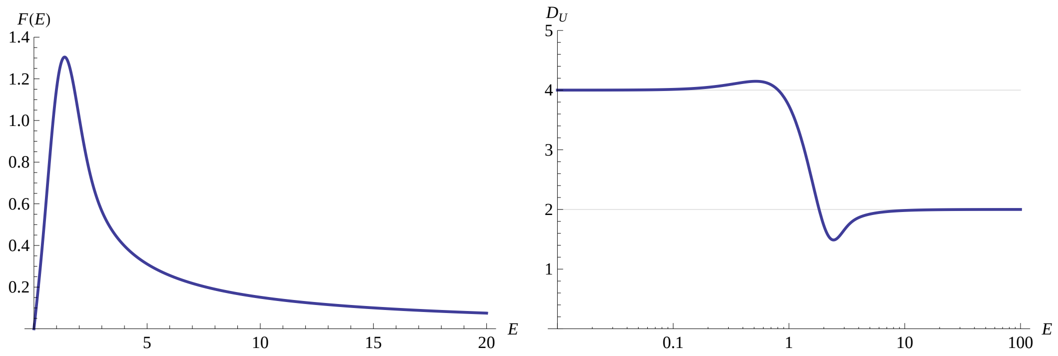

Figure 12: Profile function $\mathcal{F}(E)$ and Unruh dimension D_U arising from (9.52) with $b_0 = 1$, $b_1 = -2$ and $b_n = 0, n \geq 2$.

Thus, for this case the model matches the Unruh rate expected for Causal Set Theory. Setting $b_0 = 1$ the full profile function is shown in Fig. 12. Both the profile function and the Unruh dimension undergo a transition when the energy scale meets the discretization scale controlled by setting $b_0 = 1$.

10 Conclusions and outlook

Due to the geometric nature of the Unruh effect, the radiation temperature (and thus the number operator) is protected against corrections originating from extra dimensions and mass terms. In order to capture possible signatures induced by quantum gravity, we investigated the relation between quantum gravity inspired models exhibiting dynamical dimensional flows and the Unruh effect. Since both the detector approach to the Unruh effect and dimensional flows originate from a non-trivial momentum dependence of the two-point correlation functions there is a natural connection between the two. Explicitly, we focused on two-point functions arising within the context of phenomenologically motivated models for dynamical dimensional reduction, multiscale models, Kaluza-Klein theories, spectral actions, and Causal Set Theory. From the viewpoint of two-point functions, these models come in two distinguished classes. In the first case the inverse two-point function has a polynomial expansion in momentum space. This case is realized within dynamical dimensional reduction, multiscale models, Kaluza-Klein theories, and certain classes of spectral actions. It is also realized in theories that break Lorentz invariance, which we did not touch upon.[17] The models forming the second class possess two-point functions which are quasi-local in the sense that their inverse consists of a first order polynomial multiplying a function which is analytic in the complex plane. This setup is realized by Causal Set Theory. Our study of these models exhibits two universal features. First, despite incorporating quantum (gravity) corrections in the two-point function, the Unruh radiation remains thermal in all cases. Moreover, the low-energy spectrum is robust with respect to corrections of the two-point functions at high energies, i.e., the response of an Unruh detector is not modified below the characteristic scale where the dimensional flow sets in.

The two-point functions occurring in the first class of models can be reduced to a sum

[16] Alternatively, one could notice that the limit in (9.51) is formally of the same type as considered in Appendix A of [31], and thus one can apply the same manipulations to conclude that the limit gives zero irrespective of n.

[17] There is a vast literature on this class of models. See for instance [43, 76, 77, 78]

of (massive) second order propagators through an Ostrogradski-type decomposition. In this case we derive a master formula which expresses the response function of the Unruh detector as a function of the mass poles. Rather than explicitly calculating the response functions, we used the KMS condition to relate the induced emission to the spontaneous emission, where the factor of proportionality is exactly the Planckian distribution. We then calculated the spontaneous emission by approximating the profile function. In the case of a massive scalar field the approximation and numerical result agree for small values of $\frac{a}{m}$, while in the high energy limit the two coincide.

As a generic feature, one finds that dynamical dimensional reduction leads to a suppression of the Unruh effect at high energies while the opening up of extra dimensions leads to an enhancement above the compactification scale. In particular, models where the spectral dimension asymptotes to $D_s \to 2$ at high energies also exhibit a universal falloff in the rate function (6.32) of the Unruh effect $\mathcal{F}(E) \propto 1/E$. We proposed here to quantify this non-trivial asymptotic behavior of the profile function through a new parameter, which we called the *Unruh dimension* of the system. This is defined through the scaling of the profile function, as in (8.7). Differently from other proposed parameters characterizing the high energy behavior induced by quantum gravity effects, this one is directly related to a physical quantity that is accessible experimentally, at least in principle. Moreover, it is directly related to the spectral dimension via the relation (9.11). The specific examples studied in this paper already indicate that different quantum gravity models come with a very distinguished signature in terms of their Unruh detector response function. This may serve as an interesting starting point towards identifying universal features among different approaches to quantum gravity. This requires the computation of positive-frequency Wightman functions within different quantum gravity programs.

Obviously, it would be quite natural to apply the formalism developed in this paper to the gravitational Asymptotic Safety program [79, 73, 80, 81, 82, 83]. In this context, the momentum dependence of two-point functions has recently been studied in [84, 85, 86]. It is clear that an investigation of the Unruh effect should be based on the renormalized propagators where all quantum (gravity) fluctuations have been integrated out. The corresponding expression for the positive-frequency Wightman function is currently not available. Nevertheless, much progress has been made in recent years towards the construction of renormalized two-point functions taking quantum fluctuations into account [87, 88, 89, 85, 86, 90]. On this basis, we expect that it is feasible to compute the fingerprints of Asymptotic Safety in the Unruh effect. This may also be relevant for understanding the fate of black holes within Asymptotic Safety [91, 92, 93, 94, 95, 96, 97, 98, 99, 100, 101] based on first principles.

Another natural extension of our work is the application to Hawking radiation. Here it was argued that the low-energy Hawking spectrum is actually insensitive to Planck scale effects [102]. The situation is quite similar to the one encountered in the present work, where the Unruh spectrum at energy scales below the scale where the dimensional flow sets in is actually unaltered. At the same time there are indications that quantum gravity effects could stop the black hole evaporation process and leave a cold remnant. In particular, it was argued in [103] that the black hole evaporation could come to an end once the spectral dimension drops to $D_s = 3$. This would be relevant for the information problem as well [104]. Applying the techniques based on two-point correlation functions used in the present work may actually allow one to develop these ideas based on a first-principle calculation. We plan to come back to this point in the near-future.

Finally, we have not analyzed the class of models displaying a minimal length. These models are important for quantum gravity phenomenology, since this effect is believed to appear quite generically [105]. It would be interesting to see if a connection to our results can be made.

From an experimental point of view, multiple proposals have been made to acquire experimental evidence for the Unruh effect. Most of these proposals focus on the detection of the Unruh effect through other phenomenologically detectable effects (e.g. the Berry phase [39], the use of the Sokulov-Ternov effect [36]). Practical issues naturally arise as a result of the small imprints left by the Unruh effect. Corrections to the Unruh effect as a result of processes taking place near the Planck-scale will then be even harder to detect with the technology currently at our disposal.

Acknowledgements. I thank my supervisor, Dr Frank Saueressig, Dr Giulio D'Odorico and Natalia Alkofer for answering all my questions, sharing their enthusiasm and introducing me to the field of research. Furthermore, I am grateful to Renz Bakx for his constructive insights on conceptual issues within the first version of this thesis.

References

[1] C. Krishnan, arXiv:1011.5875.

[2] S. Carlip, AIP Conf. Proc. **1196** (2009) 72, arXiv:0909.3329.

[3] S. Carlip, AIP Conf. Proc. **1483** (2012) 63, arXiv:1207.4503.

[4] J. Ambjorn, A. Goerlich, J. Jurkiewicz and R. Loll, Phys. Rept. **519** (2012) 127, arXiv:1203.3591.

[5] J. Ambjorn, J. Jurkiewicz and R. Loll, Phys. Rev. Lett. **95** (2005) 171301, hep-th/0505113.

[6] O. Lauscher and M. Reuter, JHEP **10** (2005) 050, hep-th/0508202.

[7] M. Reuter and F. Saueressig, JHEP **12** (2011) 012, arXiv:1110.5224.

[8] S. Rechenberger and F. Saueressig, Phys. Rev. D **86** (2012) 024018, arXiv:1206.0657.

[9] G. Calcagni, A. Eichhorn and F. Saueressig, Phys. Rev. D **87** (2013) 124028, arXiv:1304.7247.

[10] L. Modesto, Class. Quant. Grav. **26** (2009) 242002, arXiv:0812.2214.

[11] F. Caravelli and L. Modesto, arXiv:0905.2170.

[12] E. Magliaro, C. Perini and L. Modesto, arXiv:0911.0437.

[13] G. Calcagni, D. Oriti and J. Thürigen, Class. Quant. Grav. **31** (2014) 135014, arXiv:1311.3340.

[14] G. Calcagni, D. Oriti and J. Thürigen, Phys. Rev. D **91** (2015) 084047, arXiv:1412.8390.

[15] T. P. Sotiriou, M. Visser and S. Weinfurtner, Phys. Rev. Lett. **107** (2011) 131303, arXiv:1105.5646.

[16] T. P. Sotiriou, M. Visser and S. Weinfurtner, Phys. Rev. D **84** (2011) 104018, arXiv:1105.6098.

[17] A. Eichhorn and S. Mizera, Class. Quant. Grav. **31** (2014) 125007, arXiv:1311.2530.

[18] S. Carlip, Class. Quant. Grav. **32** (2015) 232001, arXiv:1506.08775.

[19] A. Belenchia, D. M. T. Benincasa, A. Marciano and L. Modesto, Phys. Rev. D **93** (2016) 044017, arXiv:1507.00330.

[20] D. Benedetti, Phys. Rev. Lett. **102** (2009) 111303, arXiv:0811.1396.

[21] V. Anjana and E. Harikumar, Phys. Rev. D **91** (2015) 065026, arXiv:1501.00254.

[22] A. V. Harikumar and E. Harikumar, Phys. Rev. D **92** (2015) 045014, arXiv:1504.07773.

[23] M. A. Kurkov, F. Lizzi and D. Vassilevich, Phys. Lett. B **731** (2014) 311, arXiv:1312.2235.

[24] N. Alkofer, F. Saueressig and O. Zanusso, Phys. Rev. D **91** (2015) 025025, arXiv:1410.7999.

[25] L. Modesto, Phys. Rev. D **86** (2012) 044005, arXiv:1107.2403.

[26] L. Modesto and I. L. Shapiro, Phys. Lett. B **755** (2016) 279, arXiv:1512.07600.

[27] T. Padmanabhan, S. Chakraborty and D. Kothawala, Gen. Rel. Grav. **48** (2016) 55, arXiv:1507.05669.

[28] J. J. Atick and E. Witten, Nucl. Phys. B **310** (1988) 291.

[29] G. Calcagni, Phys. Rev. E **87** (2013) 012123, arXiv:1205.5046.

[30] G. Amelino-Camelia, M. Arzano, G. Gubitosi and J. Magueijo, Phys. Rev. D **88** (2013) 103524, arXiv:1309.3999.

[31] S. Aslanbeigi, M. Saravani and R. D. Sorkin, JHEP **1406** (2014) 024, arXiv:1403.1622.

[32] S. A. Fulling, Phys. Rev. D **7** (1973) 2850.

[33] P. C. W. Davies, J. Phys. A **8** (1975) 609.

[34] W. G. Unruh, Phys. Rev. D **14** (1976) 870.

[35] N. D. Birrell and P. C. W. Davies, *Quantum Fields in Curved Space*, Camb. Univ. Press (Cambridge) 1982.

[36] E. T. Akhmedov and D. Singleton, Int. J. Mod. Phys. A **22** (2007) 4797, hep-ph/0610391.

[37] E. T. Akhmedov and D. Singleton, Pisma Zh. Eksp. Teor. Fiz. **86** (2007) 702, arXiv:0705.2525.

[38] D. Kharzeev and K. Tuchin, Nucl. Phys. A **753** (2005) 316, hep-ph/0501234.

[39] E. Martin-Martinez, I. Fuentes and R. B. Mann, Phys. Rev. Lett. **107** (2011) 131301, arXiv:1012.2208.

[40] A. Belenchia, D. M. T. Benincasa, E. Martin-Martinez and M. Saravani, arXiv:1605.03973.

[41] V. Mukhanov and S. Winitzki, *Introduction to quantum effects in gravity*, Camb. Univ. Press (Cambridge) 2007.

[42] W. G. Unruh and N. Weiss, Phys. Rev. D **29** (1984) 1656.

[43] M. Rinaldi, Phys. Rev. D **77** (2008) 124029, arXiv:0802.0618.

[44] P. Nicolini and M. Rinaldi, Phys. Lett. B **695** (2011) 303, arXiv:0910.2860.

[45] I. Agullo, J. Navarro-Salas, G. J. Olmo and L. Parker, New J. Phys. **12** (2010) 095017, arXiv:1010.4004.

[46] E. Martin-Martinez, M. Montero and M. del Rey, Phys. Rev. D **87** (2013) 064038, arXiv:1207.3248.

[47] A. M. Alhambra, A. Kempf and E. Martin-Martinez, Phys. Rev. A **89** (2014) 033835, arXiv:1311.7619.

[48] W.J.P Beenakker, *Reader for the course Quantum Field Theory*,2015-2016.

[49] L. C. B. Crispino, A. Higuchi and G. E. A. Matsas, Rev. Mod. Phys. **80** (2008) 787, arXiv:0710.5373.

[50] Claude Itzykson, Jean-Michel Drouffe, *Statistical Field Theory Volume 1: From Brownian motion to renormalization and lattica gauge theory*, Cambridge University Press, Cambridge, 1989.

[51] J. Hensen, *The causal set approach to Quantum Gravity*, chapter 18, *Approaches to Quantum Gravity*, edited by Daniele Oriti, Cambridge University Press, Cambridge, 2009.

[52] S.W. Hawking, *Quantum gravity and path integrals*, PhysRevD.18.1747, volume 18, number 6, 1978.

[53] J. Petitot, *Noncommutative geometry and physics*, ArXiv:1505.00132.

[54] A. H. Chamseddine and A. Connes, Commun. Math. Phys. **186** (1997) 731, hep-th/9606001.

[55] W. D. van Suijlekom, *Noncommutative geometry and particle physics*, Springer (Heidelberg), 2015.

[56] A. H. Chamseddine and A. Connes, Phys. Rev. Lett. **77** (1996) 4868, hep-th/9606056.

[57] A. Connes and M. Marcolli, *Noncommutative Geometry, Quantum Fields and Motives* American Mathematical Society, 2008.

[58] K. van den Dungen and W. D. van Suijlekom, Rev. Math. Phys. **24** (2012) 1230004, arXiv:1204.0328.

[59] D. Bailint, A. Love, *Kaluza-Klein theories*, Rep. Prog. Phys. 50 (1987) 1087-1170.

[60] W. G. Unruh and R. M. Wald, Phys. Rev. D **29** (1984) 1047.

[61] B. S. de Witt in *General Relativity: an Einstein centenary survey*, S. W. Hawking and W. Israel (Eds.), Camb. Univ. Press (Cambridge), 1979.

[62] G. L. Sewell, Annals Phys. **141** (1982) 201.

[63] S. Takagi, Prog. Theor. Phys. Suppl. **88** (1986) 1.

[64] D. A. Eliezer and R. P. Woodard, Nucl. Phys. B **325** (1989) 389.

[65] D. W. Chiou, arXiv:1605.06656.

[66] D. V. Vassilevich, Phys. Rept. **388** (2003) 279, hep-th/0306138.

[67] A. O. Barvinsky and G. A. Vilkovisky, Nucl. Phys. B **282** (1987) 163.

[68] A. O. Barvinsky and G. A. Vilkovisky, Nucl. Phys. B **333** (1990) 471.

[69] I. G. Avramidi, Lect. Notes Phys. M **64** (2000) 1.

[70] B. Iochum, C. Levy and D. Vassilevich, Commun. Math. Phys. **316** (2012) 595, arXiv:1108.3749.

[71] A. Codello and O. Zanusso, J. Math. Phys. **54** (2013) 013513, arXiv:1203.2034.

[72] M. A. Kurkov, F. Lizzi, M. Sakellariadou and A. Watcharangkool, Phys. Rev. D **91** (2015) 065013, arXiv:1412.4669.

[73] A. Codello, R. Percacci and C. Rahmede, Annals Phys. **324** (2009) 414, arXiv:0805.2909.

[74] A. Belenchia, D. M. T. Benincasa and S. Liberati, JHEP **03** (2015) 036, arXiv:1411.6513.

[75] M. Saravani and S. Aslanbeigi, Phys. Rev. D **92** (2015) 103504, arXiv:1502.01655.

[76] B. R. Majhi and E. C. Vagenas, Phys. Lett. B **725** (2013) 477, arXiv:1307.4195.

[77] S. Gutti, S. Kulkarni and L. Sriramkumar, Phys. Rev. D **83** (2011) 064011, arXiv:1005.1807.

[78] I. Agullo, J. Navarro-Salas, G. J. Olmo and L. Parker, Phys. Rev. D **77** (2008) 124032, arXiv:0804.0513.

[79] M. Niedermaier and M. Reuter, Living Rev. Rel. **9** (2006) 5.

[80] D. F. Litim, Phil. Trans. Roy. Soc. Lond. A **369** (2011) 2759, arXiv:1102.4624.

[81] M. Reuter and F. Saueressig, New J. Phys. **14** (2012) 055022, arXiv:1202.2274.

[82] M. Reuter and F. Saueressig, Lect. Notes Phys. **863** (2013) 185, arXiv:1205.5431.

[83] S. Nagy, Annals Phys. **350** (2014) 310, arXiv:1211.4151.

[84] P. Donã, A. Eichhorn and R. Percacci, Phys. Rev. D **89** (2014) 084035, arXiv:1311.2898.

[85] N. Christiansen, B. Knorr, J. Meibohm, J. M. Pawlowski and M. Reichert, Phys. Rev. D **92** (2015) 121501, arXiv:1506.07016.

[86] J. Meibohm, J. M. Pawlowski and M. Reichert, Phys. Rev. D **93** (2016) 084035, arXiv:1510.07018.

[87] A. Codello, G. D'Odorico and C. Pagani, Phys. Rev. D **89** (2014) 081701, arXiv:1304.4777.

[88] N. Christiansen, D. F. Litim, J. M. Pawlowski and A. Rodigast, Phys. Lett. B **728** (2014) 114, arXiv:1209.4038.

[89] N. Christiansen, B. Knorr, J. M. Pawlowski and A. Rodigast, Phys. Rev. D **93** (2016) 044036, arXiv:1403.1232.

[90] A. Eichhorn, A. Held and J. M. Pawlowski, arXiv:1604.02041.

[91] A. Bonanno and M. Reuter, Phys. Rev. D **60** (1999) 084011, gr-qc/9811026.

[92] A. Bonanno and M. Reuter, Phys. Rev. D **62** (2000) 043008, hep-th/0002196.

[93] A. Bonanno and M. Reuter, Phys. Rev. D **73** (2006) 083005, hep-th/0602159.

[94] M. Reuter and E. Tuiran, hep-th/0612037.

[95] M. Reuter and E. Tuiran, Phys. Rev. D **83** (2011) 044041, arXiv:1009.3528.

[96] D. Becker and M. Reuter, JHEP **07** (2012) 172, arXiv:1205.3583.

[97] K. Falls and D. F. Litim, Phys. Rev. D **89** (2014) 084002, arXiv:1212.1821.

[98] D. Becker and M. Reuter, arXiv:1212.4274.

[99] B. Koch and F. Saueressig, Class. Quant. Grav. **31** (2014) 015006, arXiv:1306.1546.

[100] B. Koch and F. Saueressig, Int. J. Mod. Phys. A **29** (2014) 1430011, arXiv:1401.4452.

[101] F. Saueressig, N. Alkofer, G. D'Odorico and F. Vidotto, PoS FFP **14** (2015) 174, arXiv:1503.06472.

[102] I. Agullo, J. Navarro-Salas, G. J. Olmo and L. Parker, Phys. Rev. D **80** (2009) 047503, arXiv:0906.5315.

[103] S. Carlip and D. Grumiller, Phys. Rev. D **84** (2011) 084029, arXiv:1108.4686.

[104] P. Chen, Y. C. Ong and D. h. Yeom, Phys. Rept. **603** (2015) 1, arXiv:1412.8366.

[105] L. J. Garay, Int. J. Mod. Phys. A **10** (1995) 145, gr-qc/9403008.